IMPROVING WELL PRODUCTIVITY OF TIGHT GAS RESERVOIRS BY USING NON-DAMAGING DRILLING FLUID

BY

TURAL JAFAROV

A Thesis Presented to the

DEANSHIP OF GRADUATE STUDIES

KING FAHD UNIVERSITY OF PETROLEUM & MINERALS

DHAHRAN, SAUDI ARABIA

In Partial Fulfillment of the
Requirements for the Degree of

MASTER OF SCIENCE

In

PETROLEUM ENGINEERING

MAY, 2017

KING FAHD UNIVERSITY OF PETROLEUM & MINERALS

DHAHRAN- 31261, SAUDI ARABIA

DEANSHIP OF GRADUATE STUDIES

This thesis, written by **TURAL JAFAROV** under the direction his thesis advisor and approved by his thesis committee, has been presented and accepted by the Dean of Graduate Studies, in partial fulfillment of the requirements for the degree of **MASTER OF SCIENCE IN PETROLEUM ENGINEERING.**

Dr. ABDULAZIZ E. AL-MAJED
(Advisor)

Dr. ABDULLAH SULTAN
Department Chairman

Dr. MOHAMMED MAHMOUD
(Member)

Dr. Salam A. Zummo
Dean of Graduate Studies

Dr. SALAHELDIN ELKATATNY
(Member)

6/6/17
Date

This work is dedicated to my father Mr. Jafarkhan Jafarov, mother Mrs. Sadagat Jafarova, sister Firuza Jafarova and beloved relatives.

ACKNOWLEDGMENTS

All praises are for our merciful creator Allah, who granted me to accomplish my master study as being first Azerbaijani graduate in the history of KFUPM and Petroleum Engineering department. Everything is on His hand. Nothing may happen without His knowledge and no one may achieve without His grants. May Allah grant me to see Him and to meet with His beloved prophet Muhammad (sallAllahu alaihi va sallam) in the Heaven.

I'm so thankful to my parents Mr. Jafarkhan Jafarov and Mrs. Sadagat Jafarova for their care and support financially and morally throughout all my life. I always feel their full support behind me. I also thank my sister Firuza Jafarova and all my beloved relatives for their support and encouragement.

All my thanks go to my thesis advisor Dr. Abdulaziz Abdulla E. Al-Majed and my committee members Dr. Mohammed Mahmoud and Dr. Salaheldin Ahmed Elkatatny because of their invaluable advice and help during my whole work. Their guidance and assistance made my thesis work significantly easy. I'm grateful to KFUPM for providing me to study in such a great environment with full financial support. My thanks go to the chairman of Petroleum Engineering department Dr. Abdullah Sultan for his kind help anytime I need it . I'm also indebted to Dr. Badr Ba geri for sharing his knowledge with me during experiments. I thank the great and very experienced PETE lab staff Mr. Abdulsamad Iddrisu, Mr. Abdulrahim Muhammadain, Mr. Assad Barri and Mr. Mobeen Murtaza. They helped me a lot during my experiments anytime I was facing difficulties. I also thank Mr. Syed Rizwanullah Hussaini from CIPR because of his quick responds to my requests for working in his lab.

Finally, I thank all my dear friends in KFUPM for their support they never left me alone, even though I was the only Azerbaijani student.

TABLE OF CONTENTS

ACKNOWLEDGMENTS ..... **III**

TABLE OF CONTENTS ..... **V**

LIST OF TABLES ..... **VIII**

LIST OF FIGURES ..... **X**

LIST OF ABBREVIATIONS ..... **XIV**

ABSTRACT ..... **XVI**

ملخص الرسالة ..... **XVIII**

CHAPTER 1 INTRODUCTION **1**

1.1 Drilling Fluid Classification **1**

1.1.1 WBM **1**

1.1.2 OBM **2**

1.1.3 Gas Mud **2**

1.2 Drill-in Fluid **2**

1.2.1 Formation Damage Mechanisms **3**

1.3 Drilling Fluid Properties **4**

1.3.1 Density **4**

1.3.2 PH **5**

1.3.3 Rheological Properties **5**

1.3.4 Filtration **6**

1.3.5 Sand Content **7**

1.3.6 Alkalinity **7**

1.3.7 Water Hardness 7
1.3.8 Electrical Conductivity 7
1.4 Unconventional Reservoirs 8
1.4.1 Tight Gas Reservoirs 9
CHAPTER 2 LITERATURE REVIEW 11
2.1 Drilling Fluids for Conventional Reservoirs 11
2.2 Drilling Fluids for Unconventional Reservoirs 13
2.3 Drill-in Fluids for Conventional Reservoirs 15
2.4 Drill-in Fluids for Unconventional Reservoirs 19
CHAPTER 3 PROBLEM STATEMENT AND RESEARCH OBJECTIVES 23
CHAPTER 4 METHODOLOGY AND EXPERIMENTAL APPARATUS 25
4.1 Work Plan 25
4.1.1 Core Samples Preparation 25
4.1.2 Density and PH Measurements 25
4.1.3 Rheology Test 26
4.1.4 Solubility Test 32
4.1.5 Static Filtration Test 35
4.1.6 Stability Test 39
4.1.7 Structural Analysis 40
4.2 Materials 41
CHAPTER 5 RESULTS AND DISCUSSIONS 44
5.1 Density and PH Results 44
5.1.1 Effect of Sodium Silicate on Density 44
5.1.2 Effect of Sodium Silicate on PH 45

5.2 Rheology Results 45
5.2.1 Effect of Sodium Silicate on Rheological Properties at Room Temperature 46
5.2.2 Effect of Sodium Silicate on Rheological Properties at 100°F 52
5.2.3 Effect of Sodium Silicate on Rheological Properties at 140°F 56
5.2.4 Effect of Sodium Silicate on Rheological Properties at 170°F 61
5.2.5 Effect of Sodium Silicate on Rheological Properties at 300°F 66
5.3 Solubility Results 69
5.4 Filtration Results 73
5.4.1 High Sodium Silicate Concentrations 73
5.4.2 Low Sodium Silicate Concentrations 78
5.4.3 Return Permeability 84
5.5 Sag Test Results 88
5.6 Structural Analysis 89
5.6.1 Slice-by-slice Analysis and CT Numbers 90
5.6.2 Cross-sectional Analysis 101
5.7 Mechanism of 0.075 wt% Na_2SiO_3 104
5.7.1 Barite Flotation Recovery 104
5.7.2 Solubility Concentration of Silica with PH 105
CHAPTER 6 CONCLUSIONS AND RECOMMENDATIONS 110
6.1 Conclusions 110
6.2 Future Work Recommendations 112
REFERENCES 113
VITAE 117

LIST OF TABLES

Table 4-1 Details of the Additives in the Drill-in Fluid Formulation 42

Table 5-1 Summary of Density and PH Values 44

Table 5-2 Torque Readings of Base Fluid and with 0.05 wt% Na_2SiO_3 at Room Temperature 49

Table 5-3 Torque Readings of Base Fluid with 0.075 and 0.1 wt% Na_2SiO_3 at Room Temperature 50

Table 5-4 Torque Readings of Base Fluid with 0.5 and 1 wt% Na_2SiO_3 at Room Temperature 50

Table 5-5 Torque Readings of Base Fluid with 1.5 and 2 wt% Na_2SiO_3 at Room Temperature 51

Table 5-6 Summary of Rheological Properties of Na_2SiO_3 Concentrations at Room Temperature 51

Table 5-7 Torque Readings of Base Fluid and with 0.05 wt% Na_2SiO_3 at 100°F 54

Table 5-8 Torque Readings of Base Fluid with 0.075 and 0.1 wt% Na_2SiO_3 at 100°F ... 54

Table 5-9 Torque Readings of Base Fluid with 0.5 and 1 wt% Na_2SiO_3 at 100°F 55

Table 5-10 Torque Readings of Base Fluid with 1.5 and 2 wt% Na_2SiO_3 at 100°F 55

Table 5-11 Summary of Rheological Properties of Na_2SiO_3 Concentrations at 100°F ... 56

Table 5-12 Torque Readings of Base Fluid and with 0.05 wt% Na_2SiO_3 at 140°F 58

Table 5-13 Torque Readings of Base Fluid with 0.075 and 0.1 wt% Na_2SiO_3 at 140°F . 59

Table 5-14 Torque Readings of Base Fluid with 0.5 and 1 wt% Na_2SiO_3 at 140°F 59

Table 5-15 Torque Readings of Base Fluid with 1.5 and 2 wt% Na_2SiO_3 at 140°F 60

Table 5-16 Summary of Rheological Properties of Na_2SiO_3 Concentrations at 140°F ... 60

Table 5-17 Torque Readings of Base Fluid and with 0.05 wt% Na_2SiO_3 at 170°F 63

Table 5-18 Torque Readings of Base Fluid with 0.075 and 0.1 wt% Na_2SiO_3 at 170°F . 64

Table 5-19 Torque Readings of Base Fluid with 0.5 and 1 wt% Na_2SiO_3 at 170°F 64

Table 5-20 Torque Readings of Base Fluid with 1.5 and 2 wt% Na_2SiO_3 at 170°F 65

Table 5-21 Summary of Rheological Properties of Na_2SiO_3 Concentrations at 170°F ... 65

Table 5-22 Summary of Rheological Properties of Base Fluid and with 0.05, 0.075, 0.1 wt% Na_2SiO_3 Concentrations at 300°F 70

Table 5-23 Calculated Solubility Percentages with Different Na_2SiO_3 Concentrations.. 72

Table 5-24 Summary of Solubility Results..... 73

Table 5-25 Summary of Filtrate Volumes at 30 Minutes of Base Fluid and High Na_2SiO_3 Concentrations..... 75

Table 5-26 Summary of Filter Cake Thicknesses with High Na_2SiO_3 Concentrations... 78

Table 5-27 Summary of Filtrate Volumes at 30 Minutes of Base Fluid and Low Na_2SiO_3 Concentrations..... 81

Table 5-28 Summary of Filter Cake Thicknesses with Low Na_2SiO_3 Concentrations.... 84

Table 5-29 Recorded Pressure Values for each Flow Rates Before and After Damage.. 87

Table 5-30 Summary of Sag Test Results with Base Fluid and 0.075 wt% Na_2SiO_3..... 89

Table 5-31 Summary of CT Numbers of 0.25" Core Sample with Base Fluid and 0.05 wt% Na_2SiO_3..... 98

Table 5-32 Summary of CT Numbers of 0.25" Core Sample with 0.075 and 0.1 wt% Na_2SiO_3 98

Table 5-33 Summary of Cumulative Average Difference of CT Numbers of 0.25" Core Samples Before and After Damage for each Na_2SiO_3 Concentration... 99

Table 5-34 Summary of CT Numbers of 2" Core Sample with 0.075 wt% Na_2SiO_3.... 101

LIST OF FIGURES

Figure 1-1 Formation Damage by Conventional and Drill-in Fluids (Mandal et al. 2006) 4

Figure 1-2 Difference between Conventional and Unconventional Deposits (Wikipedia) 8

Figure 1-3 Resource Triangle for Gas Reservoirs (Lake et al. 2007) 9

Figure 4-1 Schematic Workflow Diagram 27

Figure 4-2 Typical 0.25" and 2" Scioto Tight Sandstone Core Samples After 100% Saturation with Brine… 28

Figure 4-3 Saturator 28

Figure 4-4 Digital Weight Balance 29

Figure 4-5 Mud Balance 29

Figure 4-6 OAKTON pH 2700 30

Figure 4-7 Grace M3600 Rheometer 31

Figure 4-8 Chandler 7550 HPHT Viscometer 31

Figure 4-9 Magnetic Stirrer 33

Figure 4-10 Modified Fann HPHT Filter Press while Doing Filtration Test 36

Figure 4-11 Modified Fann HPHT Filter Press with Flow Rate Controller while Measuring Permeability 38

Figure 4-12 Static Sag Test Unit 40

Figure 4-13 Toshiba CT Scanner 41

Figure 5-1 Effect of Na_2SiO_3 on Density 45

Figure 5-2 Effect of Na_2SiO_3 on PH 46

Figure 5-3 Effect of Na_2SiO_3 on PV at Room Temperature 48

Figure 5-4 Effect of Na_2SiO_3 on YP at Room Temperature 48

Figure 5-5 Effect of Na_2SiO_3 on Gel Strength at Room Temperature 49

Figure 5-6 Effect of Na_2SiO_3 on PV at 100°F 52

Figure 5-7 Effect of Na_2SiO_3 on YP at 100°F 53
Figure 5-8 Effect of Na_2SiO_3 on Gel Strength at 100°F 53
Figure 5-9 Effect of Na_2SiO_3 on PV at 140°F 57
Figure 5-10 Effect of Na_2SiO_3 on YP at 140°F 57
Figure 5-11 Effect of Na_2SiO_3 on Gel Strength at 140°F 58
Figure 5-12 Effect of Na_2SiO_3 on PV at 170°F 62
Figure 5-13 Effect of Na_2SiO_3 on YP at 170°F 62
Figure 5-14 Effect of Na_2SiO_3 on Gel Strength at 170°F 63
Figure 5-15 Effect of Na_2SiO_3 on PV at 300°F 67
Figure 5-16 Effect of Na_2SiO_3 on YP at 300°F 68
Figure 5-17 Effect of Na_2SiO_3 on 10-second Gel Strength at 300°F 68
Figure 5-18 Effect of Na_2SiO_3 on 10-minute Gel Strength at 300°F 69
Figure 5-19 Effect of Na_2SiO_3 on Barite Solubility 72
Figure 5-20 Effect of High Na_2SiO_3 Concentrations on Filtrate Volumes 74
Figure 5-21 Effect of High Na_2SiO_3 Concentrations on Filter Cake Thicknesses 76
Figure 5-22 Formed Filter Cake with Base Fluid on 0.25” Core Sample 76
Figure 5-23 Formed Filter Cake with 0.5 wt% Na_2SiO_3 on 0.25” Core Sample 77
Figure 5-24 Formed Filter Cake with 1 wt% Na_2SiO_3 on 0.25” Core Sample 77
Figure 5-25 Formed Filter Cake with 1.5 wt% Na_2SiO_3 on 0.25” Core Sample 78
Figure 5-26 Effect of Low Na_2SiO_3 Concentrations on Filtrate Volumes 80
Figure 5-27 Effect of Low Na_2SiO_3 Concentrations on Filter Cake Thicknesses 82
Figure 5-28 Formed Filter Cake with 0.1 wt% Na_2SiO_3 on 0.25” Core Sample 82
Figure 5-29 Formed Filter Cake with 0.075 wt% Na_2SiO_3 on 0.25” Core Sample 83
Figure 5-30 Formed Filter Cake with 0.05 wt% Na_2SiO_3 on 0.25” Core Sample 83
Figure 5-31 Formed Filter Cake with 0.075 wt% Na_2SiO_3 on 2” Core Sample 84

Figure 5-32 Voltage Readings of *Omega* Software Before (a) and After (b) Damage ... 86

Figure 5-33 Plotted q vs. ΔP Relationships Before (a) and After (b) Damage 87

Figure 5-34 Sag Test Results with Base Fluid and 0.075 wt% Na_2SiO_3 89

Figure 5-35 Slice-by-slice View of 0.25" Core Sample with Base Fluid Before (a) and After (b) Damage….. 92

Figure 5-36 Comparison between CT Numbers of 0.25" Core Sample with Base Fluid Before and After Damage 93

Figure 5-37 Slice-by-slice View of 0.25" Core Sample with 0.05 wt% Na_2SiO_3 Before (a) and After (b) Damage….. 93

Figure 5-38 Comparison between CT Numbers of 0.25" Core Sample with 0.05 wt% Na_2SiO_3 Before and After Damage..... 94

Figure 5-39 Slice-by-slice View of 0.25" Core Sample with 0.075 wt% Na_2SiO_3 Before (a) and After (b) Damage….. 95

Figure 5-40 Comparison between CT Numbers of 0.25" Core Sample with 0.075 wt% Na_2SiO_3 Before and After Damage..... 96

Figure 5-41 Slice-by-slice View of 0.25" Core Sample with 0.1 wt% Na_2SiO_3 Before (a) and After (b) Damage….. 96

Figure 5-42 Comparison between CT Numbers of 0.25" Core Sample with 0.1 wt% Na_2SiO_3 Before and After Damage..... 97

Figure 5-43 Cumulative Average Difference of CT Numbers of 0.25" Core Sample Before and After Damage for each Na_2SiO_3 Concentration..... 98

Figure 5-44 Slice-by-slice View of 2" Core Sample with 0.075 wt% Na_2SiO_3 Before (a) and After (b) Damage….. 99

Figure 5-45 Comparison between CT Numbers of 2" Core Sample with 0.075 wt% Na_2SiO_3 Before and After Damage..... 100

Figure 5-46 Cross-sectional View of Typical 0.25" Core Sample Before Damage 102

Figure 5-47 Cross-sectional View of 0.25" Core Sample with Base Fluid After Damage 102

Figure 5-48 Cross-sectional View of 0.25" Core Sample with 0.05 wt% Na_2SiO_3 After Damage…… 102

Figure 5-49 Cross-sectional View of 0.25” Core Sample with 0.075 wt% Na_2SiO_3 After Damage…… 103

Figure 5-50 Cross-sectional View of 0.25” Core Sample with 0.1 wt% Na_2SiO_3 After Damage…… 103

Figure 5-51 Cross-sectional View of 2” Core Sample with 0.075 wt% Na_2SiO_3 Before (left) and After (right) Damage 103

Figure 5-52 Barite Flotation Recovery with respect to $Na_2SiO_3/BaSO_4$ Ratio 105

Figure 5-53 Solubility Concentration of Silica with respect to PH 106

LIST OF ABBREVIATIONS

WBM	:	Water-Based Mud
OBM	:	Oil-Based Mud
ROP	:	Rate of Penetration
PV	:	Plastic Viscosity
YP	:	Yield Point
PAC	:	Polyanionic Cellulose
MRC	:	Maximum Reservoir Contact
HPHT	:	High Pressure High Temperature
LPLT	:	Low Pressure Low Temperature
MWCNT	:	Multi-Walled Carbon Nanotube
SAGD	:	Steam-Assisted Gravity Drainage
MMH	:	Mixed Metal Hydroxide
EGMBE	:	Ethylene Glycol Monobutylether
OA	:	Organic Acid
N/A	:	Not Applicable
N/P	:	Not Provided

RPM	:	Rotation per Minute
DTPA	:	Diethylene Triamine Penta Acetic Acid
K-DTPA	:	Potassium-based Diethylene Triamine Penta Acetic Acid
∆P	:	Differential Pressure
CT	:	Computed Tomography

ABSTRACT

Full Name : Tural Jafarov

Thesis Title : Improving Well Productivity of Tight Gas Reservoirs by Using Non-Damaging Drilling Fluid

Major Field : Petroleum Engineering

Date of Degree : May 2017

Selection of the suitable drilling fluid is one of the most essential parts of drilling processes. The main objectives of circulating a fluid during drilling a well are to carry the rock cuttings to the surface, to cool and lubricate the bit, to maintain wellbore stability, to reduce friction between the drill string and the borehole walls, to prevent fluid flow from penetrated permeable rocks, and to form a thin and a low-permeability filter cake with the minimum formation damage. However, recent advancement in drilling and completion plans showed that conventional drilling fluids are not effective and can damage the formation severely. In some cases, this damage becomes irreversible and permeability around the wellbore decreases considerably. This led the petroleum industry to the development of new type of drilling fluids, which is called non-damaging drilling fluids or drill-in fluids, to minimize formation damage and to improve well productivity as the main goals beside the environmental consideration.

On the other hand, rapid increase in energy demand already forces oil companies to develop methods for producing from unconventional reservoirs as well as conventional ones. Tight gas reservoirs are the typical examples for such type of reservoirs. In case of unconventional reservoirs, due to complexity of drilling methods, formation damage by drilling fluids become more severe. The wells drilled in tight gas formations suffer mainly from water blockage problem. This is due

to much lower viscosity of gas than water, because water fills smaller pores of tight formation. Consequently, capillary forces cause water blockage.

In this thesis work, damage mechanisms of conventional and non-damaging drilling fluids to the formations were studied by conducting a comprehensive literature review.

The main objective of this work was to explore the possibility of formulating a proper non-damaging water-based drilling fluid for tight gas reservoirs. The results showed that the optimum concentration of sodium silicate (Na_2SiO_3) reduces solid invasion completely, minimizes fluid invasion and prevents water blockage problem of the wells. It formed very thin, impermeable and easily removable filter cake, which led to increase in well productivity by obtaining the high return permeability. In addition to these objectives, the effect of sodium silicate was observed on the rheological properties of the formulated drill-in fluid, barite solubility and the sag performance.

ملخص الرسالة

الاسم الكامل: تورال جعفروف

عنوان الرسالة: تحسين انتاجية الابار في المكامن قليلة النفاذية باستخدام موائع حفر غير ضارّة

التخصص: هندسة البترول

تاريخ الدرجة العلمية: مايو ٢٠١٧

إن اختيار مائع الحفر المناسب يمثل واحدا من الأركان الأساسية لعملية الحفر. من أهم وظائف ضخ مائع الحفر داخل البئر هو حمل الصخور المقطوعة إلى السطح، تبريد وتزييت حفّارة البئر، المحافظة على ثبات جدار البئر، تقليل الاحتكاك بين عمود الحفر وجدار البئر، منع دخول الموائع من الطبقات المحفورة عالية النفاذية وتشكيل طبقة رقيقة ذات نفاذية قليلة بأقل تخريب للطبقات المحفورة. ولكن، التطور الحديث لخطط الحفر وتكملة الآبار أوضح أن موائع الحفر العادية لا تستطيع التعامل معها بصورة جيدة وتتسبب في تخريب حاد للطبقات المحفورة. في بعض الحالات، هذا التخريب يكون دائما ولا يمكن معالجته مما سبب نقصانا شديدا في النفاذية حول البئر. وقد قاد هذا التغير صناعة النفط إلى تطوير موائع حفر جديدة تسمي موائع الحفر غير التخريبية أو موائع الحفر الداخلي، لتقليل التخريب الطبقي وتحسين إنتاجية البئر وهو الهدف الأساسي بجانب مراعاة البيئة.

في المقابل، الزيادة السريعة لطلب الطاقة أجبرت مؤسسات النفط على تطوير طرق حديثة للإنتاج من المكامن غير الاعتيادية والاعتيادية على حد سواء. المكامن قليلة النفاذية هي مثال نمطي لهذه المكامن غير الاعتيادية. في حالة المكامن غير الاعتيادية، نسبة لتعقيدات عمليات وطرق الحفر فإن التخريب الطبقي الناتج من موائع الحفر يصبح أكثر حدّة. الابار المحفورة في طبقات قليلة النفاذية تعاني من مشاكل أهمها الانسداد المائي. هذه المشكلة تنتج نسبة للزوجة المنخفضة للغاز مقارنة بالماء، مما يؤدي الي امتلاء الفجوات الصغيرة بالماء وتتسبب القوى الشعرية بانسداد مائي.

في هذا البحث، طرق تخريب الطبقات الناتجة عن موائع الحفر الاعتيادية، الغير الاعتيادية وموائع الحفر غير المخرّبة (موائع الحفر الداخلي) قد درست عن طريق بحث شامل للمصادر العلمية.

إن الهدف الأساسي من هذا البحث هو لمحاولة تحضير مائع حفر غيّر مخّرب للطبقات مبني على أساس مائي مع تركيز مثالي من سيليكات الصوديوم (Na_2SiO_3) يستخدم في حفر الطبقات قليلة النفاذية للحد من تسرب المائع الي الطبقات ومنع مشكلة الانسداد المائي في هذه الطبقات. وذلك بتكوين طبقة رقيقة، غير نفّاذة وسهلة الازالة على جدار البئر. الهدف النهائي يتمثل في

زيادة إنتاجية البئر نسبة للكسب العالي في نفاذية البئر المسترجعة. بالإضافة لهذه الأهداف، تاثير سيليكات الصوديوم الملاحظ على الخصائص الحركية لمائع الحفر والتأثير على اذابة مادة البارايت واختبار سقوط مائع الحفر (sag performance) سيدرس.

CHAPTER 1

INTRODUCTION

1.1 Drilling Fluid Classification

Drilling fluid is a vital part of drilling operations. Drilling fluids have several functions that play an important role in choosing them. These are:

- Removing and carrying cuttings to the surface
- Cooling and lubricating the bit
- Reducing friction between the drill string and the borehole walls
- Maintaining wellbore stability
- Preventing fluid flow from penetrated permeable rocks
- Forming a thin and a low-permeability filter cake.

They are classified into three broad categories: water-based mud (WBM), oil-based mud (OBM) and gas mud. Each of them have their own properties and applicability conditions (Caenn et al. 2011).

1.1.1 WBM

WBMs are the most common types of drilling fluids. Saltwater and freshwater are used as their base components. They have several advantages, such as less loss of circulation due to formed filter cake by clay particles, increasing of viscosity because of clay hydration

that helps to carry cuttings to the surface more easily and low cost. Water-based drilling fluids constitute around 10% of total well cost. However, WBMs have also some disadvantages, like reduction in rate of penetration (ROP) and more pressure loss because of friction.

1.1.2 OBM

OBMs' water content variees between 2 – 5%. Their applicability conditions are too broad and range from high pressure to deep wells and from unconsolidated formations to shale formations. This is because they introduce less drilling problems and less formation damage. Although, OBMs provide such superiorities than WBMs, they have limitations as well. These are mainly their very high cost and environmental pollution. Since, nowadays, HSE issues have already been more dominant in the decisions, OBMs are strictly prohibited by most countries. Therefore, oil companies are trying to avoid using them.

1.1.3 Gas Mud

Gas muds are used when formations are impermeable, which it limits their usage. They are different types as air or foam drilling muds. Main advantages of gas muds are higher ROP, better hole cleaning and less damage to formation. They have also some important disadvantages, such as inefficient borehole support and drilling in only underbalanced regime (Hossain and Al-Majed 2015).

1.2 Drill-in Fluid

Recent development in drilling (e.g. horizontal wells, maximum reservoir contact wells multi-lateral wells etc.) and completion plans showed that aforementioned conventional

drilling fluids are not effective and has resulted in severe formation damage and reduction in well productivity. This concern directed the petroleum industry to formulate non-damaging drilling or so called drill-in fluids, such that formation damage and reduced well productivity became considerably smaller compared to conventional ones. Despite drill-in fluids decrease the damage level, still formulations require much attention due to different natures of the formations. Because of this reason, there is no unique solution and damage mechanisms should be identified clearly before starting to formulate drill-in fluid so that to achieve lower damage.

1.2.1 Formation Damage Mechanisms

There are several types of formation damage mechanisms. These mainly depend on composition and chemistry of drill-in fluid, used bridging material, spurt loss characteristics of drill-in fluid, maximum level of overbalance drilling etc (Amanullah and Allen 2013). **Fig. 1-1** illustrates comparison between formation damage of conventional and drill-in fluids, respectively. Less formation damage means more hydrocarbon production. So, the drill-in fluid should be formulated by considering this fact so that to make damage as less as possible. Ideal drill-in fluid should have degradable solids, minimum drill cuttings, reduced fluid invasion, not chemically reactive filtrate with formation fluid, filtrate that is not swellable with shale and so on (Mandal et al. 2006).

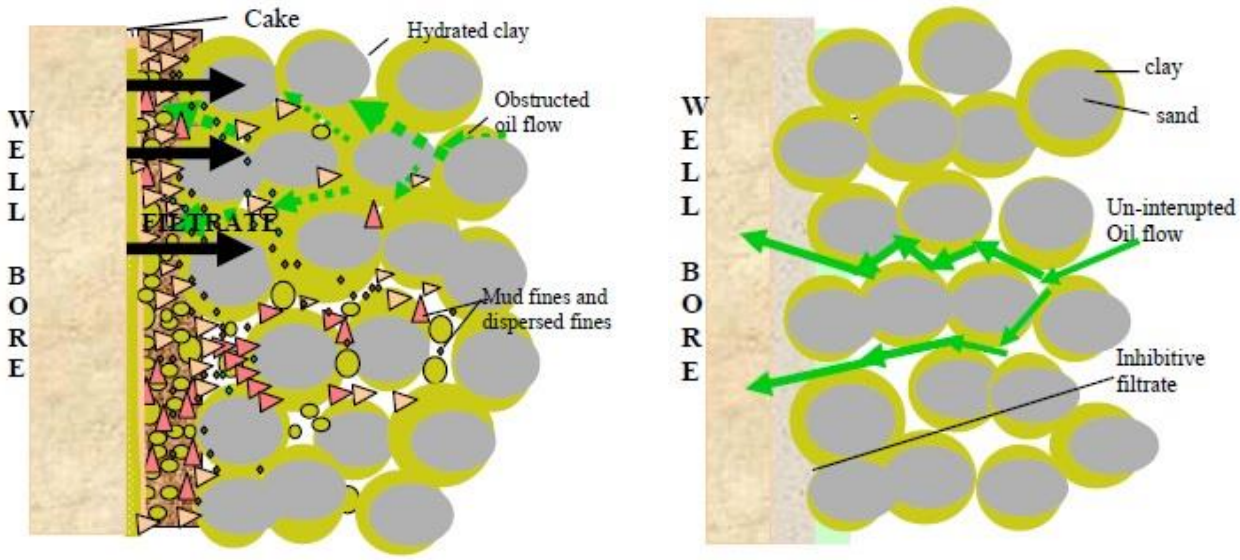

Figure 1-1. Formation Damage by Conventional and Drill-in Fluids (Mandal et al. 2006)

1.3 Drilling Fluid Properties

Drilling fluid properties include mud density, rheological properties, filtration, sand content, PH, alkalinity, water hardness, electrical conductivity. All these properties must be controlled.

1.3.1 Density

Mud density is an important parameter in determining hydrostatic pressure of mud column, which allows to decide to drill the well either in underbalanced or overbalanced regimes. For controlling density, several weighting agents can be added to the mud, such as barite ($BaSO_4$), ilmenite ($FeO \cdot TiO_2$), magnetite (Fe_3O_4), manganese tetra oxide (Mn_3O_4) etc.

1.3.2 PH

PH determines acidity or alkalinity of mixing water. If PH=7, drilling fluid is called neutral. Water is acidic below this value and it is alkaline above seven. Rarely PH value decreases below 7. Typical value for PH is in between 8 and 12.5. Generally, the values above 10 are sign of corrosion. Therefore, PH for desired operating muds lies between 8.5 and 9.5. PH control is an important for detection and treatment of some contaminants, reduction in corrosion and maintenance of lime-treated drilling muds.

1.3.3 Rheological Properties

Rheological properties of drilling fluids consist of plastic viscosity (PV), yield point (YP) and gel strength. Viscosity is a measurement of resistance to flow. Apparent viscosity is obtained by the division of shear stress by shear rate:

$$\mu = \frac{\tau_s}{\gamma} = \frac{F/A}{dv/dl} \qquad (1)$$

where A – cross-sectional area, cm^2; l – layer thickness, cm; F – force, dynes; v – velocity, cm/s; μ – apparent or dynamic viscosity, poise or dynes-sec/cm^2; τ_s – shear stress, dynes/cm^2; γ – shear rate, sec^{-1}; dv/dl – velocity gradient, sec^{-1}.

Fluids are classified into two types: Newtonian and Non-Newtonian. Newtonian fluids are those, which their viscosities do not change with shear rate, e.g. water, light hydrocarbon oils, air etc. Apparent viscosity is constant for Newtonian fluids. However, the viscosity of plastic or Non-Newtonian fluids depends on shear stress, e.g. drilling fluids. Drilling fluids with high solid content may be expressed based on Bingham Plastic theory. The theory explains that a finite stress should be applied to allow flow of fluids and it will be

Newtonian at higher stresses. Decreasing of apparent viscosity with increasing of shear rate is called shear thinning. Shear thinning is an important property for reducing apparent viscosity. Viscosity will be low at high shear rates and high at low shear rates. Consequently, shear thinning increases carrying capacity of drill cuttings. Shear thinning fluids are called pseudo-plastic (Rao 2007). Thixotropic fluids are those in which their apparent viscosity decreases under constant shear stress and rate. The behavior of anti-thixotropic fluids is completely opposite of thixotropic fluids, their apparent viscosity increases under constant shear stress and rate. Anti-thixotropic fluids are also known as rheopectic fluids by the industry (Tropea et al. 2007). Plastic viscosity (PV) is the flow resistance caused by mechanical friction, which occurs between solid content of the mud and the dispersed phase's viscosity. Yield point (YP) is the required stress for fluid to start flowing. Gel strength can be decreased by adding thinners and increased by adding bentonite to the mud. It should be high enough for suspending drill cuttings in case of circulation stopped.

1.3.4 Filtration

Since the pressure of mud column must be greater than formation pressure for preventing fluid flow, drilling fluid would continuously invade the formation in case filter cake was not formed properly. For forming a filter cake, mud should have bridging particles that can prevent invasion of smaller particles to the formation. After trapping the finer particles with bridging particles, mud invades the formation. Fluid invasion process during mud cake forming is called filtration or mud spurt. There are two types of filtration in the well: static and dynamic. Static filtration is made when the circulation of drilling fluid is stopped, whilst dynamic filtration is made with the circulation of drilling fluid. Since dynamic tests

are time consuming, all the tests are done under static conditions. Common filtration control materials are starch, polymers, polyanionic cellulose (PAC), thinners etc.

1.3.5 Sand Content

Sand content of drilling fluid is identified as any particles of it larger than 74 μm. Periodic sand content determination is important as too much sand can result in the deposition of thick mud cake on the borehole.

1.3.6 Alkalinity

In addition to PH analysis, alkalinity is also important for the quality of drilling fluid. Alkalinity measurements can be used to estimate the concentration of hydroxyl (OH^-), carbonate (CO_3^{2-}) and bicarbonate (HCO_3^-). Drilling fluid additives require alkaline environment for functioning properly, especially some organic de-flocculants.

1.3.7 Water Hardness

Water hardness of mud is because of calcium (Ca^{2+}) and magnesium (Mg^{2+}) ions that are present in the water. Hard water has hard mineral contents such as calcium, magnesium and sometimes bicarbonates and sulfates.

1.3.8 Electrical Conductivity

The resistivity of WBMs is controlled and measured from electrical logs. To lower the resistivity, salt is used, to raise the resistivity, fresh water is used. This is because usually, salt has low resistivity and fresh water has high resistivity. The electrical stability test indicates the stability of OBMs.

1.4 Unconventional Reservoirs

Unconventional reservoirs are the reservoirs that have low permeability and porosity, which make production of hydrocarbon very difficult. It requires advanced technology and special recovery operations. Example for unconventional resources are shale gas, shale oil, heavy oil, tight gas, coalbed methane etc. Rapid increase in energy demand forces oil companies to develop methods for producing hydrocarbons from unconventional reservoirs. **Fig. 1-2** graphically explains the difference between conventional and unconventional deposits. As we see from the graph, unlike conventional, unconventional resources are in source rock, which makes difficult to drill wells to those formations and needs special attentions because of having high risk.

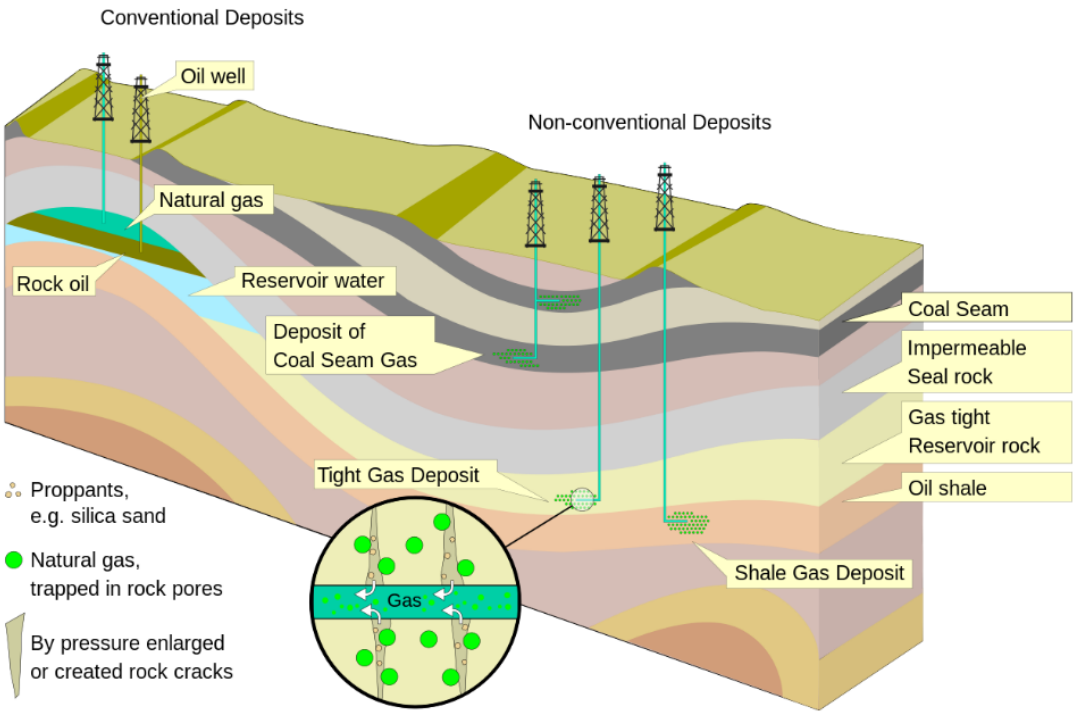

Figure 1-2. Difference between Conventional and Unconventional Deposits (Wikipedia)

1.4.1 Tight Gas Reservoirs

Tight gas reservoirs are typical type of unconventional gas reservoirs with permeability less than 0.1 mD and produce mainly dry gas. **Fig. 1-3** shows quality for all types of gas resources. Main challenge in this type of reservoirs is wells cannot produce at economic flow rate and require expensive technologies. For this reason, many wells should be drilled to the formation. Advanced well drilling technologies, such as drilling horizontal, multilateral or even maximum reservoir contact (MRC) wells, can be applied to increase overall flow rate. Best drilling plan is to drill a well in a near balanced regime for minimizing wellbore washouts and drilling mud invasion. Large hydraulic fracturing as a stimulation technique must also be done in order to increase the recovery percentage (Lake et al. 2007).

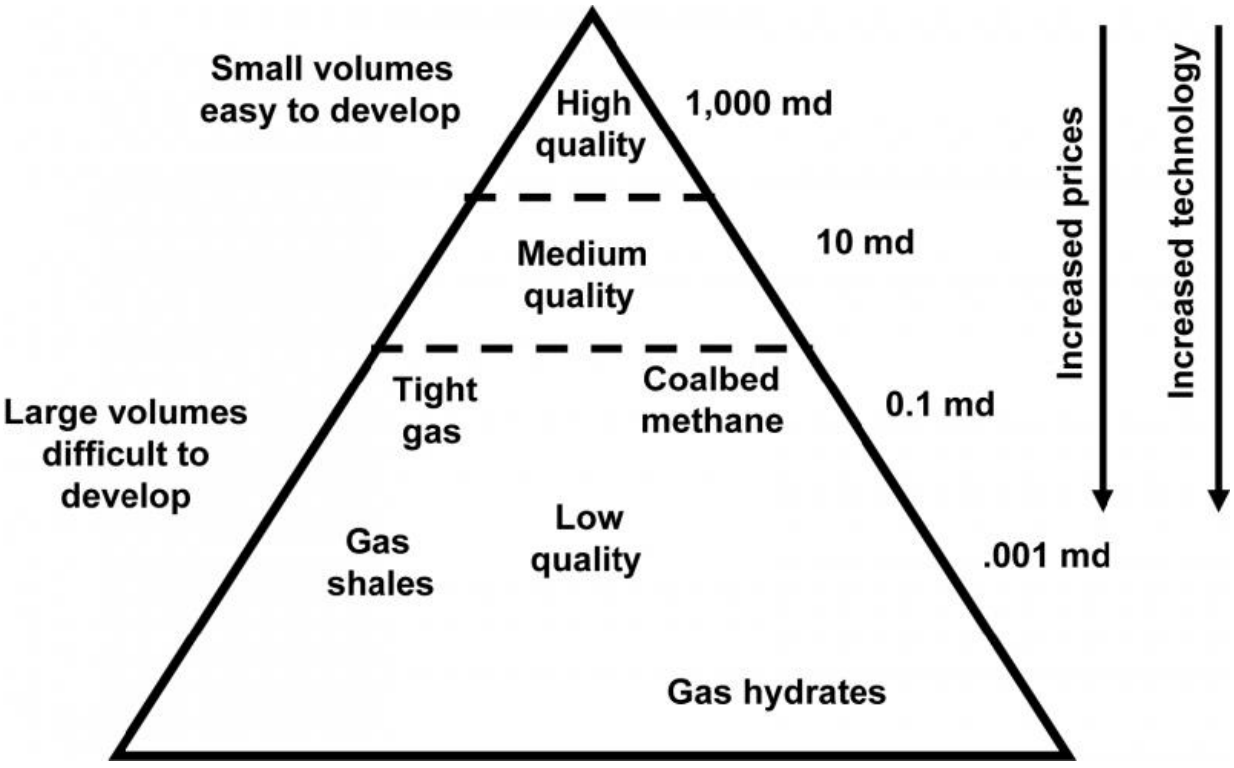

Figure 1-3. Resource Triangle for Gas Reservoirs (Lake et al. 2007)

The wells drilled to tight gas reservoirs mainly suffer from water blockage problem due to the interaction between water-based drilling fluid and formation. This is because of much lower viscosity of gas than water. Water fills smaller pores of tight formation and causes liquid build-up. In another word, capillary forces cause water blockage. As a result, gas production of the wells decreases considerably, which is a significant challenge for tight gas reservoirs as normally their production rate is low. To prevent water blockage, compatibility between formulated drill-in fluid and formation should be verified (Van Zanten et al. 2011). Liquid sodium silicate (Na_2SiO_3) is a strongly inhibitive material. Its particles in fresh water become in gel state and form a film-like barrier throughout the rock (Guo et al. 2005). Our study mainly investigates whether this gel will fill the micro pores of the tight rocks in order to minimize fluid invasion and prevent water blockage problem of tight gas reservoirs by forming a very thin and impermeable filter cake. A very thin filter cake has easily breakable character, which allows to have a high return permeability. On the other hand, obtaining a high return permeability means formation damage becomes considerably less. Moreover, fractures are also easily opened during fracturing job as a part of stimulation due to the soft breakable behavior of a formed gel.

CHAPTER 2

LITERATURE REVIEW

2.1 Drilling Fluids for Conventional Reservoirs

William et al. (2014) studied the effects of nano sized copper oxide (CuO) and zinc oxide (ZnO) separately, in xanthan gum based drilling fluid and WBM with nanoparticle concentrations – 0.1, 0.3 and 0.5 wt%. Nanoparticle size was around 50 nm. The prepared nanofluid added to the WBM as 1 vol%. They reported that thermal conductivity increases with the increase of nanoparticle concentration for both xanthan and water based drilling fluids. For both cases, the results became higher for CuO nanofluids. Nanofluid WBMs showed about 35% higher thermal conductivity than WBM. Higher thermal conductivity means faster mud cooling and viscosity preservation, which is very important for HPHT environments. Similarly, electrical conductivity was also enhanced. Higher electrical conductivity observed for CuO nanofluids from 44 to 49%. The authors also observed the rheological properties at temperatures 25, 70, 90 and 110℃ and pressures 0.1 and 10 MPa. It was found that nanofluids stabilize the viscosity at higher temperatures.

Barry et al. (2015) investigated rheological properties and fluid losses of a new drilling fluid with low solid bentonite that contains iron oxide (Fe_2O_3) nanoparticles (3 and 30 nm), iron oxide and aluminosilicate ($Al_2O_3 \cdot SiO_2$) clay hybrid nanoparticles under LPLT and HPHT conditions. Their experiments demonstrated that adding iron oxide and aluminosilicate clay hybrid nanoparticles reduces fluid loss by 37% and 47% for LPLT and

HPHT, respectively. This was because of reduced filter cake permeability, which created strong electrostatic repulsion between hybrid particles and clay platelets. On the other hand, adding 0.5 wt% 3 and 30 nm iron oxide particles increased fluid loss to 14% for LPLT, but decreased to 28% for HPHT. The reason for reduction in HT is that nanoparticle iron oxide replaces Na^{2+} cations, which leads to a low filter cake permeability.

Ismail et al. (2016) did the experiments for studying the effects of multi-walled carbon nanotube (MWCNT), nanosilica and glass beds in WBMs for rheological properties. The concentrations for both 21 nm MWCNT and 12 nm nanosilica were 0.001 ppb, 0.002 ppb, 0.01 ppb, 0.02 ppb, 0.1 ppb, 0.2 ppb, whereas glass beds sizes were chosen as 90-150 μm and 250-425 μm to investigate for 2 ppb, 4 ppb, 6 ppb, 8 ppb, 10 ppb and 12 ppb concentrations. They reported that PV, YP, gel strength increased, whilst filtrate volume and mud cake thickness decreased for all nanofluids. MWCNT provided less fluid loss compared than others because of its high surface area and nanotube structure with 0.01 ppb 4.8 ml and 0.01 ppb 4.5 ml. Their experiments also showed that friction coefficient decreases with adding nanoparticles to WBM, about 38%, 44%, 28% with MWCNT, nanosilica and glass beds (90-150 μm), respectively. Authors concluded that selection of MWCNT as a nanomaterial for WBMs can be better.

Mahmoud et al. (2016) studied the effect 50 nm ferric oxide (Fe_2O_3) and 12 nm silica nanoparticles in bentonite-based drilling fluids for HPHT (500 psi, 350°F) conditions using Indiana limestone cores. They found that both nanoparticles increase rheological properties. 0.5 wt% ferric oxide increases YP more than 0.5 wt% silica. They also reported that using both additives together increases rheological properties, but the value is still less than 0.5 wt% ferric oxide. Both nanoparticles increased PV and gave almost similar results.

The experiments of the authors under static conditions demonstrated that 0.5 wt% ferric oxide nanoparticle reduces filtration loss by 42.7%. However, silica nanoparticles increased filtration loss and cake thickness adversely. They also reported that filter cake permeability decreased considerably by 76.38% and became 0.000345 mD with 0.5 wt%. Using ferric oxide in different conditions and silica resulted in higher permeability values. They also observed the effect of pressure (200-500 psi) and temperature (175, 200, 250, 300, 350°F) on the filter cake behavior using 0.5 wt% ferric oxide nanoparticle. Observations showed that as the temperature increases at constant 300 psi, filter cake quality remains good and its permeability reduces to 0.000296 mD. The experiments also showed that temperature is dominant than pressure on filter cake behavior.

2.2 Drilling Fluids for Unconventional Reservoirs

Guo et al. (2005) prepared KCl/sodium silicate based drilling fluid for shaly Aradeiba and Abu Gabra formations in Sudan. Authors reported that new formulated mud system gave better rheological properties and filtration volume in comparison with previous systems, such as KCl/polymer, KCl/lime/polymer and KCl/Partially Hydrolized Polyacrylamide. The authors recommended that the ratio of KCl, silicate and bentonite should be kept in the range of (5-8):(7-11):(1-3). The reported filtrate volume at HPHT condition was ranging between 11-13 ml.

Lakatos et al. (2010) studied effect of using water-based drilling fluids for tight gas reservoirs. They investigated that because of small pore structure and water-wetness of unconventional gas reservoirs, very high capillary forces dominate the flow and this

resulted in water blockage problem, if water-based drilling fluid is used. Consequently, it causes serious formation damage. They recommended to use non-ionic surfactants, like ethoxylated alkyl phenols with different ethoxy number for lowering surface tension and altering wettability i.e. from strongly water-wet to intermediate or oil-wet. They also suggested to use organic or oil-based muds for drilling wells to tight gas reservoirs.

McDonald (2012) offered new high ratio potassium silicate water-based drilling fluid formula for shale gas and tar sand reservoirs. The new ratio was ranging between 4 and 12. He determined that high ratio potassium silicate is chemically more reactive and can easily enter to polymerization and precipitation reactions, since it is believed to be the mechanism of shale stabilization. His investigations showed that the new formula increases the effectiveness of shale hydration prevention and wellbore stabilization such as micro fractures seal. This new formula gave also good results in tar sand reservoirs for SAGD operation, which it prevented expansion of bitumen as well as providing shale stabilization.

Young & Friedheim (2013) studied the effect of water-based drilling fluid with 3% wt. nano sized silica solution for Mancos shale and Texas shale gas core samples. They researched that 3% wt. nanosilica particles successfully plug small pores of shale formations. The permeability of Mancos and Texas gas shale samples decreased to 98% and 100%, respectively. The experiments showed that very small amount of water could invade into the pores, which is negligible. The reported filtrate volume at 200°F/500 psi was 8.8 ml.

Yadav et al. (2015) formulated water-based drilling fluid for shale gas reservoir in Saudi Arabia to drill horizontal, deviated and extended-reach wells for maximizing recovery.

They reported that drilling fluid with nano-based polyacrylamide + polyamine derivative prevents shale hydration and swelling better than KCl polymer based drilling fluid, where the difference is about 5%. KCl polymer based mud showed also poor results in fluid loss compared than nano-based drilling fluid, where nano-based mud gave 15 ml filtrate volume. It is dispersed to micronized particles and provided enhanced wellbore stability. Their study also showed that the formula with high temperature lubricant and ROP enhancer reduces lubricity coefficient significantly than other formulated fluids such as OBM and WBM with ester-based lubricant.

2.3 Drill-in Fluids for Conventional Reservoirs

Conners & Bruton (1979) used clear brine completion fluids – calcium chloride/calcium bromide ($CaCl_2/CaBr_2$) with densities 13.5 to 13.6 lb/gal as a drill-in fluid for the wells drilled into the Cal Canal field in California, USA. Initially, barite weighted WBM has been used, which later resulted in very high skin damage (+74.3) because of pore plugging of barite particles. Consequently, it was decided to prepare a fluid with no solid and not damaging additives. Calcium chloride/calcium bromide was selected containing viscosifiers and fluid loss control agents. It was considered as Newtonian, because hole cleaning was a function of velocity, not viscosity. Because of this reason, density of the brine remained constant. However, fluid loss of brine became 25% in total, which was higher than barite weighted WBM. Production remained the same. The authors also reported that its initial cost is high, but with the comprehensive drilling planning, it can be reduced substantially.

Fraser et al. (1999) studied the performances of polymer/sized KCl, polymer/sized carbonate and bentonite/mixed metal hydroxide (MMH)/sized carbonate drill-in fluids for Ketton limestone, Clashach and Birchover sandstone core samples. Dynamic filtration results showed that bentonite/MMH rapidly forms a cake. Fluid loss data showed that with barite-weighted bentonite/MMH was lower than polymer/sized KCl, which measured for Ketton and Clashach core samples under static and dynamic conditions. The recorded volumes was 6, 2.2, 1.6 ml with bentonite/MMH, polymer/sized carbonate and polymer sized KCl, respectively, under API conditions. The authors also investigated that polymer/sized KCl caused more damage to the rock samples than carbonated-weighted fluids.

Dobson et al. (2000) formulated silica (SiO_2)/polymer calcium bromide ($CaBr_2$) brine drill-in fluid with 13.2 lb/gal density to drill geopressured horizontal wells at 185°F bottom hole temperature in the Gulf of Mexico. The fluid loss was ranging between 32-55 ml. The authors reported that formic acid (HCOOH) was used to remove the filter cake and return permeability was more than 90%. They also mentioned that this novel drill-in fluid system provided good lubricity and shale stabilization and density without adding weighting agent.

Cobianco et al. (2001) designed a statistical experiment under dynamic conditions for scleroglucan and xanthan gum/$CaCO_3$ drill-in fluids to study many variables at 200°F with STATISTICA v. 5.0 software package. The study included viscosity inducing polymers, the bridging particle concentration, the fluid density and the rock permeability. They determined that filter cake permeability and filtrate volume is influenced by scleroglucan concentration. Increasing its concentration decreases cake permeability and filtrate volume. They also determined that the concentration of cross-linked starch also influences

filtration properties. Simultaneous increasing the concentration of both scleroglucan and cross-linked starch decreases permeability and filtrate volume. However, xanthan gum has reverse effect, as it increases cake permeability and filtrate volume. The authors found that density has the same effect on both fluid types, as filtration properties increase with higher density values. The typical spurt loss was 14 ml for polymer/$CaCO_3$. Their statistical analysis also showed that bridging agent concentration, ranging between 5% and 20%, of $CaCO_3$ doesn't have effect on filtration properties. Therefore, for minimizing possible problems that occurs by solid particles, it is recommended to use minimum amount (5%) of calcium carbonate. The authors also studied return permeability values for both drill-in fluids. Formation damage test results showed that scleroglucan/$CaCO_3$ gives 100% return permeability, while xanthan gum/$CaCO_3$ gives only 75% at 200°F.

Nasr-El-Din et al. (2002) studied the efficiency of solvents – ethylene glycol monobutylether (EGMBE) and 15 vol% blend of glycol ethers (E-2) for removing water blockage problem by decreasing surface tension of water droplets in tight oil carbonate reservoir of the Ghawar field area in Saudi Arabia. The reservoir temperature was 200-220°F. They reported that increasing the concentration of both solvents beyond 10% doesn't have any significant effect on lowering surface tension. E-2 at 100% concentration causes significant damage with 60% permeability loss for the high permeability core and 84 permeability loss for the low permeability core. This is because of salt and emulsion precipitation by E-2 solvent. The authors also investigated that both solvent treatments give almost the same permeability recoveries for the low permeability cores – 84.9% and 83.5% by E-2 and EGMBE, respectively. Similar results also obtained for the high permeability cores such as 92.7% and 87.4% by E-2 and EGMBE, respectively.

Sanchez et al. (2004) observed the performance of scleroglucan and xanthan polymers separately for three drill-in fluid formulas with different additive concentrations and made the comparisons among them. Clashach sandstone cores used for the experiments. Since the polymer doesn't behave as stable at about 120℃ temperature, the authors proposed to use scleroglucan as an alternative to xanthan gum in the drill-in fluid formula. They prepared the optimized scleroglucan drill-in fluid for high temperature/high permeability reservoirs, because it was already proposed for low permeability reservoirs. Static filtration experiments demonstrated that lowest filtrate volume and mud cake permeability are obtained by scleroglucan polymer. Dynamic filtration experiments on core samples showed that the invasion rate of scleroglucan-based drill-in fluid is half of the xanthan-based one at 250°F temperature. The obtained minimum filtrate volume was 8.2 ml with scleroglucan-based drill-in fluid at 80℃ temperature under 35 bar pressure.

Al-Yami et al. (2010) studied the behavior of the three – $KCl/BaSO_4/CaCO_3$, $KCOOH/CaCO_3$ and Mn_3O_4 water-based drill-in fluids for Unayzah sandstone formation in Saudi Arabia, where shale stabilization is one of the main problems in this reservoir. It requires about 95 lbm/ft^3 drilling fluid density. Their experiments showed that all the three fluid types damage the core samples. However, the highest damage level occurred by $KCl/BaSO_4/CaCO_3$. $KCOOH/CaCO_3$ and Mn_3O_4 water-based drill-in fluids followed it. Although, the highest return permeability obtained by Mn_3O_4 water-based fluid with 66%, but fluid loss was also higher than other drill-in fluids, which was ranging between 9-13 ml under dynamic and static conditions.

Huang et al. (2011) introduced a new surfactant micellar-based polymer and solid free drill-in fluid with 10 wt% organic acid (OA) + 2 vol% surfactant + 0.2 vol% internal

breaker base composition for carbonate reservoirs. They explained that as surfactant micellar fluids have a strong shear-thinning viscosity property, very high viscosity can be achieved with low shear rate, which is desirable. The authors reported that this drill-in fluid without internal breaker achieves the high viscosity – 100000 cp with almost zero shear rate, which reduces fluid loss and carries drill cuttings to the surface. The reported filtrate volume was around 325 ml at 150°F under 100 psi pressure. After drilling the targeted formation, internal breaker is added to the fluid and it decreases fluid viscosity significantly, where the acid reacts with $CaCO_3$ and PH decreases. Reduced viscosity forces fluid to flow back and consequently, make a very low formation damage.

2.4 Drill-in Fluids for Unconventional Reservoirs

Zabala et al. (1999) prepared drill-in fluid, which is called Stable Mul System, for heavy oil – Bare, Melones and Arecuna fields in Venezuela. Basic components of Stable Mul System were any type of oil i.e. mineral, vegetal, diesel, polyalphaolefins etc. and surfactant Stable Mul - stabilizers and emulsifiers. They used this drill-in fluid for more than 100 wells, including vertical, horizontal and multilateral wells. Since the oil was heavy, ranging between 8 and 12 API, the reservoir pressure was very low. On the other hand, since, the wells drilled 5500 ft deeper, the temperature increases by going deeper as well. As a result, both of these conditions should be considered, when drill-in fluid is formulated. Stable Mul System provided 7.4 ppg density as free from solid and showed stable temperature up to 300°F. They reported that this drill-in mud demonstrated no formation damage, which the maximum filtrate volume became 5 ml and return

permeability was 89%. The authors also did comparisons with those wells that where drilled with WBM and OBM and reported that the production rate of wells, drilled with Stable Mul, increased about 30%.

Siddiqui & Nasr-El-Din (2005) investigated the effectiveness of various cleaning fluids, such as acidic brines, non-ionic surfactant, mutual solvent – ethyleneglycol monobutylether, specific enzymes and combination of them, in removing the filter cake made by water-based drill-in fluids. They did the experiments for seven core samples that have been taken from the horizontal wells drilled in Unayzah B tight gas reservoir in Saudi Arabia. The reported filtrate volume at 280°F was 18 ml. The authors determined the return permeability values for each core sample with different washing scenarios. They observed that washing core samples alone with neither acidic brines, nor surfactant, nor mutual solvent and nor enzymes gives good results and combination of them should be applied for better performance. Final observations showed that using 7 wt% KCl brine that contains surfactant and mutual solvent minimizes water blockage. Specific enzymes treatment was applied after cleaning with 15 wt% HCl brine and the combination gave 61% return permeability, which it is 20% higher than washing with only acid. Since formation damage could not be removed completely, authors recommended also performing organic acid treatment before or after enzyme treatment, because enzymes cannot remove calcium carbonate particles.

Van Zanten et al. (2011) studied the effect of surfactant treatments after using water or brine-based drill-in fluids for altering wettability and elimination of emulsion blockage in tight oil and water blockage in tight gas formations. Core sample for tight oil has been taken from carbonate formation of North America and for tight gas from Crab Orchard

sandstone formation. They used surfactant packages – MS1, MS2, S1, SS1, SS2, SS3, FS1 and FS2 as an additive. The authors observed that two Windsor IV microemulsion forming surfactant packages – MS1 and MS2 are the most effective ones for gaining higher return permeability values. Especially, MS1 treatment showed highest results with 103% and 100% regain permeability values for tight oil and tight gas cores, respectively. They also reported that two common damage types that were caused by lubricant and corrosion inhibitor additives also decreased by using surfactant additives.

El Bialy et al. (2011) designed a drill-in fluid with potassium formate (KCOOH) brine and manganese tetra oxide (Mn_3O_4) weighting agent to provide 114 lb/ft^3 density. It was used for drilling a vertical appraisal well to Unayzah A and B sandstone tight gas reservoirs in Saudi Arabia. They reported that using manganese tetra oxide as a weighting agent allowed density increase compared than calcium carbonate ($CaCO_3$). On the other hand, friction and drag reduced due to reduced particle size and spherical shape of manganese tetra oxide. As a result, it improved equivalent circulating density (ECD) and plastic viscosity control. The authors mentioned that since manganese tetra oxide is acid and enzyme soluble, they got very high – about 99.3% return permeability (k_i = 0.0606 mD, k_f = 0.0602 mD) with less than 14 ml filtrate volume. It was also reported that the formulated drill-in fluid showed very high stability at the bottom hole temperatures exceeding 155°C.

Han et al. (2012) formulated sodium chloride **(**NaCl) brine-based drill-in fluid with 3.5% potassium chloride (KCl) and 3% glycol additives to drill 4 horizontal wells to Peregrino heavy oil field in Brazil. The wells completed as an open-hole with sand screens and gravel packing. The oil density was 13 API. To make comparisons, the authors designed three WBMs – with NaCl/KCl, NaCOOH and $CaCl_2$ and two OBMs – with barite-weighted

OBM and brine-weighted Low Solid OBM. Based on their observations, they determined that 3.5% potassium chloride (KCl) and 3% glycol additives are ideal for inhibition of moderately reactive shales, which is present in Peregrino filed. The experiments showed that return permeability is almost the same for each of the five formulas. They used mineral oil as a washing fluid and got permeability vales for NaCl/KCl WBM and LS OBM between 68% and 76% with 6.8-7.2 and 1.9-2.9 ml fluid losses, respectively. The authors indicated that formation damage is low and NaCl/KCl formula can be accepted as non-damaging according to the industry standards, where its return permeability is higher than 60%.

CHAPTER 3

PROBLEM STATEMENT AND RESEARCH OBJECTIVES

Having reviewed the previous research and studies, it can be concluded that previous studies mainly focused on elimination of water blockage problem of tight gas formations induced by water-based drill-in fluids during drilling process rather than to prevent it from the commencement of drilling. Based on this observation, our study focuses on investigating the performance of sodium silicate (Na_2SiO_3) in the formulated non-damaging drilling fluid. The main objective is to determine the optimum sodium silicate concentration that will minimize fluid invasion, prevent water blockage and reduce solid invasion problems of the wells drilled into tight gas formation.

The specific objectives of this research are as follows:

- ✓ Formulating a proper non-damaging barite-weighted water-based drilling fluid and determining the optimum sodium silicate concentration
- ✓ Evaluating the effect of sodium silicate on the rheological properties of the formulated drill-in fluid
- ✓ Evaluating the effect of sodium silicate on the barite solubility
- ✓ Improving well productivity by obtaining the high return permeability after forming the very thin, impermeable and easily removable filter cake

- ✓ Assessing the effect of optimum concentration of sodium silicate on the sag performance of the formulated drill-in fluid.

CHAPTER 4

METHODOLOGY AND EXPERIMENTAL APPARATUS

4.1 Work Plan

The diagram in **Fig. 4-1** schematically illustrates the work plan.

4.1.1 Core Samples Preparation

The obtained core block is belong to Scioto tight sandstone formation. The samples have been plugged from the block with 2.5" diameter bit and cut in 0.25" and 2" lengths. Typical core samples with aforementioned specifications are shown in **Fig. 4-2**. After that they have been vacuumed for 6 h, then 100% saturated in 3 wt% potassium chloride (KCl) brine under 2000 psi pressure for 24 h with Saturator as shown in **Fig. 4-3**. It should be noted that since the core samples are sandstone, they were saturated with 3 wt% KCl brine. The reason is pores of sandstone cores have clay inside them. Saturating with water leads to loosening of clay particles, which is undesirable. Loosening of clay particles may result in change in permeability and pore structure from original condition. Because of it, sandstone cores should only be saturated with KCl brine.

4.1.2 Density and PH Measurements

The density and PH of the drill-in fluid have been measured with Mud Balance and OAKTON pH 2700, respectively, as shown in **Figs. 4-4** and **4-5**. The measurements have

been carried for the base fluid and for 0.05, 0.075, 0.1, 0.5, 1, 1.5 and 2 wt% sodium silicate concentrations in the base fluid.

4.1.3 Rheology Test

4.1.3.1 Plastic Viscosity and Yield Point Measurements

Plastic Viscosity (PV) and Yield Point (YP) have been measured at room temperature, 100°F, 140°F and 170°F under atmospheric pressure with Grace M3600 Rheometer as shown in **Fig. 4-7** and at 300°F under 300 psi pressure with Chandler 7550 HPHT Viscometer shown in **Fig. 4-8**.

$$PV = \Phi_{600} - \Phi_{300}$$

$$YP = \Phi_{300} - PV$$

where PV – plastic viscosity, cp; YP – yield point, lb/100ft^2; Φ_{600} and Φ_{300} – torque readings at 600 and 300 RPM, respectively, RPM.

4.1.3.1.1 Measuring by Grace M3600 Rheometer

The prepared fluid sample was put into the stainless steel sample cup by raising till the scribed line of a rotor. The rotor produces torque on the bob. The machine has two operational modes: standalone and PC integrated. It has been operated through PC by using *M3600DAQ*™ software. Since this equipment can only be operated under atmospheric pressure, maximum temperature cannot exceed 200°F. The sequence below was followed to perform the tests:

- Prepared the base drill-in fluid and with the added 0.05, 0.075, 0.1, 0.5, 1, 1.5 and 2

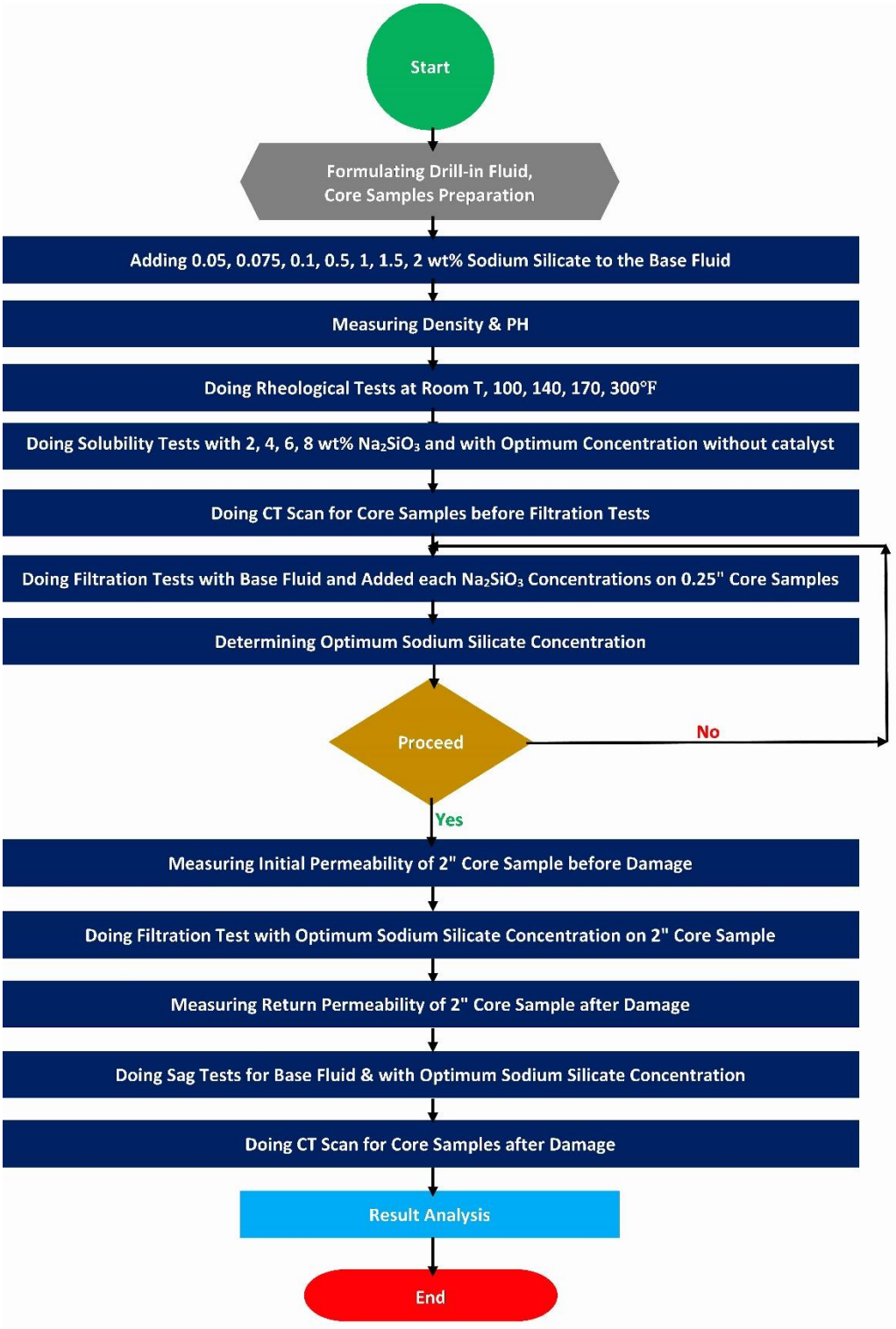

Figure 4-1. Schematic Workflow Diagram

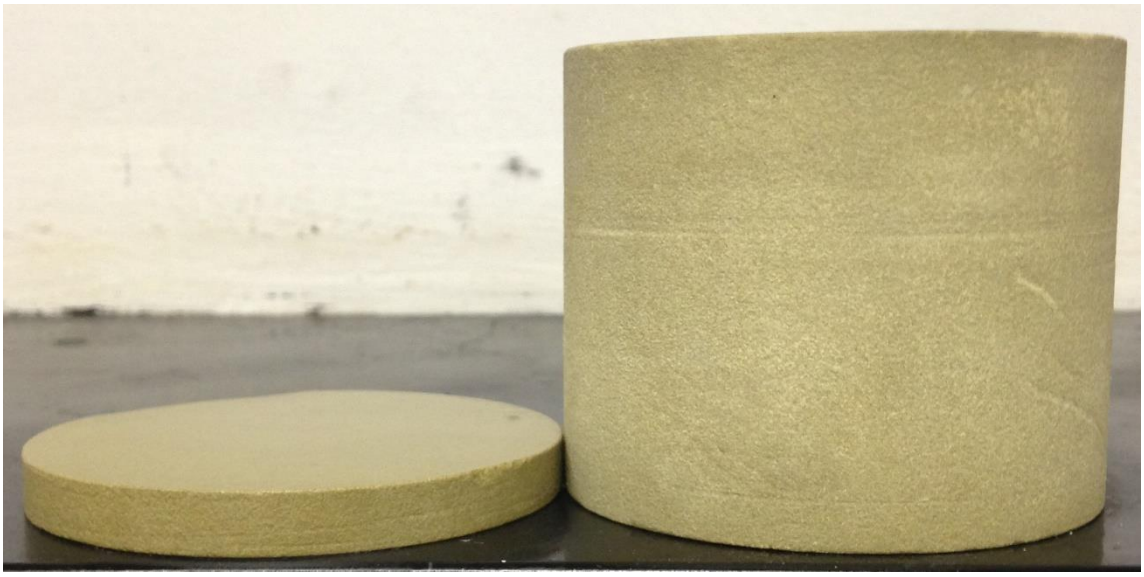

Figure 4-2. Typical 0.25” and 2” Scioto Tight Sandstone Core Samples After 100% Saturation with Brine

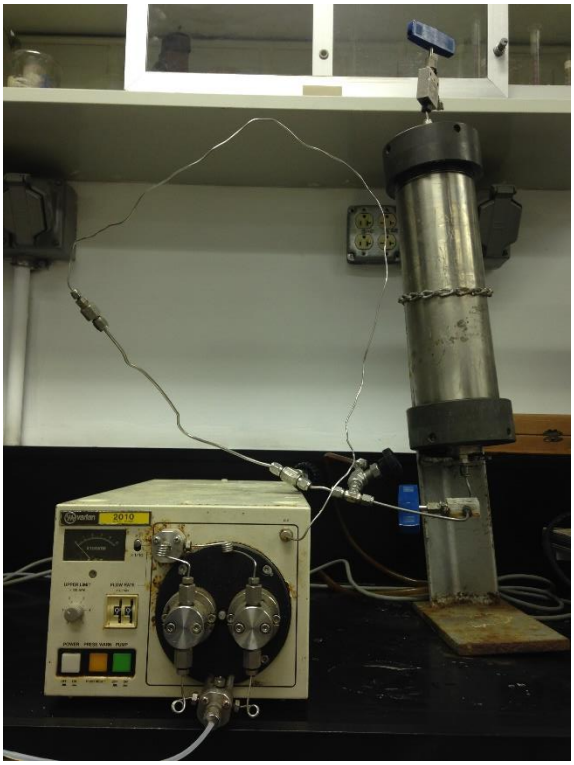

Figure 4-3. Saturator

Figure 4-4. Digital Weight Balance

Figure 4-5. Mud Balance

Figure 4-6. OAKTON pH 2700

wt% sodium silicate concentrations

- Filled the sample cup with 150 ml and raised it up to scribed line
- Determined the correct test sequence for each temperature from the setup of *M3600DAQ*™ software and done the tests at room temperature, 100°F, 140°F and 170°F
- Started to the real time test by using aforementioned software
- Got the results in Excel sheet at the end of the test
- Performed the tests for all the base fluid and with the added sodium silicate concentrations
- Turned off the machine after finishing the test
- Cleaned the bob and sample cup.

4.1.3.1.2 Measuring by Chandler 7550 HPHT Viscometer

The equipment has been operated through PC by using *Rheo 7500* software. 300 psi

pressure was applied so that to prevent evaporation at 300°F. The sequence below was followed to perform the tests:

Figure 4-7. Grace M3600 Rheometer

Figure 4-8. Chandler 7550 HPHT Viscometer

- Prepared the base drill-in fluid and with the added 0.05, 0.075, 0.1, 0.5, 1, 1.5 and 2 wt% sodium silicate concentrations
- Filled the sample cup with 110 ml fluid sample
- Turned on heater and set the temperature as 300°F
- Turned of pressure pump and applied 300 psi to prevent evaporation
- Started *Rheo 7500* software and chose the appropriate schedule to perform the real time test
- Turned off the heater and pressure pump
- Once the equipment cooled down, disassembled the parts for cleaning
- Performed the tests for all the base fluid and with the added sodium silicate concentrations

4.1.3.2 Gel Strength Measurements

Gel strength values both for 10-second and 10-minute have also been obtained at room temperature, 100°F, 140°F and 170°F under atmospheric pressure by using Grace M3600 Rheometer and at 300°F under 300 psi pressure with Chandler 7550 HPHT Viscometer. All the steps have already been explained in the section 4.1.2.1 and the gel strength values were also obtained by the similar way.

4.1.4 Solubility Test

A number of solubility tests have been performed to check the effect of sodium silicate on barite ($BaSO_4$) solubility based on the single stage barite filter cake removal method of Ba geri et al. (2015). The tests have been done with the magnetic stirrers as shown in **Fig. 4-**

9. By following the standards, the experiments have been conducted with 350 RPM stirring rate and at 200°F temperature for 24 h using condensers to make sure that there is no evaporation. 50 ml solution, including 20 wt% chelating agent – potassium-based diethylene triamine penta acetic acid (DTPA), 6 wt% catalyst – potassium formate (KCOOH) and 7 wt% enzyme, was prepared for mixing with 2 g barite. By doing sieve analysis, 75 μm-sized barite has been used in the experiments. After that 2, 4, 6 and 8 wt% sodium silicate concentrations have been added to the prepared solutions. Additionally, after finding the optimum sodium silicate concentration, the experiment has been repeated without catalyst as well. After 24 h, the solutions have been filtered with 2 μm filter paper by using vacuum machine. Before filtering, the weight of filter paper has been measured. After filtering,

Figure 4-9. Magnetic Stirrer

filter paper with the remained barite has been put into the oven to dry at 300°F for 1h. After drying, the weight of remained barite and filter paper have been measured together. By extracting before and after weights, the weight of remained barite has been recorded. Dissolved weight of barite has been calculated by extracting initial (2g) and remained barite weight. The solubility was measured by dividing dissolved and initial weight of barite:

$$Solubility\ \% = \frac{Dissolved\ Weight\ of\ Barite}{Initial\ Weight\ of\ Barite}\ x\ 100\%$$

Below sequence was followed to perform the tests:

- Prepared the solution – 20 wt% potassium-based DTPA, 6 wt% potassium formate and 7 wt% enzyme to mix with 2 g 75 μm-sized barite
- Added 2, 4, 6 and 8 wt% sodium silicate to the solution
- Put the solution on the magnetic stirrer with 350 RPM stirring rate and at 200°F temperature for 24 h
- Measured the weight of 2 μm filter paper
- Filtered the solution on the filter paper by using vacuum machine
- Put the filter paper with the remained barite into the oven to dry at 300°F for 1 h
- Measured the weight of filter paper and remained barite after drying
- Extracted the weight of filter paper + remained barite and the weight of filter paper to find the remained weight of barite
- Extracted the initial and remained weights of barite to find the dissolved weight of barite
- The solubility has been determined by dividing dissolved and initial weight of barite

- Above steps have been repeated by the same way for each sodium silicate concentrations
- Prepared the solution without catalyst (potassium carbonate) with the optimum sodium silicate concentration and repeated above steps to get the solubility.

4.1.5 Static Filtration Test

4.1.5.1 Collecting Filtrate Volume and Measuring Filter Cake Thickness

Importance of filtration process has already been mentioned under Drilling Fluid Properties section in the Chapter I. Since dynamic filtration test is time-consuming, usually static filtration test is performed. The static filtration experiments have been performed by the Modified Fann HPHT Filter Press shown in **Fig. 4-10**. The setup has been installed in the PETE lab. By performing filtration test, filtrate volume and filter cake thickness were measured. Filtration characteristics of the drill-in fluid were observed based on these measurements. Below sequence was followed to perform the tests:

- Stirred the fluid sample for 10 minutes with high speed mixer
- Placed the 0.25" or 2" core sample into the cell by covering with Teflon. For 2" core sample, the spacer inside the cell has been modified
- Tightened the lower cell cap and filled the fluid sample by leaving an enough space for expansion
- Tightened the top cell cap and placed the cell into the heating jacket
- Turned on the equipment and increased temperature up to 300°F by adjusting through thermostat. Pilot light indicates the temperature on the heating jacket
- Opened pressure valve of nitrogen tank and applied 250 psi back pressure
- Put the thermometer in the cell and waited until increasing to 300°F temperature

- Put the glass cylinder under the filtrate line to collect the filtrate volume
- Applied 500 psi inlet pressure to make 250 psi delta pressure (ΔP) once the temperature reached to 300°F and filtration started automatically
- Recorded the volume from 10 second until 30 minutes
- After finishing the filtration, closed the top valve and main pressure source
- Bleed the pressure carefully by opening the pressure line that goes to main pressure source
- Removed the core sample from the cell
- Washed it with water gently and measured the filter cake thickness by using caliper

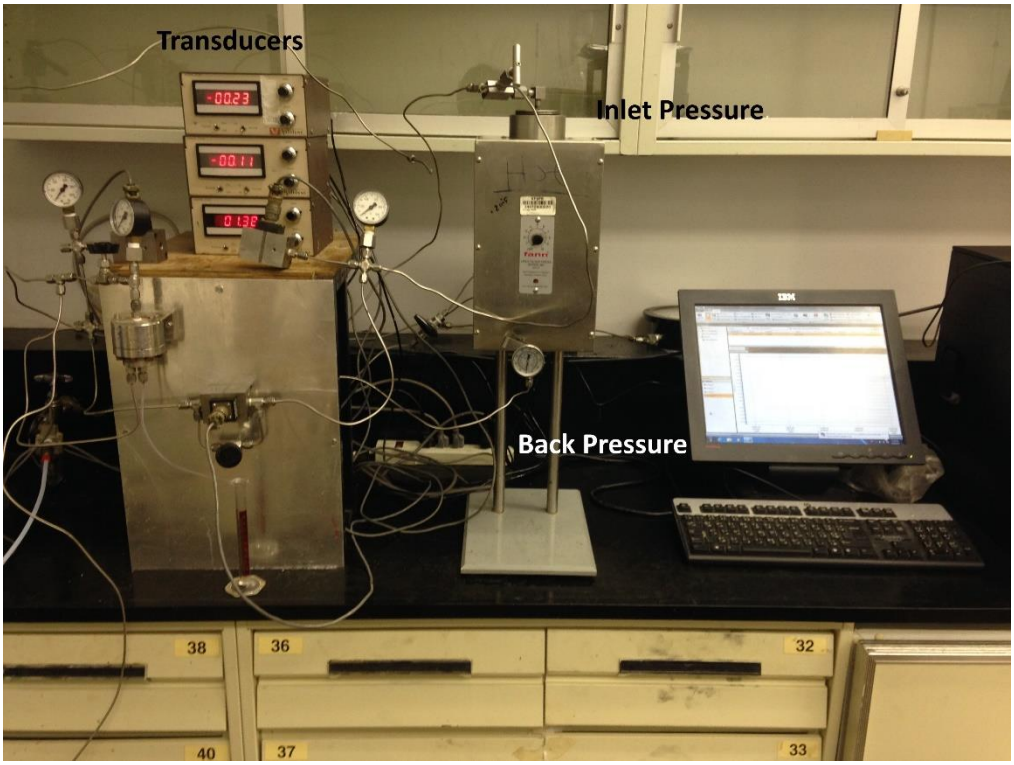

Figure 4-10. Modified Fann HPHT Filter Press while Doing Filtration Test

- Did the experiments for the base fluid and with added 0.05, 0.075, 0.1, 0.5, 1, 1.5 wt% sodium silicate concentrations

4.1.5.2 Measuring Initial and Return Permeabilities

To make a clear comparison, the initial and return permeability values have been calculated before and after damaging the core sample. Similar to filtration test, these measurements have also been carried with Modified Fann HPHT Filter Press, but with addition of Flow Rate Controller as shown in **Fig. 4-11**. 2" core sample was used for this reason. Below sequence was followed to perform the measurements:

- Measured brine viscosity
- Placed the 2" core sample into the cell by covering with Teflon
- Tightened the lower cell cap and filled with brine
- Tightened the top cell cap and placed the cell into the heating jacket (without heating)
- Filled the cell with brine that is connected to the flow rate controller so that to inject brine under constant flow rate inside the cell that the core sample placed
- Opened pressure valve of nitrogen tank and applied over 200 psi back pressure
- Turned on the flow rate controller for applying constant flow rate
- Put the cup to collect brine once the required pressure under constant flow rate passed the applied back pressure
- Started *Omega* software to read the voltage readings of transducers corresponding to each flow rate
- The recorded voltages converted to pressure values based on the calibration data in real time
- Recorded the stabilized delta pressure (ΔP) values corresponding to the flow rates (q)

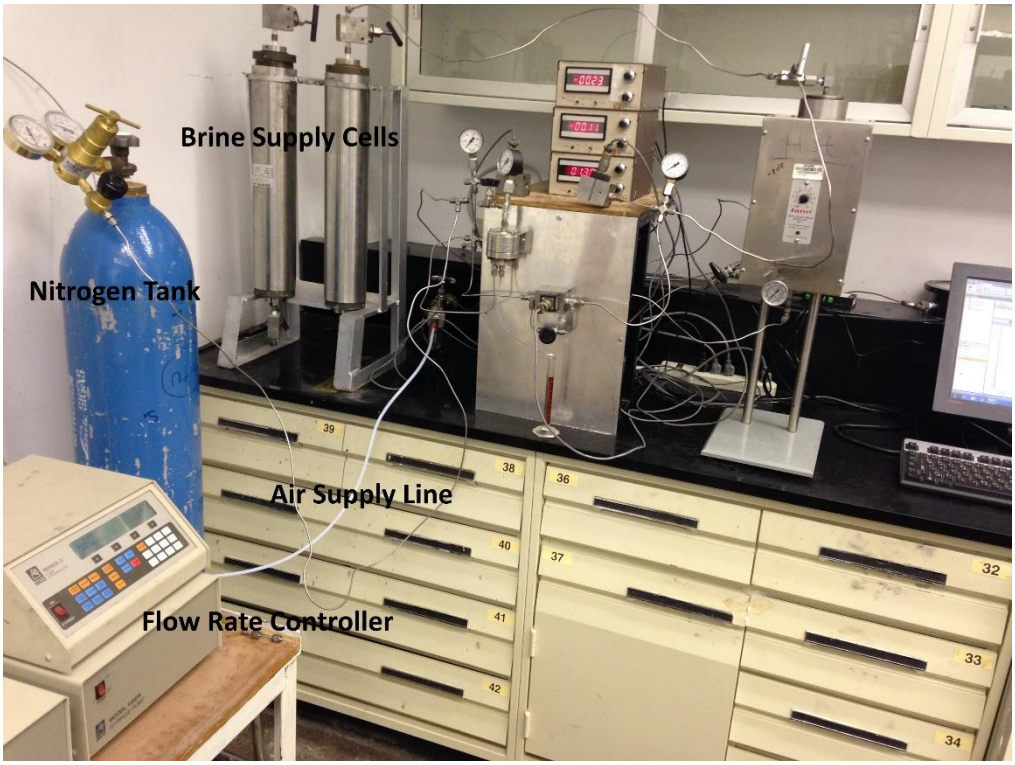

Figure 4-11. Modified Fann HPHT Filter Press with Flow Rate Controller while Measuring Permeability

- The same sequence repeated for 0.5, 1, 1,5 and 2 ml/min constant flow rates
- Plotted the ΔP values against corresponding to the q values in Excel sheet and obtained slope
- Obtained slope used in the below equation to calculate the initial and return permeability values:

$$k = \frac{m \cdot \mu \cdot l}{A} \qquad (2)$$

where, k – permeability, D; m – obtained slope from q vs. ΔP; μ – brine viscosity, cp; l – length of the core sample, cm; A – surface area of the core sample, cm^2.

The calculation of the return permeability is slightly different than the calculation of initial permeability. The return permeability is calculated after doing the filtration test or with

another word, after damaging the core sample. The formed filter cake was removed by any convenient tool, completely. For not to break the core sample, the removing of filter cake was done gently. Afterwards, non-filter cake formed or production side of the core sample was placed in the cell as an upper side. Rest of the procedures are applied same as the initial permeability calculation.

4.1.6 Stability Test

4.1.6.1 Static Sag Test

Static sag test is done mainly, when barite is used as a weighting material in the drilling fluid. It is because barite separates from the liquid and settles at the bottom. As a result, the density is fluctuating and it may cause problems during drilling process. Typical static sag test unit is shown in **Fig. 4-12**. First of all, the fluid has been stirred by a high speed fluid mixer for 10 minutes. Meantime, a Teflon was placed in the cell to reduce the amount of the used fluid sample. The cell with Teflon has been filled with the fluid and tightly closed with the screws. 300 psi pressure was applied to prevent from evaporation at 300°F and then put to the oven vertically for 24 hours. After 24 hours, the cell was taken carefully and cooled down without releasing the pressure. Once it was cooled, the pressure was released. Thereafter, using by syringe, the free fluid on the sample was removed from it in case of presence and two fluid samples were taken, one from top and one from bottom, respectively. Their densities were calculated and sag factor was determined by using below equation:

$$Sag\ Factor = \frac{\rho_{bottom}}{\rho_{bottom} + \rho_{top}} \qquad (3)$$

where ρ_{bottom} – density at the bottom, g/ml and ρ_{top} – density at the top, g/ml.

The sag factor for the fluid must be between 0.5 and 0.53 for having a sag good performance. Having the sag factor higher than 0.53 means, the fluid has a poor sag performance and most likely, the solid particles are going to settle.

4.1.7 Structural Analysis

4.1.7.1 Slice-by-slice Analysis and Computed Tomography (CT) Numbers of Core Samples

The core samples have been scanned before and after filtration test by Toshiba Computed Tomography (CT) Scanner as shown in **Fig. 4-13**. Being done CT Scan of the core samples provides a clear idea how fluid has invaded. CT Scan imaging has been done as slice-by-slice. 0.25" cores were divided to 6 slices, while 2" core was divided to 50 slices. By using *VoxelCalc* software, CT numbers were obtained for each slice. Based on these CT numbers, fluid invasion could be characterized and compared as before and after damage.

Figure 4-12. Static Sag Test Unit

Figure 4-13. Toshiba CT Scanner

4.1.7.2 Cross-sectional Analysis of Core Samples

By working with *PerGeos* software on the obtained CT scanning data of the core samples, the cross-sectional views were extracted and compared as before and after damage. These images allowed to observe how fluid has invaded as an addition to the slice-by-slice images.

4.2 Materials

The whole work was done on the actual drilling fluid formula that is currently used in one of the tight gas reservoirs in Middle East region. The list of the additives is given in **Table 4-1**. Some of the chemicals were excluded from the formula, due to their unavailability in our PETE lab stocks. These are:

- Resinex

- Drill Zone
- OES Liquid Gilsonite
- Lubricant CBR600
- Steelseal Fine & Super Fine
- Marble Medium Mi Sch
- Sureseal

In the table, the amount, primary function and mixing time of the additives are given, except mixing times of the excluded ones. On the other hand, instead of fresh water, distilled water has been used, even though the original formula includes fresh one.

Table 4-1. Details of the Additives in the Drill-in Fluid Formulation

Additives	Amount	Primary Function	Mixing Time
Distilled Water	241.5 ml	-	-
Soda Ash (Na_2CO_3)	0.5 g	Contaminant Remover	10 min
Defoamer	0.01 g	Defoamer	30 sec
Bentonite	5 g	Viscosifier	15 min
XC Polymer	1 g	Viscosifier	20 min
Caustic Soda (NaOH)	0.25 g	PH Adjustment	10 min
Sodium Sulphite (Na_2S)	0.3 g	Oxygen Scavenger	10 min
Sodium Chloride (NaCl)	22 g	Weighting Material	10 min
Starch	4 g	Fluid Loss Additive at Low Temperatures	20 min
$CaCO_3$ 25 & <38 mic.	3 + 3 g	Bridging Material	10 min
Barite	278 g	Weighting Material	20 min
Resinex	3 – 6 g	Fluid Loss Additive at High Temperatures	-
Drill Zone	2 – 3 %	ROP Enhancer	-
OES Liquid Gilsonite	3.34 g	Shale Stabilizer	-
Lubricant CBR600	3%	Lubricant	-
Steelseal Fine & Super Fine	2 + 2 g	Bridging Material	-
Marble Medium Mi Sch	10 g	Weighting Material	-
Sureseal	2 g	Bridging Material	-
Sodium Silicate (Na_2SiO_3)	0.05, 0.075, 0.1, 0.5, 1, 1.5, 2 wt%	Inhibitive Additive against Fluid Invasion	10 min

CHAPTER 5

RESULTS AND DISCUSSIONS

5.1 Density and PH Results

Table 5-1 summarizes all density and PH measurements.

Table 5-1. Summary of Density and PH Values

Na_2SiO_3 Concentration, wt%	PH	Density, lb/gal	Density, pcf
0	9.86	14.3	107
0.05	9.9	14.3	107
0.075	10	14.3	107
0.1	10.05	14.3	110
0.5	10.23	14.85	111
1	10.38	15	112
1.5	10.48	15.1	113
2	10.45	15.1	113

5.1.1 Effect of Sodium Silicate on Density

The experiments showed that adding sodium silicate to the base formula doesn't have any significant effect on density and stays almost constant as can be observed in **Fig. 5-1**. It ranges between 107-113 pcf, which these values are desirable. As tight gas is located in very deep formations, this density range is quite enough to drill wells up to that level.

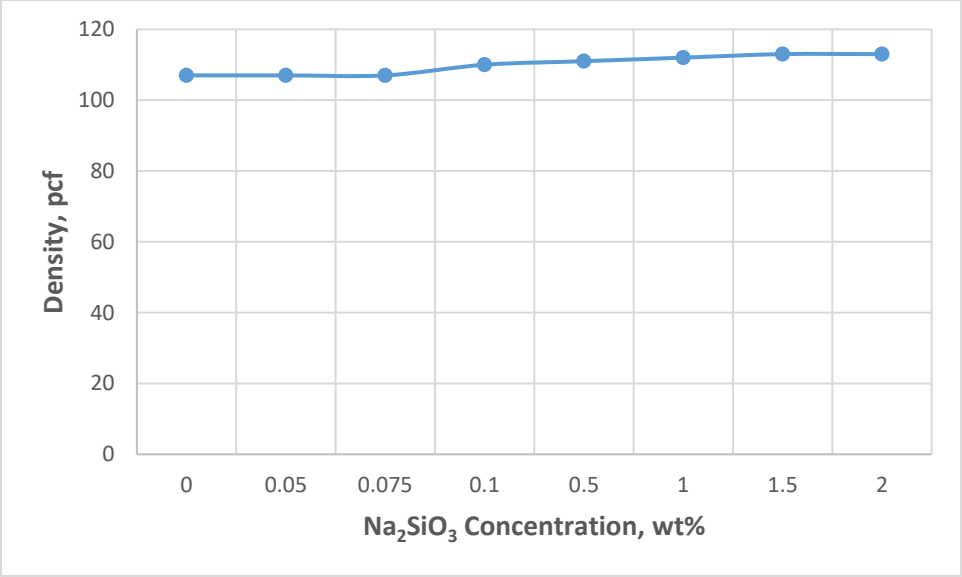

Figure 5-1. Effect of Na_2SiO_3 on Density

5.1.2 Effect of Sodium Silicate on PH

Like in density measurements, sodium silicate showed negligible effect on PH as well. It is clearly observed in **Fig. 5-2** that PH stays constant around 10. Having PH around 10 means corrosion rate is very low.

5.2 Rheology Results

As discussed in **Chapter 4**, the rheology tests up to 170°F have been performed under atmospheric and at 300°F under 300 psi pressure. In the beginning the plan for rheology tests was to observe 0.5, 1, 1.5 and 2 wt% sodium silicate concentrations. However, later on the plan was updated due to the filtration test results and made a decision to observe lower concentrations like 0.05, 0.075 and 0.1 wt% as well. On the other hand, high

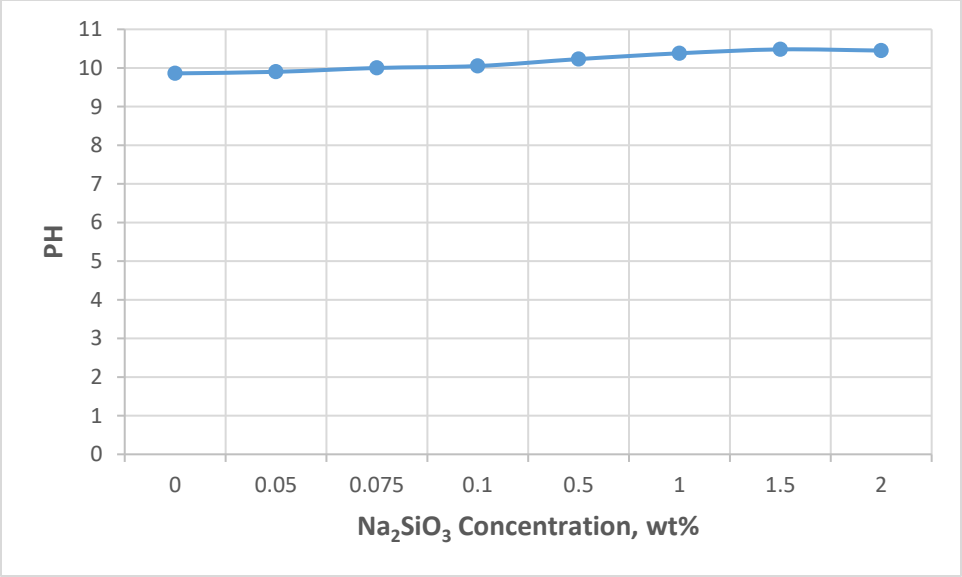

Figure 5-2. Effect of Na_2SiO_3 on PH

temperature rheology measurements were also done for only low concentrations up to 0.1 wt%. This will be discussed in the filtration results detailed.

5.2.1 Effect of Sodium Silicate on Rheological Properties at Room Temperature

Analyzing **Fig. 5-3** demonstrates that 0.05 wt% sodium silicate has almost same PV value with base fluid. However, adding more sodium silicate increases it, as it can be observed a big jump from 25 to 35 cp for 0.05 to 0.075 wt%, respectively. PV stabilizes for 0.1, 0.5 and 1 wt% around 30 cp, while it again increases to 35 cp with 1.5 and 2 wt%. These observations show that higher concentrations increase PV, while lower concentrations do not affect as higher ones, except 0.075 wt% at room temperature. This concentration's unique behavior will be discussed later.

Unlike PV relationship, YP jumps from 60 to over 80 lb/100ft^2 immediately after adding 0.05 wt% sodium silicate to base fluid as shown in **Fig. 5-4**. Then, we observe a slow decreasing till 0.5 wt%. After this concentration, sodium silicate doesn't show any effect in YP and stabilizes around 55 lb/100ft^2 at room temperature.

Fig. 5-5 shows that 10-second gel strength increases with added sodium silicate concentration up to 1 wt% and stabilizes around 35 lb/100ft^2. 10-minute gel strength also shows same trend and stabilizes around 45 lb/100ft^2. It should be noted that initial gel strength of 0.1 wt% slightly decreases, instead of following the trend. The reason is the sample temperature. Since the tests performed under atmospheric pressure with Grace M3600 Rheometer, the sample cup is open and room temperature directly affects the sample temperature. So, achieving the desired temperature is not easy. This leads to such errors sometimes. Otherwise, the trend could be upward for 0.1 wt% sodium silicate as well as other concentrations. Analyzing the torque readings at room temperature that are given in **Tables 5-2, 5-3, 5-4** and **5-5** clearly proves this explanation. **Table 5-5** summarizes all rheology test results for each sodium silicate concentration at room temperature.

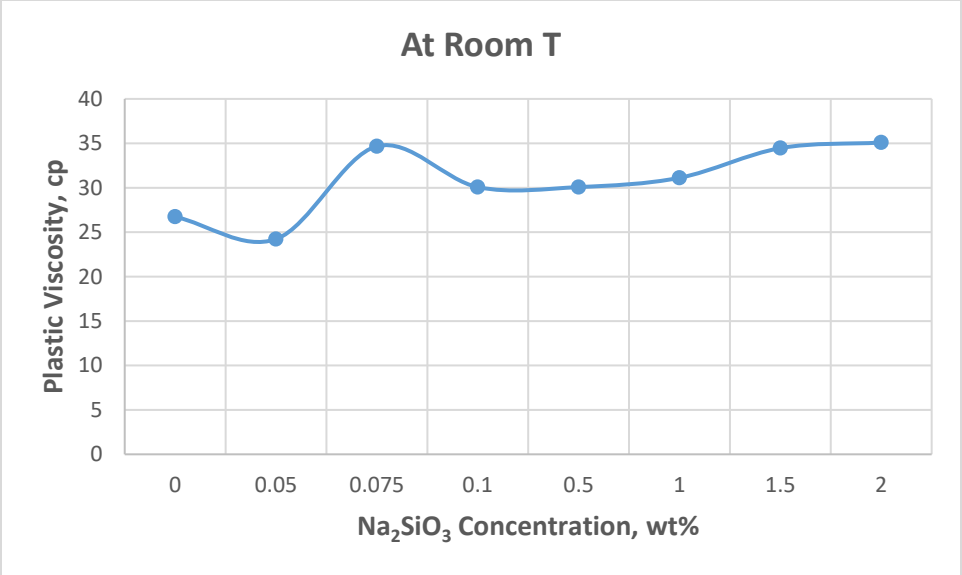

Figure 5-3. Effect of Na_2SiO_3 on PV at Room Temperature

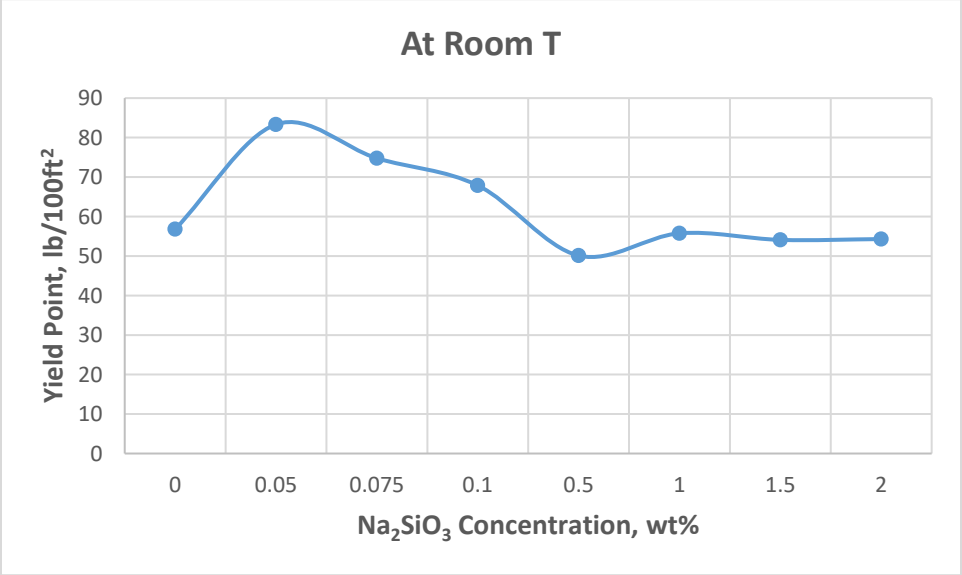

Figure 5-4. Effect of Na_2SiO_3 on YP at Room Temperature

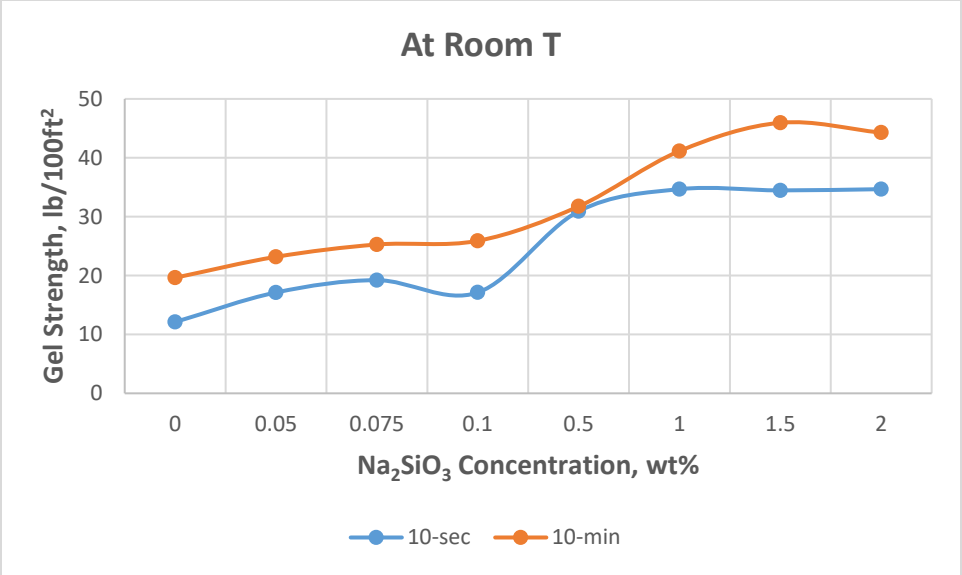

Figure 5-5. Effect of Na_2SiO_3 on Gel Strength at Room Temperature

Table 5-2. Torque Readings of Base Fluid and with 0.05 wt% Na_2SiO_3 at Room Temperature

Base Fluid				0.05 wt%			
T, °F	Speed, RPM	Shear Stress, lb/100ft²	Gel Strength, lb/100 ft²	T, °F	Speed, RPM	Shear Stress, lb/100ft²	Gel Strength, lb/100 ft²
80	600	110,3	111,9	77	600	131,8	132,6
80	300	83,5	110,5	77	300	107,6	132
80	200	65,2	83,5	77	200	87,3	107,8
79	100	45,3	65,4	77	100	60,6	85,8
79	60	35,5	45,3	76	60	46,4	59,3
79	30	26,5	35,5	76	30	34	45,5
79	6	14,6	26,3	76	6	19,6	34
79	3	11,9	18,2	76	3	16,9	23,6
79	600	109	109,4	76	600	130,5	131
79	0	0	109,4	76	0	111,9	136,8
78	3	11,9	12,1	76	3	16,9	17,1
78	300	83,5	83,8	76	300	47,8	77,5
76	0	0	83,8	74	0	0	103,6
76	3	13,8	19,6	74	3	18,2	23,2

Table 5-3. Torque Readings of Base Fluid with 0.075 and 0.1 wt% Na_2SiO_3 at Room Temperature

0.075 wt%				0.1 wt%			
T, °F	Speed, RPM	Shear Stress, lb/100ft^2	Gel Strength, lb/100 ft^2	T, °F	Speed, RPM	Shear Stress, lb/100ft^2	Gel Strength, lb/100 ft^2
81	600	144,1	144,7	79	600	128	128,4
81	300	109,4	144,5	79	300	98	128,4
81	200	89	109,6	79	200	79,8	98,2
81	100	62,4	87,5	78	100	56,6	78,9
81	60	48,2	61,2	79	60	44,1	55,8
81	30	36,3	47,8	78	30	33,2	43,7
81	6	21,9	36,3	79	6	19,8	33
81	3	18,6	26,1	79	3	17,3	24
82	600	134,5	134,9	78	600	123,2	123,6
82	0	111,8	141,8	78	0	102,8	126,1
82	3	19	19,2	78	3	17,1	17,1
82	300	54,3	85,8	78	300	48,4	76,2
82	0	0	107,6	77	0	0	97,1
82	3	20,5	25,3	77	3	19,4	25,9

Table 5-4. Torque Readings of Base Fluid with 0.5 and 1 wt% Na_2SiO_3 at Room Temperature

0.5 wt%				1 wt%			
T, °F	Speed, RPM	Shear Stress, lb/100ft^2	Gel Strength, lb/100 ft^2	T, °F	Speed, RPM	Shear Stress, lb/100ft^2	Gel Strength, lb/100 ft^2
82	600	110,2	110,7	81	600	118	118,6
81	300	80,2	110,7	80	300	86,9	118,6
80	200	67,7	78,7	80	200	73,1	85,4
80	100	53,9	68,1	80	100	58,7	73,3
80	60	47	53,9	80	60	51,4	58,9
79	30	40,9	46,8	80	30	44,3	51,4
79	6	32,6	40,7	80	6	37	44,3
79	3	30,5	34,7	81	3	35,7	38,2
79	600	110,9	111,1	80	600	117,6	117,6
79	0	91,1	111,3	80	0	92,9	117,6
79	3	30,7	30,9	80	3	34,5	34,7
79	300	53,3	72,5	80	300	57	76,2
76	0	0	82,3	79	0	0	87,7
76	3	15,5	31,7	79	3	19,2	41,1

Table 5-5. Torque Readings of Base Fluid with 1.5 and 2 wt% Na_2SiO_3 at Room Temperature

1.5 wt%				2 wt%			
T, °F	Speed, RPM	Shear Stress, lb/100ft²	Gel Strength, lb/100 ft²	T, °F	Speed, RPM	Shear Stress, lb/100ft²	Gel Strength, lb/100 ft²
81	600	123	123,2	81	600	124,5	124,7
81	300	88,6	122,8	81	300	89,4	124,3
81	200	75,6	88,3	81	200	76,4	89,6
81	100	59,9	76,2	81	100	59,5	76,7
81	60	52,2	59,9	81	60	51,1	59,5
81	30	44,5	52,4	82	30	43,4	51
81	6	36,3	44,3	82	6	35,7	43
81	3	36,1	37,4	82	3	35,5	36,8
81	600	122,4	122,6	81	600	123,4	124,7
81	0	97,1	122,6	81	0	101,3	123,4
81	3	34,5	34,5	81	3	34,5	34,7
81	300	60,4	80,6	81	300	58,7	78,9
80	0	0	89,4	81	0	0	89,6
80	3	23,4	45,9	81	3	21,1	44,3

Table 5-6. Summary of Rheological Properties of Na_2SiO_3 Concentrations at Room Temperature

Na_2SiO_3 Concentration, wt%	PV, cp	YP, lb/100ft²	10-sec, lb/100ft²	10-min, lb/100ft²
0	26,7	56,8	12,1	19,6
0,05	24,2	83,3	17,1	23,2
0,075	34,7	74,8	19,2	25,3
0,1	30,1	67,9	17,1	25,9
0,5	30,1	50,1	30,9	31,7
1	31,1	55,8	34,7	41,1
1,5	34,5	54,1	34,5	45,9
2	35,1	54,3	34,7	44,3

5.2.2 Effect of Sodium Silicate on Rheological Properties at 100°F

Analyzing **Figs. 5-6**, **5-7** and **5-8** show that PV, YP and gel strength values at 100°F follow the same trend like at room temperature. The main difference is YP values are decreasing only for low sodium silicate concentrations up to 0.1 wt%. However, it is observed that starting from 0.5 wt%, those values are keeping constant for the higher concentrations same as room temperature. Decreasing of PV and YP values at a bit high temperature is the first sign of deflocculation at the lower concentrations. Whilst both gel strength values are keeping constant at 100°F, as shown in **Fig. 5-8**, compared with the values at room temperature. **Table 5-11** summarizes all rheology test results for each sodium silicate concentration at 100°F.

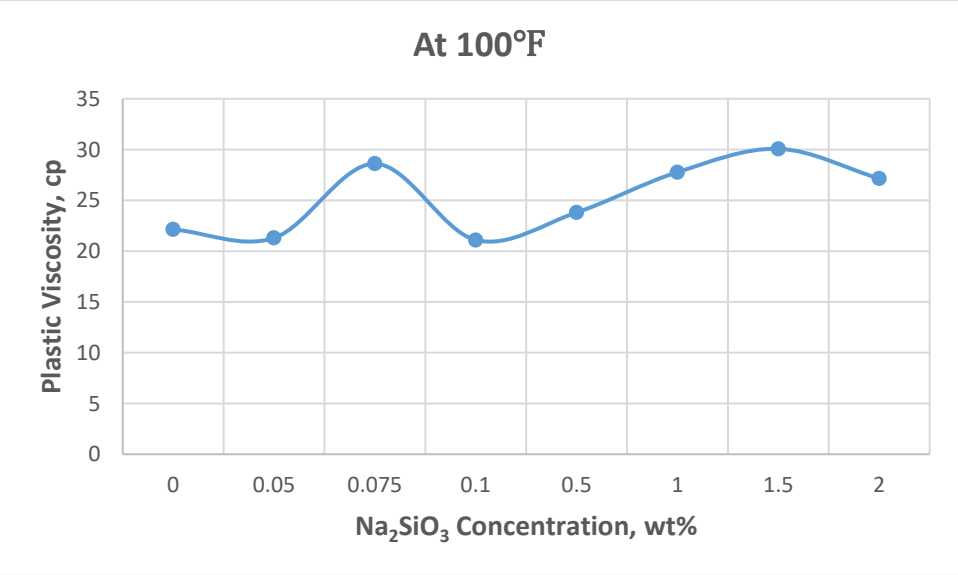

Figure 5-6. Effect of Na_2SiO_3 on PV at 100°F

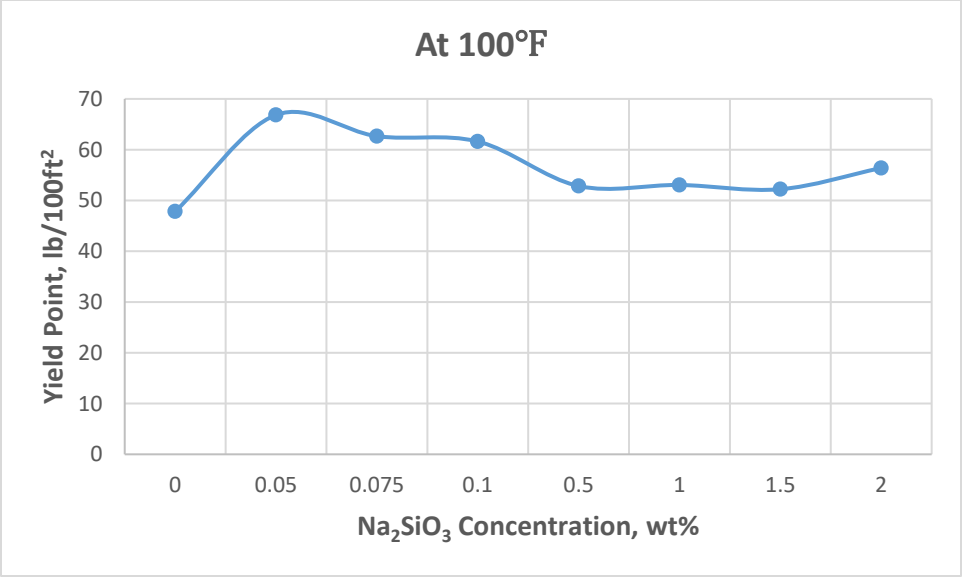

Figure 5-7. Effect of Na_2SiO_3 on YP at 100°F

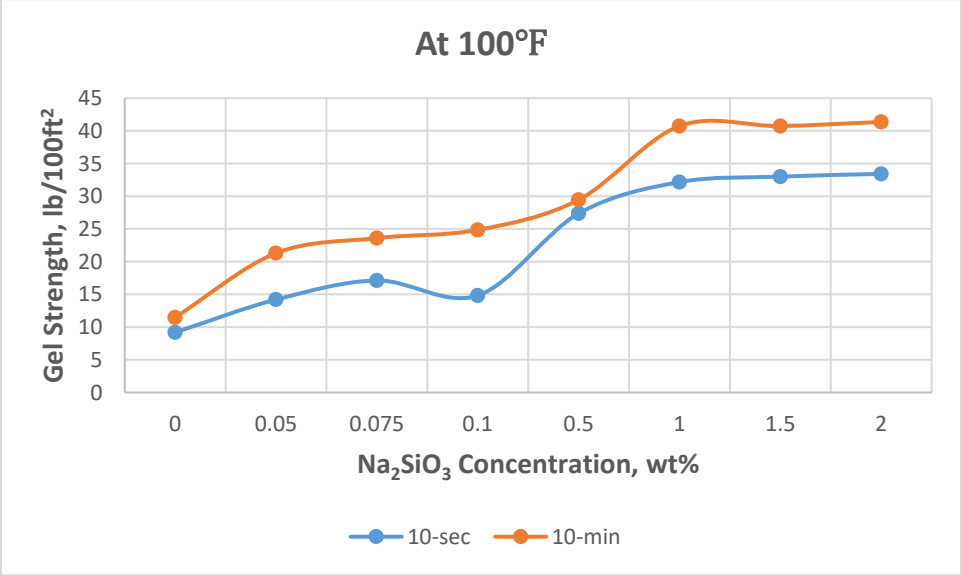

Figure 5-8. Effect of Na_2SiO_3 on Gel Strength at 100°F

Table 5-7. Torque Readings of Base Fluid and with 0.05 Na_2SiO_3 at 100°F

Base Fluid				0.05 wt%			
T, °F	Speed, RPM	Shear Stress, lb/100ft^2	Gel Strength, lb/100 ft^2	T, °F	Speed, RPM	Shear Stress, lb/100ft^2	Gel Strength, lb/100 ft^2
101	600	92,1	95,4	102	600	109,4	113,4
102	300	70	92,3	102	300	88,1	109,6
102	200	55,8	69,8	102	200	70,6	88,3
102	100	39,3	55,1	103	100	49,3	69,1
103	60	30,7	39,1	104	60	38,6	48,7
104	30	22,3	30,7	105	30	28,6	38,2
105	6	11,9	22,6	106	6	16,9	28,8
106	3	9,6	15,2	107	3	14	20,3
106	600	86,5	86,9	105	600	106,5	106,9
106	0	70,2	89,4	105	0	91,1	110,7
106	3	9,2	9,2	106	3	14,2	14,2
106	300	31,7	52,8	106	300	42	67,3
116	0	0	69,8	107	0	0	86,9
116	3	5,6	11,5	107	3	15,7	21,3

Table 5-8. Torque Readings of Base Fluid with 0.075 and 0.1 wt% Na_2SiO_3 at 100°F

0.075 wt%				0.1 wt%			
T, °F	Speed, RPM	Shear Stress, lb/100ft^2	Gel Strength, lb/100 ft^2	T, °F	Speed, RPM	Shear Stress, lb/100ft^2	Gel Strength, lb/100 ft^2
105	600	119,9	127,6	104	600	103,8	111,5
105	300	91,3	120,3	104	300	82,7	104,2
105	200	73,7	91,5	104	200	67	82,9
105	100	52,2	72,7	104	100	47,6	65,8
105	60	41,4	51,6	105	60	37,8	47,2
105	30	31,3	40,7	105	30	28,6	37,6
105	6	18,8	31,3	105	6	17,3	28,6
106	3	15,9	22,1	106	3	14,8	20,5
107	600	113	113,4	108	600	99,8	100,3
107	0	98,2	119	108	0	84	102,1
108	3	16,5	17,1	108	3	14,8	14,8
108	300	43,9	70,2	108	300	38,4	61
109	0	0	92,1	112	0	0,0	82,1
109	3	18	23,6	111	3	17,3	24,9

Table 5-9. Torque Readings of Base Fluid with 0.5 and 1 wt% Na_2SiO_3 at 100°F

0.5 wt%				1 wt%			
T, °F	Speed, RPM	Shear Stress, lb/100ft²	Gel Strength, lb/100 ft²	T, °F	Speed, RPM	Shear Stress, lb/100ft²	Gel Strength, lb/100 ft²
99	600	100,5	100,7	99	600	108,6	109
99	300	76,7	102,5	99	300	80,8	108,6
101	200	64,1	73,9	100	200	68,3	78,9
102	100	51,8	64,1	101	100	55,3	68,9
103	60	45,3	52	102	60	48,7	55,6
104	30	39,1	45,3	103	30	42,2	48,7
105	6	30,1	39,1	105	6	34	42,4
105	3	27,4	32,8	106	3	32,6	35,9
102	600	100,7	101,1	103	600	106,7	107,1
102	0	84	101,7	103	0	89,2	107,1
103	3	27,4	27,4	103	3	32,2	32,2
103	300	48,2	66,6	103	300	54,3	72,7
115	0	0	78,1	115	0	0	81,7
115	3	14,6	29,4	115	3	20,7	40,7

Table 5-10. Torque Readings of Base Fluid with 1.5 and 2 wt% Na_2SiO_3 at 100°F

1.5 wt%				2 wt%			
T, °F	Speed, RPM	Shear Stress, lb/100ft²	Gel Strength, lb/100 ft²	T, °F	Speed, RPM	Shear Stress, lb/100ft²	Gel Strength, lb/100 ft²
102	600	112,4	112,8	107	600	110,7	112,4
102	300	82,3	111,3	107	300	83,5	111,3
103	200	70,4	81,2	108	200	71,8	83,3
104	100	56,6	70,6	109	100	57,6	72,5
105	60	48,9	56,4	110	60	50,1	57,6
105	30	41,8	49,1	111	30	42,8	50,1
106	6	34	41,8	112	6	35,3	42,6
107	3	33	35,5	113	3	34,5	36,1
106	600	109,4	109,9	110	600	110,3	112,8
106	0	87,1	109	110	0	91,3	109,9
106	3	32,8	33	112	3	32,6	33,4
106	300	53,7	72,1	112	300	55,6	74,4
112	0	0	82,5	115	0	0,2	82,7
112	3	20,1	40,7	115	3	20,9	41,4

Table 5-11. Summary of Rheological Properties of Na_2SiO_3 Concentrations at 100°F

Na_2SiO_3 Concentration, wt%	PV, cp	YP, lb/100ft^2	10-sec, lb/100ft^2	10-min, lb/100ft^2
0	22,1	47,8	9,2	11,5
0,05	21,3	66,8	14,2	21,3
0,075	28,6	62,7	17,1	23,6
0,1	21,1	61,6	14,8	24,9
0,5	23,8	52,8	27,4	29,4
1	27,8	53	32,2	40,7
1,5	30,1	52,2	33	40,7
2	27,2	56,4	33,4	41,4

5.2.3 Effect of Sodium Silicate on Rheological Properties at 140°F

Similarly, the same trends are observed for PV, YP and gel strength values at 140°F in **Figs. 5-9**, **5-10** and **5-11**. PVs are decreasing for all concentrations, while YPs are decreasing only for low concentrations of sodium silicate. By the decrement of low concentrations, YP values at this temperature are keeping almost constant for all concentrations between around 50-55 lb/100ft^2. These results are also showing that deflocculation effect remains for low concentrations. When it comes to gel strength values, both 10-second and 10-minute are decreasing about 5 lb/100ft^2 compared with 100°F. Another observation is gel strength values at 140°F stabilize from 1.5 wt% compared to 1 wt% at lower temperatures, it was starting with 1 wt%. **Table 5-16** summarizes all rheology test results for each sodium silicate concentration at 140°F.

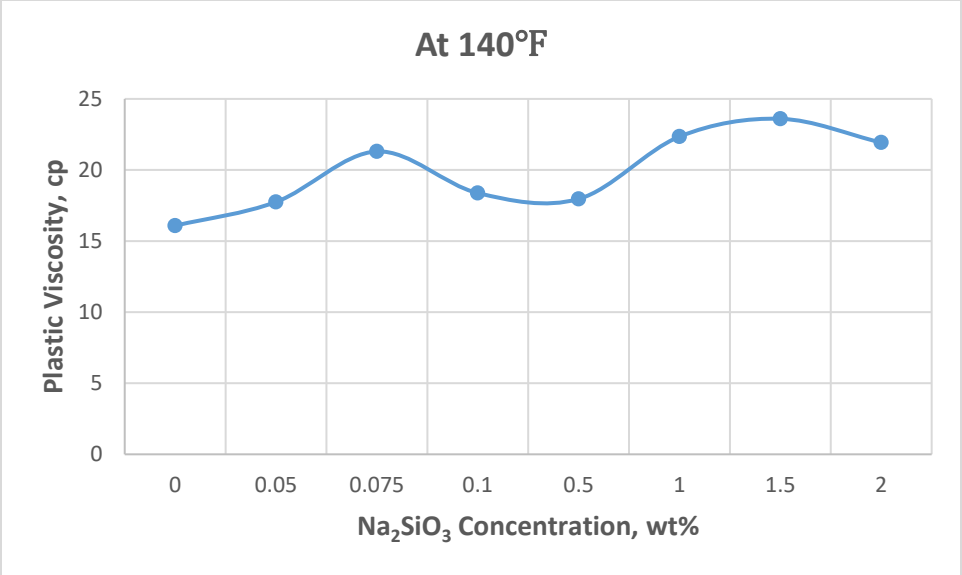

Figure 5-9. Effect of Na_2SiO_3 on PV at 140°F

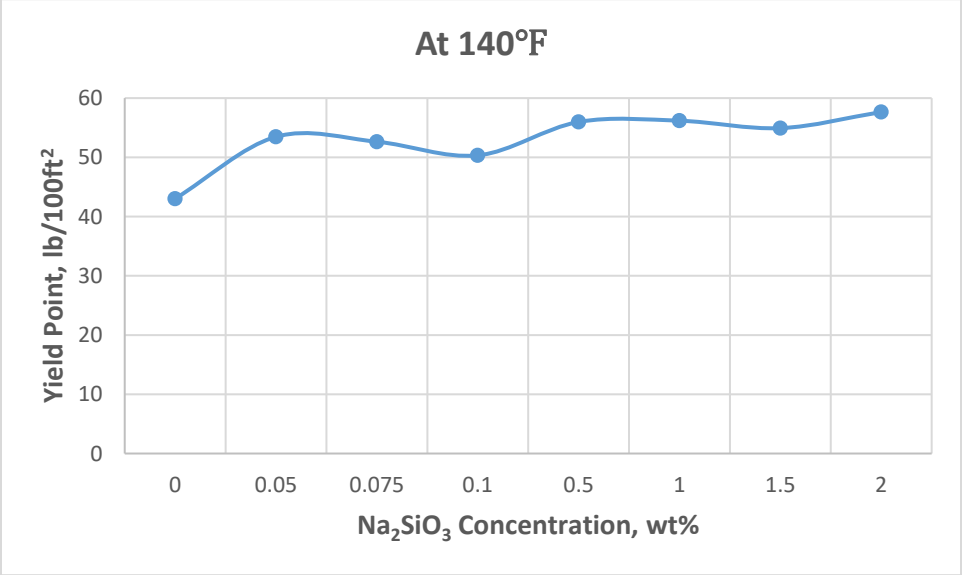

Figure 5-10. Effect of Na_2SiO_3 on YP at 140°F

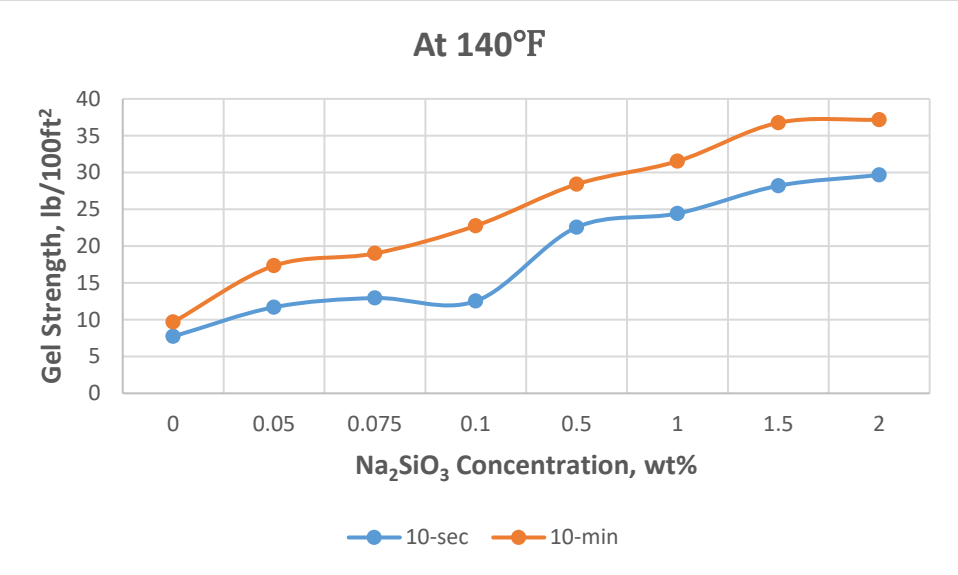

Figure 5-11. Effect of Na_2SiO_3 on Gel Strength at 140°F

Table 5-12. Torque Readings of Base Fluid and with 0.05 wt% Na_2SiO_3 at 140°F

Base Fluid				0.05 wt%			
T, °F	Speed, RPM	Shear Stress, lb/100ft²	Gel Strength, lb/100 ft²	T, °F	Speed, RPM	Shear Stress, lb/100ft²	Gel Strength, lb/100 ft²
136	600	75,2	76,7	138	600	89	90,4
136	300	59,1	76,9	139	300	71,2	89,4
136	200	47,6	58,5	139	200	57,2	71,4
136	100	33,8	47,4	140	100	40,7	56,8
136	60	26,3	33,6	141	60	32,0	40,3
136	30	19	26,1	142	30	23,6	31,7
137	6	9,6	19	143	6	13,8	23,8
137	3	7,9	12,3	144	3	11,3	16,9
135	600	75,4	75,8	142	600	87,9	88,3
135	0	63,9	77,5	142	0	74,8	90,4
135	3	7,5	7,7	143	3	11,5	11,7
135	300	25,9	44,3	143	300	34,5	55,8
134	0	0	60,8	141	0	0	72,3
134	3	9,5	9,7	141	3	12,7	17,3

Table 5-13. Torque Readings of Base Fluid with 0.075 and 0.1 wt% Na_2SiO_3 at 140°F

0.075 wt%				0.1 wt%			
T, °F	Speed, RPM	Shear Stress, lb/100ft^2	Gel Strength, lb/100 ft^2	T, °F	Speed, RPM	Shear Stress, lb/100ft^2	Gel Strength, lb/100 ft^2
141	600	95,2	99,2	139	600	87,1	91,9
141	300	73,9	95,4	139	300	68,7	87,1
142	200	60,4	74,1	139	200	56	68,9
142	100	43	59,5	139	100	40,5	55,1
142	60	34	42,6	139	60	32,2	40,1
142	30	25,7	33,8	140	30	24,4	32,2
142	6	14,8	25,5	140	6	14,6	24,6
143	3	12,3	18,0	141	3	12,3	17,5
145	600	92,5	93,2	142	600	84,6	84,6
144	0	79,2	95,2	142	0	71,2	85,8
144	3	12,9	12,9	142	3	12,5	12,5
144	300	35,3	57,0	143	300	34,7	54,5
143	0	0	76,0	143	0	0	70,4
143	3	14,2	19,0	143	3	14,8	22,8

Table 5-14. Torque Readings of Base Fluid with 0.5 and 1 wt% Na_2SiO_3 at 140°F

0.5 wt%				1 wt%			
T, °F	Speed, RPM	Shear Stress, lb/100ft^2	Gel Strength, lb/100 ft^2	T, °F	Speed, RPM	Shear Stress, lb/100ft^2	Gel Strength, lb/100 ft^2
133	600	91,9	92,3	135	600	100,9	101,5
132	300	73,9	94,8	134	300	78,5	102,5
133	200	60,4	70,4	134	200	64,7	76,2
134	100	48,5	60,2	135	100	51,6	64,7
135	60	42,2	49,1	137	60	44,3	51,4
135	30	35,1	42	138	30	36,8	44,3
135	6	24,4	34,7	139	6	26,1	36,8
136	3	21,1	27,8	139	3	23,4	29
133	600	94,4	94,6	136	600	100,3	100,7
133	0	80,2	95,4	136	0	81,9	101,1
133	3	22,1	22,6	136	3	24,2	24,4
133	300	44,1	64,1	136	300	45,1	64,7
135	0	0	74,6	139	0	0,6	79,2
135	3	15,2	28,4	139	3	16,7	31,5

Table 5-15. Torque Readings of Base Fluid with 1.5 and 2 wt% Na_2SiO_3 at 140°F

1.5 wt%				2 wt%			
T, °F	Speed, RPM	Shear Stress, lb/100ft²	Gel Strength, lb/100 ft²	T, °F	Speed, RPM	Shear Stress, lb/100ft²	Gel Strength, lb/100 ft²
145	600	102,1	102,5	141	600	101,5	102,5
144	300	78,5	101,7	140	300	79,6	103,4
144	200	67,3	77,3	140	200	68,3	78,7
145	100	54,3	67,3	142	100	54,9	68,3
146	60	46,8	54,1	142	60	47,6	54,9
146	30	39,3	46,6	143	30	40,3	47,6
146	6	29,4	39,1	144	6	31,5	40,1
146	3	26,5	32,0	144	3	29,7	33,8
144	600	101,5	101,9	141	600	103,4	103,8
144	0	85,8	101,7	140	0	86,5	102,8
143	3	28	28,2	141	3	29,4	29,7
143	300	49,7	69,1	142	300	49,5	68,1
141	0	2,1	78,7	141	0	0,2	78,9
141	3	20,7	36,8	141	3	19,4	37,2

Table 5-16. Summary of Rheological Properties of Na_2SiO_3 Concentrations at 140°F

Na_2SiO_3 Concentration, wt%	PV, cp	YP, lb/100ft²	10-sec, lb/100ft²	10-min, lb/100ft²
0	16,1	43	7,7	9,7
0,05	17,8	53,5	11,7	17,3
0,075	21,3	52,6	12,9	19
0,1	18,4	50,3	12,5	22,8
0,5	18	56	22,6	28,4
1	22,3	56,2	24,4	31,5
1,5	23,6	54,9	28,2	36,8
2	21,9	57,6	29,7	37,2

5.2.4 Effect of Sodium Silicate on Rheological Properties at 170°F

It is observed that the trends of PV and YP are slightly changing for lower concentrations of sodium silicate as shown in **Figs. 5-12** and **5-13**. While PVs of 0.05 and 0.1 wt% are not changing, 0.075 wt% are decreasing and all low concentrations are becoming constant at about 18 cp. Similar decrement is observed for YP with 0.075 wt%, while low concentrations are showing constant trend around 47 lb/100 ft^2. Like lower temperatures, YP values are ranging between the same values at 170°F. On the other hand, the constant values show that unlike low concentrations, still flocculation occurs at high concentrations up to 170°F under atmospheric pressure. In comparison with 140°F, both gel strength values are decreasing at 170°F with high concentrations as shown in **Fig. 5-14**. However, low concentrations do not show any significant change for initial gel strength. Unlike 10-second, 10-minute gel strength values are already not stabilizing at even 1.5 wt%. This observation shows that as the temperature increases, gel strength of high concentrations loses their stability. **Table 5-21** summarizes all rheology test results for each sodium silicate concentration at 170°F.

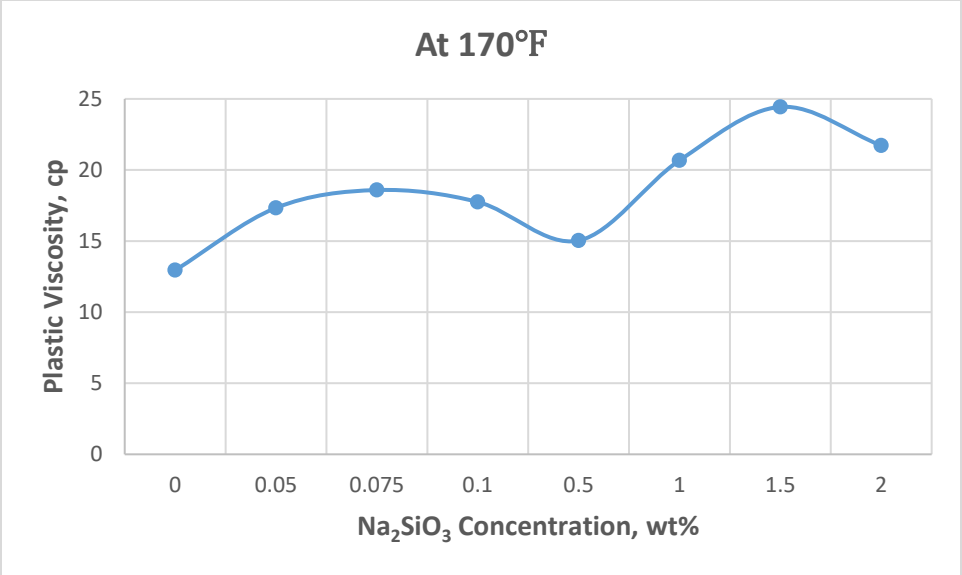

Figure 5-12. Effect of Na_2SiO_3 on PV at 170°F

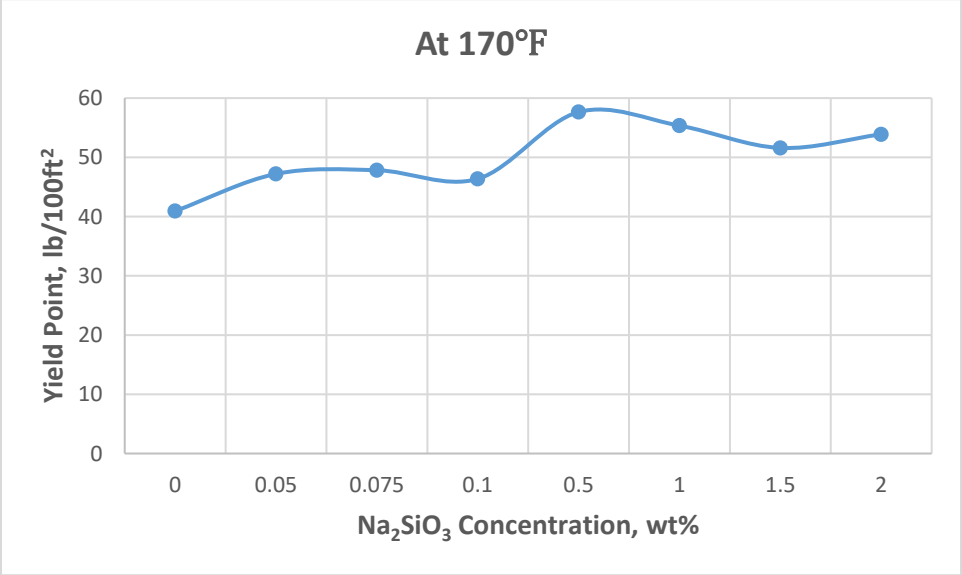

Figure 5-13. Effect of Na_2SiO_3 on YP at 170°F

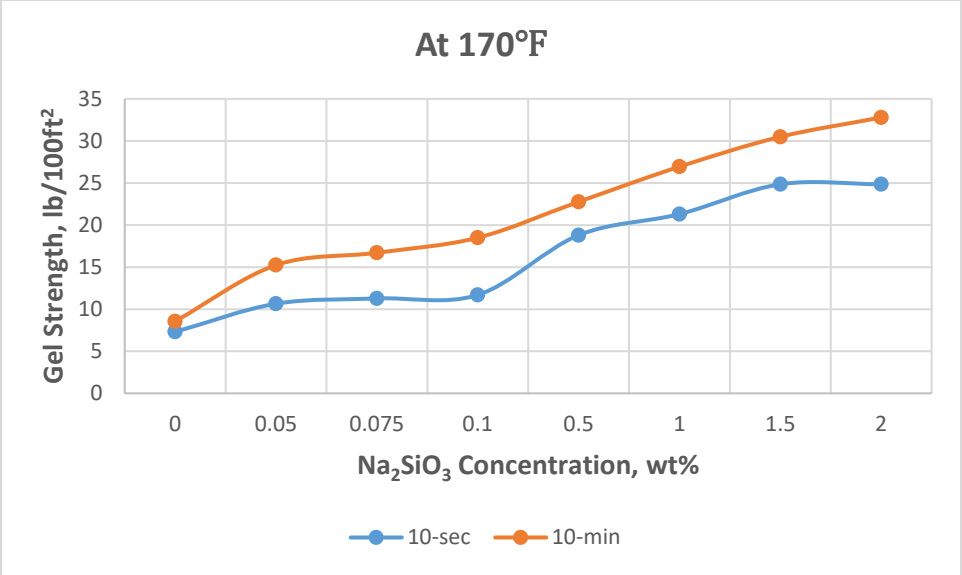

Figure 5-14. Effect of Na_2SiO_3 on Gel Strength at 170°F

Table 5-17. Torque Readings of Base Fluid and with 0.05 wt% Na_2SiO_3 at 170°F

Base Fluid				0.05 wt%			
T, °F	Speed, RPM	Shear Stress, lb/100ft²	Gel Strength, lb/100 ft²	T, °F	Speed, RPM	Shear Stress, lb/100ft²	Gel Strength, lb/100 ft²
167	600	66,8	68,5	167	600	81,9	82,5
167	300	53,9	68,9	167	300	64,5	82,5
168	200	43,2	53,5	167	200	52,2	64,7
168	100	30,3	43	168	100	37,2	51,8
168	60	23,2	30,3	168	60	28,8	36,8
168	30	16,5	23,4	169	30	21,1	28,8
168	6	8,6	16,7	170	6	12,1	21,1
168	3	7,1	10,9	171	3	9,8	14,6
169	600	69,1	69,3	168	600	82,1	82,5
168	0	56,2	71,2	168	0	67,3	84,4
168	3	7,1	7,3	168	3	10,7	10,7
168	300	25,5	42,8	168	300	32	52
173	0	0	55,1	165	0	0	66,6
172	3	3,3	8,6	165	3	11,9	15,2

Table 5-18. Torque Readings of Base Fluid with 0.075 and 0.1 wt% Na_2SiO_3 at 170°F

0.075 wt%				0.1 wt%			
T, °F	Speed, RPM	Shear Stress, lb/100ft²	Gel Strength, lb/100 ft²	T, °F	Speed, RPM	Shear Stress, lb/100ft²	Gel Strength, lb/100 ft²
171	600	85	85,4	165	600	81,9	85
170	300	66,4	85,6	165	300	64,1	82,1
170	200	54,3	66,6	165	200	52,2	64,1
171	100	38,6	53,5	166	100	37,8	51,6
171	60	30,1	38,2	166	60	30,1	37,6
171	30	22,1	30,1	166	30	22,6	29,9
171	6	12,5	22,3	166	6	13,6	22,6
172	3	10,4	15,9	167	3	11,3	16,5
172	600	86,3	86,7	166	600	80,2	80,6
172	0	73,7	88,6	167	0	68,3	82,3
172	3	11,1	11,3	166	3	11,5	11,7
172	300	31,7	52,2	166	300	30,9	49,7
169	0	0	69,1	166	0	0	66,6
168	3	12,322	16,708	166	3	13,8	18,5

Table 5-19. Torque Readings of Base Fluid with 0.5 and 1 wt% Na_2SiO_3 at 170°F

0.5 wt%				1 wt%			
T, °F	Speed, RPM	Shear Stress, lb/100ft²	Gel Strength, lb/100 ft²	T, °F	Speed, RPM	Shear Stress, lb/100ft²	Gel Strength, lb/100 ft²
164	600	87,7	88,1	162	600	96,7	97,1
164	300	72,7	91,5	161	300	76	98,4
165	200	58,3	69,3	160	200	62,2	73,7
166	100	45,1	57,6	162	100	48,5	62
167	60	38	45,1	163	60	40,9	48,5
168	30	30,5	38	165	30	32,8	40,7
169	6	19,4	30,3	165	6	21,7	33
170	3	16,3	22,3	167	3	18,6	24,4
164	600	91,1	91,5	162	600	97,5	97,7
164	0	75	92,3	161	0	83,1	98,4
165	3	18	18,8	161	3	20,5	21,3
165	300	38	57,4	162	300	41,4	61,6
175	0	0,2	72,1	174	0	0,4	76,4
175	3	12,5	22,8	174	3	14,6	26,9

Table 5-20. Torque Readings of Base Fluid with 1.5 and 2 wt% Na_2SiO_3 at 170°F

1.5 wt%				2 wt%			
T, °F	Speed, RPM	Shear Stress, lb/100ft²	Gel Strength, lb/100 ft²	T, °F	Speed, RPM	Shear Stress, lb/100ft²	Gel Strength, lb/100 ft²
161	600	100,5	100,7	168	600	97,3	98,2
159	300	76	100,3	166	300	75,6	99,4
160	200	64,7	74,6	168	200	64,5	74,6
162	100	51,4	64,7	169	100	51,0	64,5
164	60	43,9	51,4	170	60	43,7	51,2
165	30	36,1	43,9	171	30	36,3	43,7
165	6	25,5	35,9	171	6	26,5	35,9
166	3	22,6	28,4	172	3	23,6	29,9
163	600	101,5	101,5	168	600	99,4	99,8
162	0	84,6	100,5	167	0	83,3	98,6
161	3	24	24,9	168	3	24,4	24,9
162	300	44,3	63,7	168	300	44,5	63,7
173	0	0,2	76,7	176	0	0,6	76,4
173	3	15,9	30,5	176	3	17,8	32,8

Table 5-21. Summary of Rheological Properties of Na_2SiO_3 Concentrations at 170°F

Na_2SiO_3 Concentration, wt%	PV, cp	YP, lb/100ft²	10-sec, lb/100ft²	10-min, lb/100ft²
0	12,9	40,9	7,3	8,6
0,05	17,3	47,2	10,7	15,2
0,075	18,6	47,8	11,3	16,7
0,1	17,8	46,4	11,7	18,5
0,5	15	57,6	18,8	22,8
1	20,7	55,3	21,3	26,9
1,5	24,4	51,6	24,9	30,5
2	21,7	53,9	24,9	32,8

5.2.5 Effect of Sodium Silicate on Rheological Properties at 300°F

As mentioned earlier, rheological properties at 300°F have been measured slightly different than other temperatures. First of all, the measurements have been done under 300 psi pressure to prevent evaporation. Secondly, only low sodium silicate concentrations have been measured at this temperature. This is due to the filtration test results that changed experimental plan from higher concentrations to lower ones. Lastly, the answer for the question "Why measurements are performed exactly at 300°F?" is because of the drilling fluid formula that is used for the reservoir, where the temperature ranges between 280-305°F. The upper temperature limit was selected.

Analyzing the data that are presented in **Figs. 5-15**, **5-16**, **5-17** and **5-18** clearly demonstrate that all rheological properties for all low concentrations up to 0.1 wt%, including PV, YP and both 10-second, 10-minute gel strengths, are decreasing with increasing temperature. PV is ranging between 10-15 cp by following similar decreasing trend of lower temperatures. Main remarkable change happens with 0.1 wt%, which is becoming even lower than base fluid. 0.075 wt% is showing slightly higher PV than others. However, the sharpest reduction occurs in YP values at 300°F. YP values ranging between 40-50 lb/100ft^2 at 170°F, but are falling below 10 lb/100 ft^2 at 300°F. This result allows us to conclude that the reason of such sharp reduction is due to the high pressure. The results demonstrate that pressure has also an important effect on YP, beside the effects of different sodium silicate concentrations and temperature. Additionally, one more conclusion can be reached is that having low YP eliminates the need for powerful pumps to inject drilling fluid into the well. Again 0.075 wt% is showing higher value. On the other hand, decrease of both PV and YP values at 300°F as well as lower temperatures shows that base fluid

itself and with all low concentrations are fully deflocculates, which means small particles cannot coalesce together and form bigger ones. In another word, the fluid completely disperses. The main reason of it is the elimination of fluid loss additive at high temperatures – Resinex.

Similarly, both gel strength values are also decreasing at 300°F. Highest values are obtained with 0.075 wt% as in PV and YP. However, interestingly, 0.1 wt% is falling below base fluid value at 10-minute again similar to PV. This can be a sign for the instability of higher sodium silicate concentrations at high temperatures and high pressures, even though 0.1 wt% itself is not high. Probably, further detailed investigations for rheology are required for higher concentrations at HPHT conditions. In filtration results, the effect of high concentrations will also be discussed.

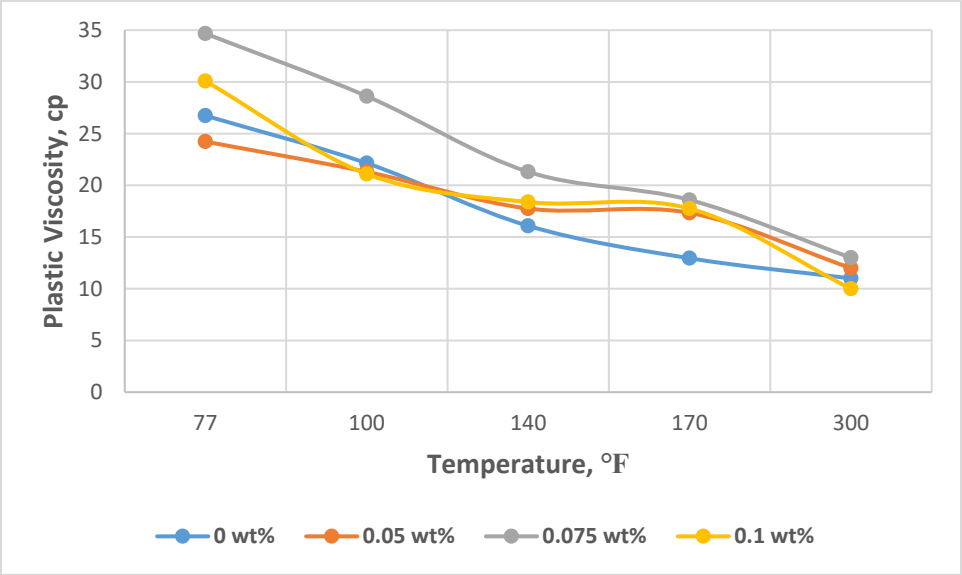

Figure 5-15. Effect of Na_2SiO_3 on PV at 300°F

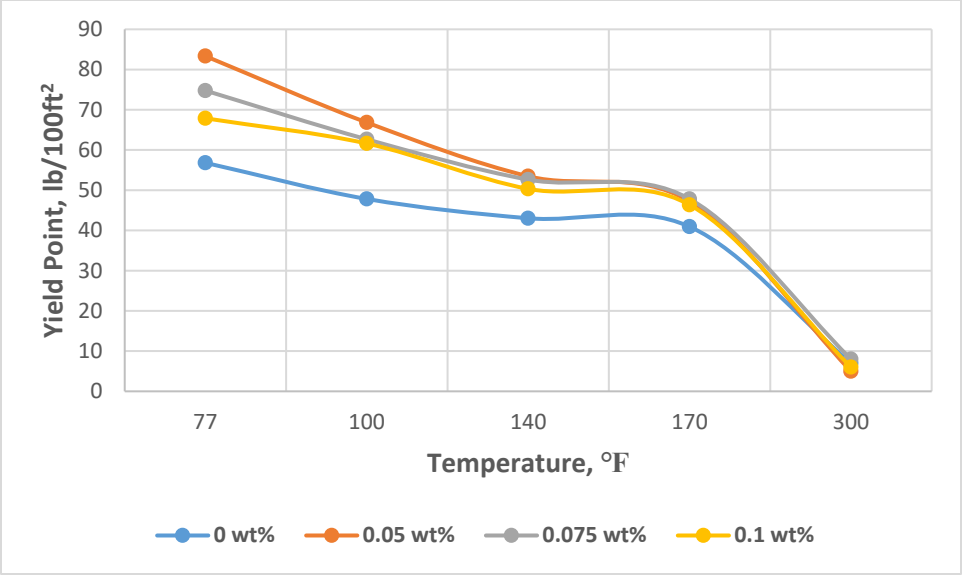

Figure 5-16. Effect of Na_2SiO_3 on YP at 300°F

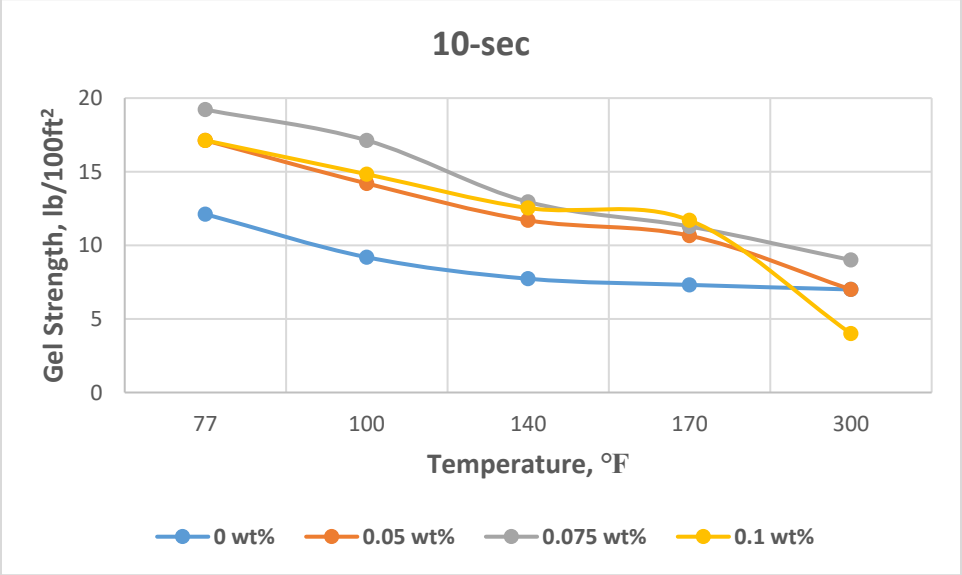

Figure 5-17. Effect of Na_2SiO_3 on 10-second Gel Strength at 300°F

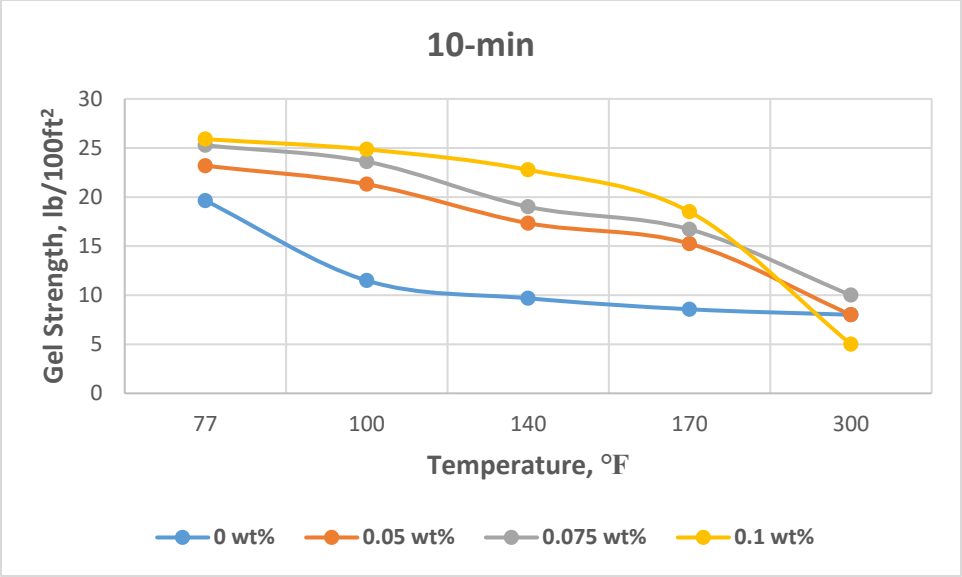

Figure 5-18. Effect of Na_2SiO_3 on 10-minute Gel Strength at 300°F

5.3 Solubility Results

The solubility experiments were conducted in two stages. In the first part, the effects of 2, 4 and 6 wt% sodium silicate on barite solubility observed. To confirm these results, the tests were repeated beside new concentration 8 wt% as well. It should be noted that in the beginning the purpose of doing solubility tests was to evaluate whether sodium silicate has reverse effect on barite solubility. The expected results were similar or slightly lower than the obtained ones of Ba geri et al. (2015). This has prompted interest to conduct further and do the researches for filtration tests. Furthermore, it was agreed to perform the experiments with high concentrations, since the used sodium silicate is in liquid state, it is very difficult to achieve adding small concentrations for 2 g barite. Indeed, if there was no considerable reverse effect at higher concentrations, it would mean there will not be also reversible effect at lower concentrations. However, the results revealed different values

Table 5-22. Summary of Rheological Properties of Base Fluid and with 0.05, 0.075, 0.1 wt% Na_2SiO_3 at 300°F

Na_2SiO_3 Concentration, wt%	T, °F	PV, cp	YP, lb/100ft^2	10-sec, lb/100ft^2	10-min, lb/100ft^2
0	77	26,7	56,8	12,1	19,6
	100	22,1	47,8	9,2	11,5
	140	16,1	43	7,7	9,7
	170	12,9	40,9	7,3	8,6
	300	11	7	7	8
0.05	77	24,2	83,3	17,1	23,2
	100	21,3	66,8	14,2	21,3
	140	17,8	53,5	11,7	17,3
	170	17,3	47,2	10,7	15,2
	300	12	5	7	8
0.075	77	34,7	74,8	19,2	25,3
	100	28,6	62,7	17,1	23,6
	140	21,3	52,6	12,9	19
	170	18,6	47,8	11,3	16,7
	300	13	8	9	10
0.1	77	30,1	67,9	17,1	25,9
	100	21,1	61,6	14,8	24,9
	140	18,4	50,3	12,5	22,8
	170	17,8	46,4	11,7	18,5
	300	10	6	4	5

values for 2, 4 and 6 wt% are the average values of two tests and both of which are provided in **Table. 5-24**. 0 wt% shows the result that Ba geri et al. (2015) obtained with 20 wt% potassium-based DTPA + 6 wt% potassium formate + 7 wt% enzyme, which it is 75%. On the other hand, adding 2, 4 and 6 wt% sodium silicate increased the solubility around 80% as an average value. Highest percentage obtained at 4 wt% with 82%. 2 and 6 wt% showed similar behavior. Additionally, 8 wt% confirmed the decreasing solubility behavior of

sodium silicate with 62%. Based on the sudden and sharp decrease, it can be concluded that 4 wt% is an optimum concentration.

After determining an optimum concentration, the solubility behavior of sodium silicate was observed in the absence of catalyst. The test presented more lower result with 45%. However, this result is consistent with the presented result of Ba geri et al. (2015), which he has gained 38% with sodium-based DTPA in the absence of catalyst. The only difference in these two tests is the used chelating agents, where our test was performed with potassium-based DTPA. Therefore, two more conclusions may also be derived. First, using sodium-based DTPA could decrease the solubility further in case of catalyst's absence. Second, these last two results prove that sodium alone has a reverse effect on barite solubility and lowers it significantly.

To summarize, 4 wt% sodium silicate improves the single stage barite filter cake removal method of Ba geri et al. (2015). His results show more than 90% of filter cake dissolved within 24 h at 270°F. Similarly, increasing the temperature will improve the effect of sodium silicate on barite solubility as well. Since the reservoir temperature is 300°F, the solubility in downhole conditions will improve further. As a result, the expected filter cake dissolution with 4 wt% sodium silicate will be more than the result without sodium silicate. It should also be stressed that since our drill-in fluid includes starch, the enzyme for starch should be used beside the enzyme for XC polymer in addition to the method of Ba geri et al. (2015) so that to dissolve starch in the filter cake. **Table 29** summarizes all solubility results.

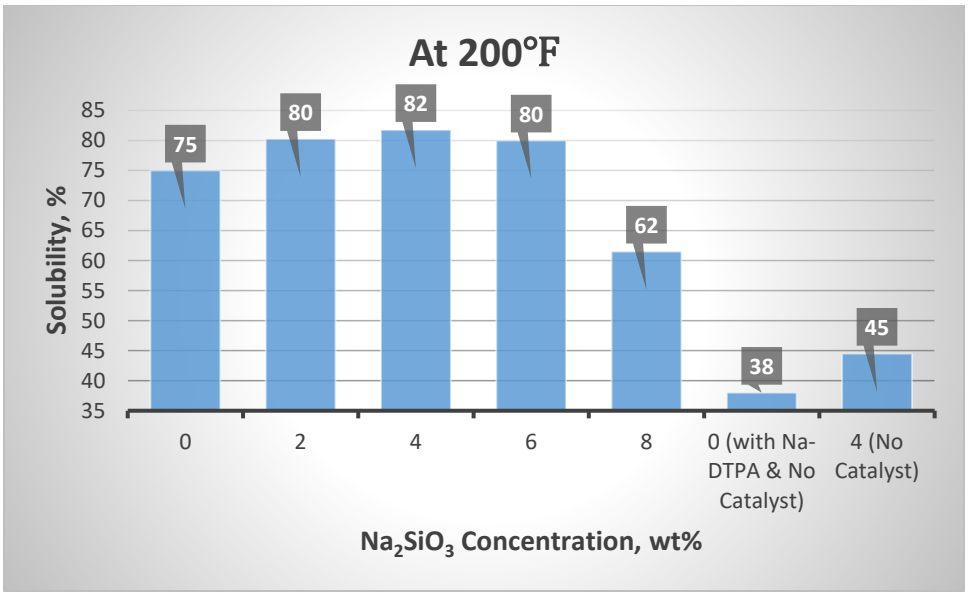

Figure 5-19. Effect of Na_2SiO_3 on Barite Solubility

Table 5-23. Calculated Solubility Percentages with Different Na_2SiO_3 Concentrations

№	Na_2SiO_3 Concentration, wt%	Na_2SiO_3 Concentration, ml	Weight of Filter Paper, g	Weight of Filter Paper + Remained Barite, g	Weight of Remained Barite, g	Dissolved Weight of Barite, g	Solubility, %
Test #1	2	0,04	0,47	0,88	0,41	1,59	80
	4	0,08	0,48	0,87	0,39	1,61	81
	6	0,12	0,47	0,91	0,44	1,56	78
Test #2	2	0,04	0,46	0,84	0,38	1,62	81
	4	0,08	0,47	0,81	0,34	1,66	83
	6	0,12	0,45	0,81	0,36	1,64	82
	8	0,16	0,48	1,25	0,77	1,23	62
	4 (No Catalyst)	0,08	0,47	1,58	1,11	0,89	45

Table 5-24. Summary of Solubility Results

Na_2SiO_3 Concentration, wt%	Average Solubility, %
0	75
2	80
4	82
6	80
8	62
0 (with Na-DTPA & No Catalyst)	38
4 (No Catalyst)	45

5.4 Filtration Results

As per the plan, the filtration experiments were performed on 0.25" tight core samples to determine the optimum sodium silicate concentration and to conduct the test with the optimum concentration on 2" core sample, finally. The reason of to perform filtration test on 2" core sample is fluid invasion can be characterized better with the big length.

5.4.1 High Sodium Silicate Concentrations

Fig. 5-20 graphically explains the filtration test results with high sodium silicate concentrations, whereas **Fig. 5-21** shows the formed filter cake thicknesses after filtration. The experiments started with base fluid so that to observe the original behavior of it. The collected filtrate volume became 7.4 ml and the filter cake thickness was 2 mm. Since the plan in the beginning was to observe high concentrations, 0.5, 1, 1.5 and 2 wt% were selected as the interest points. However, the poor filtration results of 0.5, 1 and 1.5 wt% presented that conducting the test with 2 wt% is unnecessary and this concentration was

cancelled. 20, 25.2 and 52 ml filtrate volumes collected with 0.5, 1 and 1.5 wt%, respectively. The cake thicknesses also followed the volumes with the high values such as 8, 13 and 25 mm. **Tables 5-25** and **5-26** summarize the filtrate volumes at 30 minutes and filter cake thicknesses for the high sodium silicate concentrations. Moreover, the formed filter cakes of base fluid and high concentrations can be viewed through **Figs. 5-22 – 5-25**.

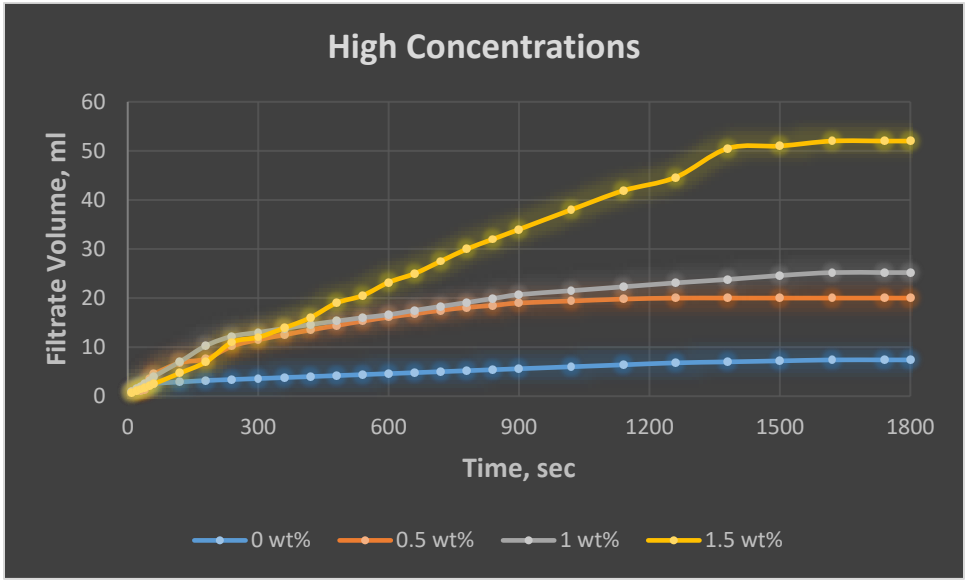

Figure 5-20. Effect of High Na_2SiO_3 Concentrations on Filtrate Volumes

Table 5-25. Summary of Filtrate Volumes at 30 Minutes of Base Fluid and High Na_2SiO_3 Concentrations

0 wt%		0.5 wt%		1 wt%		1.5 wt%	
Time, sec	Volume, ml	Time, sec	Volume, ml	Time, sec	Volume, ml	Time, sec	Volume, ml
10	1	10	1	10	1	10	0,7
20	1,5	20	1,1	20	1,5	20	1,2
30	1,7	30	1,2	30	1,9	30	1,4
40	2	40	1,3	40	2,5	40	1,8
50	2,3	50	3,5	50	3,2	50	2,1
60	2,6	60	4,5	60	4	60	2,5
120	2,9	120	6,8	120	7	120	4,7
180	3,2	180	7,6	180	10,3	180	7
240	3,4	240	10,2	240	12,2	240	11
300	3,6	300	11,5	300	13	300	12
360	3,8	360	12,5	360	13,8	360	13,9
420	4	420	13,5	420	14,6	420	16
480	4,2	480	14,4	480	15,3	480	19
540	4,4	540	15,3	540	16	540	20,5
600	4,6	600	16,1	600	16,6	600	23,2
660	4,8	660	16,8	660	17,5	660	25
720	5	720	17,5	720	18,3	720	27,5
780	5,2	780	18,1	780	19,1	780	30
840	5,4	840	18,5	840	19,9	840	32
900	5,6	900	19	900	20,7	900	34
1020	6	1020	19,4	1020	21,5	1020	38
1140	6,4	1140	19,8	1140	22,3	1140	41,9
1260	6,8	1260	20	1260	23,1	1260	44,6
1380	7	1380	20	1380	23,8	1380	50,5
1500	7,2	1500	20	1500	24,6	1500	51
1620	7,4	1620	20	1620	25,2	1620	52
1740	7,4	1740	20	1740	25,2	1740	52
1800	7,4	1800	20	1800	25,2	1800	52

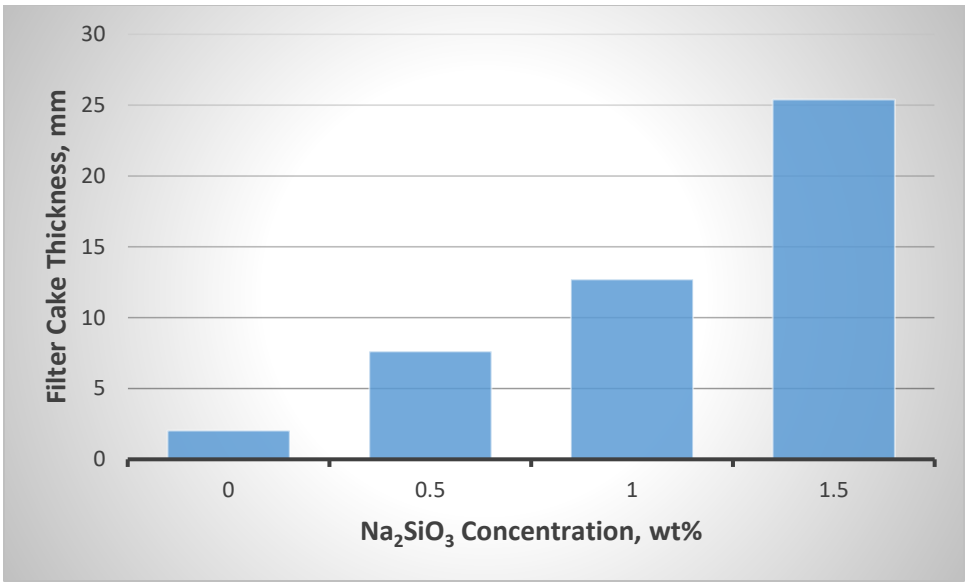

Figure 5-21. Effect of High Na_2SiO_3 Concentrations on Filter Cake Thicknesses

Figure 5-22. Formed Filter Cake with Base Fluid on 0.25" Core Sample

Figure 5-23. Formed Filter Cake with 0.5 wt% Na_2SiO_3 on 0.25" Core Sample

Figure 5-24. Formed Filter Cake with 1 wt% Na_2SiO_3 on 0.25" Core Sample

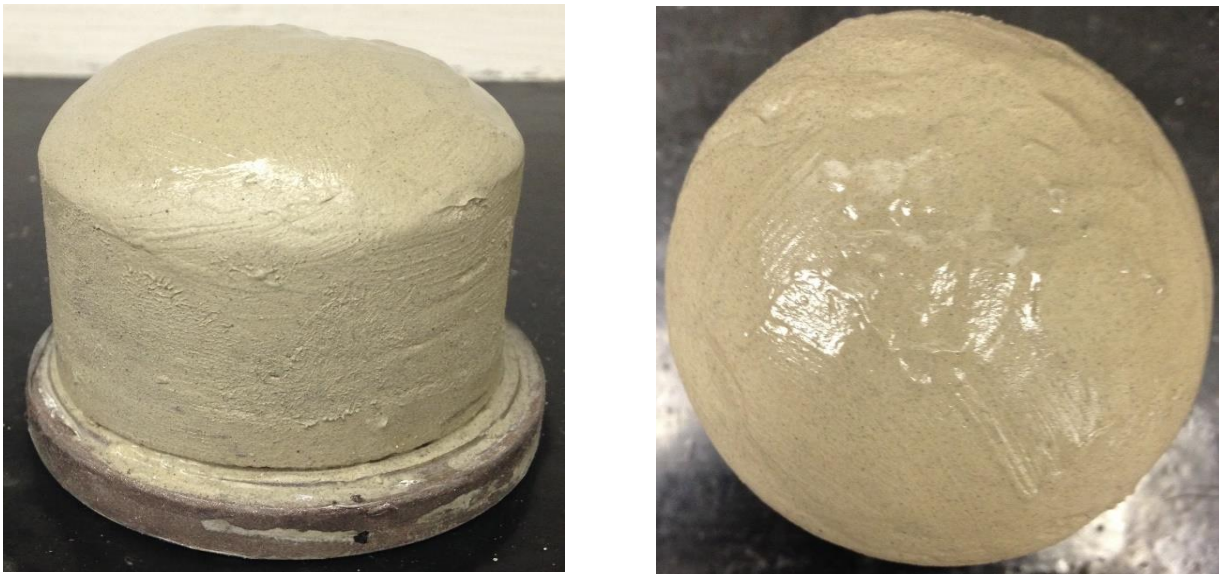

Figure 5-25. Formed Filter Cake with 1.5 wt% Na_2SiO_3 on 0.25" Core Sample

Table 5-26. Summary of Filter Cake Thicknesses with High Na_2SiO_3 Concentrations

Na_2SiO_3 Concentration, wt%	Filter Cake Thickness, 1/32 inch	Filter Cake Thickness, mm
0	2.6	2
0.5	9.6	8
1	16	13
1.5	32	25

5.4.2 Low Sodium Silicate Concentrations

Obtaining the poor filtrate volumes at the high concentrations directed us to conduct the experiments with the lower concentrations to investigate their behavior as well. For this reason, 0.1 wt% was selected, initially, and 5 ml filtrate volume collected, as illustrated in **Fig. 5-26**. The filter cake thickness also decreased to 1.3 mm, as shown in **Fig. 5-27**. In the next stage, a more lower concentration – 0.075 wt% observed, because of getting such

improvement for both parameters with 0.1 wt%. As it was expected, adding 0.075 wt% sodium silicate to base fluid improved both filtrate volume and filter cake thickness more. The collected filtrate volume was just 3.5 ml and the filter cake thickness decreased even to 0.7 mm. The filtrate volume and cake thickness reduced by 53% and 65% with 0.075 wt% Na_2SiO_3, respectively, compared than the base fluid's results. However, going one more step below 0.075 wt%, namely with 0.05 wt%, didn't show improvement, instead got worse. The volume and filter cake thickness increased to 6.5 ml and 1.8 mm, respectively. Although, these findings with 0.05 wt% can be seen as poor, but still they are better than base fluid's results.

Consequently, above findings allowed us to conclude that 0.075 wt% sodium silicate concentration is an optimum one. In fact, the filtration results are confirming rheology results. Having higher PV, YP, 10-second and 10-minute gel strength values with 0.075 wt% than other low concentrations at 300°F is consistent with its filtration properties. According to these results, the last filtration experiment was performed with 0.075 wt% on 2" core sample. Though the selected concentration was 0.075 wt%, the filtrate volume and filter cake thickness could not be obtained for 2" core sample same as 0.25" one. The collected volume and cake thickness were 6.4 ml and 1.6 mm, respectively. The main explanation of this inconsistency is used bridging material. Poor bridging may cause to such result. Two types of bridging materials have been used in the drill-in fluid formula: calcium carbonate 25 and <38 μm. The fluctuations in the results is due to <38 μm, because this bridging size can be very low and very high up to 38 μm. So, we can understand from here that most probably, bigger sized bridging materials have been in the drill-in fluid that used for 2" core sample in comparison with 0.25" ones. However, still there is a significant

improvement in the filtrate volume and cake thickness compared to base fluid. As a result, less fluid invasion will fill the pores of tight formation with less fluid and water blockage problem of tight gas wells will decrease substantially by newly formulated drill-in fluid. **Tables 5-27** and **5-28** summarize the filtrate volumes at 30 minutes and filter cake thicknesses for the low sodium silicate concentrations. Furthermore, the formed filter cakes of low concentrations with 0.25" and 2" core samples can be observed through **Figs. 5-28 – 5-31**.

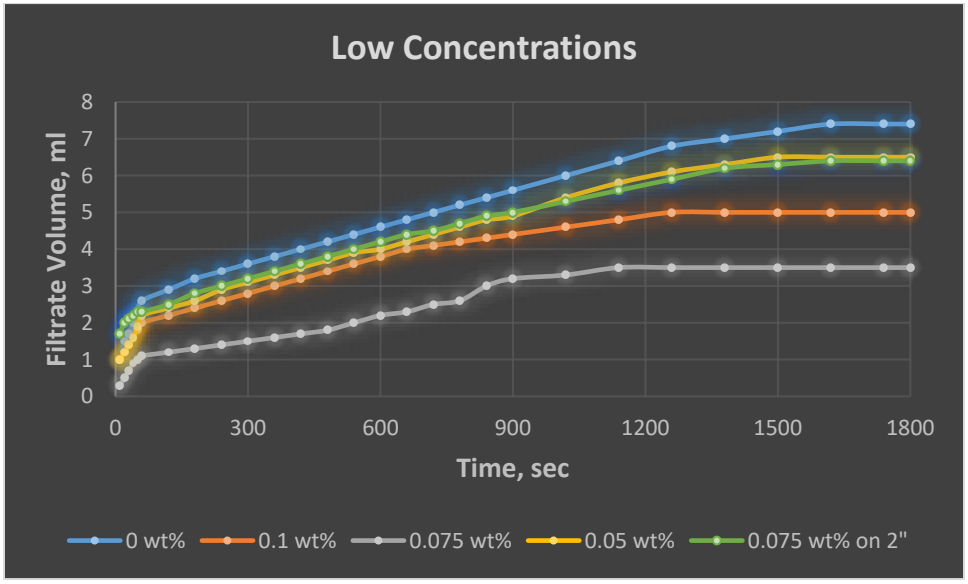

Figure 5-26. Effect of Low Na_2SiO_3 Concentrations on Filtrate Volumes

Table 5-27. Summary of Filtrate Volumes at 30 Minutes with Low Na_2SiO_3 Concentrations

0.05 wt%		0.075 wt%		0.1 wt%		0.075 wt% on 2"	
Time, sec	Volume, ml	Time, sec	Volume, ml	Time, sec	Volume, ml	Time, sec	Volume, ml
10	1	10	0,3	10	1	10	1,7
20	1,2	20	0,5	20	1,2	20	2
30	1,4	30	0,7	30	1,4	30	2,1
40	1,6	40	0,9	40	1,6	40	2,2
50	1,9	50	1	50	1,8	50	2,3
60	2,2	60	1,1	60	2	60	2,3
120	2,4	120	1,2	120	2,2	120	2,5
180	2,6	180	1,3	180	2,4	180	2,8
240	2,9	240	1,4	240	2,6	240	3
300	3,1	300	1,5	300	2,8	300	3,2
360	3,3	360	1,6	360	3	360	3,4
420	3,5	420	1,7	420	3,2	420	3,6
480	3,7	480	1,8	480	3,4	480	3,8
540	3,9	540	2	540	3,6	540	4
600	4	600	2,2	600	3,8	600	4,2
660	4,2	660	2,3	660	4	660	4,4
720	4,4	720	2,5	720	4,1	720	4,5
780	4,6	780	2,6	780	4,2	780	4,7
840	4,8	840	3	840	4,3	840	4,9
900	4,9	900	3,2	900	4,4	900	5
1020	5,4	1020	3,3	1020	4,6	1020	5,3
1140	5,8	1140	3,5	1140	4,8	1140	5,6
1260	6,1	1260	3,5	1260	5	1260	5,9
1380	6,3	1380	3,5	1380	5	1380	6,2
1500	6,5	1500	3,5	1500	5	1500	6,3
1620	6,5	1620	3,5	1620	5	1620	6,4
1740	6,5	1740	3,5	1740	5	1740	6,4
1800	6,5	1800	3,5	1800	5	1800	6,4

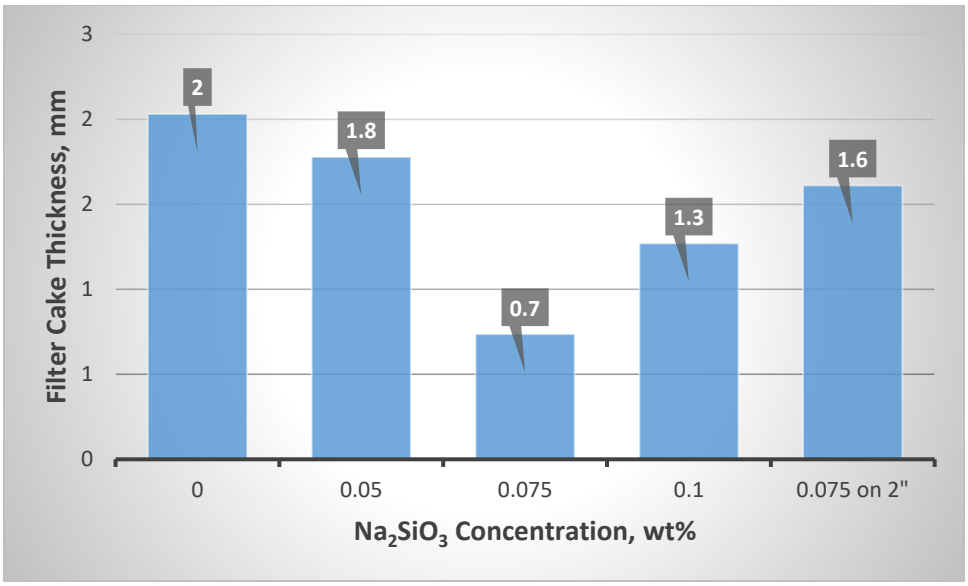

Figure 5-27. Effect of Low Na_2SiO_3 Concentrations on Filter Cake Thicknesses

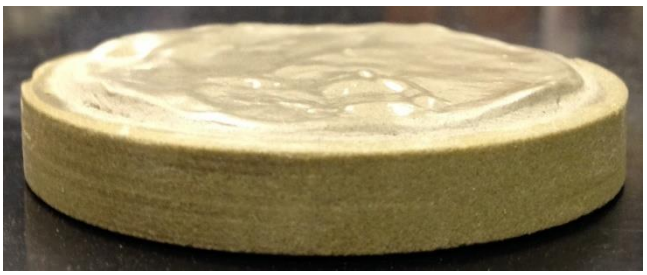

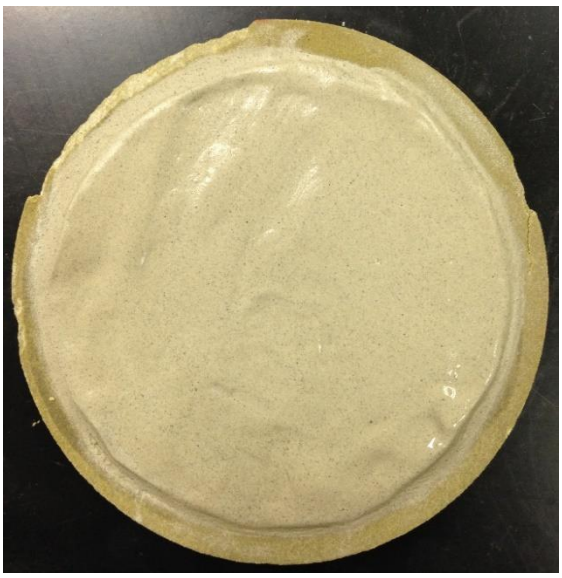

Figure 5-28. Formed Filter Cake with 0.1 wt% Na_2SiO_3 on 0.25" Core Sample

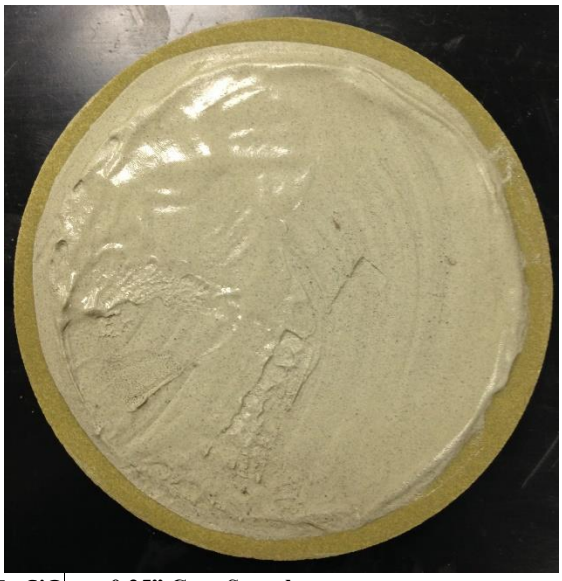

Figure 5-29. Formed Filter Cake with 0.075 wt% Na_2SiO_3 on 0.25" Core Sample

Figure 5-30. Formed Filter Cake with 0.05 wt% Na_2SiO_3 on 0.25" Core Sample

Figure 5-31. Formed Filter Cake with 0.075 wt% Na_2SiO_3 on 2" Core Sample

Table 5-28. Summary of Filter Cake Thicknesses with Low Na_2SiO_3 Concentrations

Na_2SiO_3 Concentration, wt%	Filter Cake Thickness, 1/32 inch	Filter Cake Thickness, mm
0	2.6	2
0.05	2.2	1.8
0.075	0.9	0.7
0.1	1.6	1.3
0.075 on 2"	2	1.6

5.4.3 Return Permeability

Initial Details:

l = 2.045" = 5.1943 cm

d = 2.5" = 6.25 cm

μ = 1.204 cp

$$A = \frac{\pi d^2}{4} = \frac{3.14 \cdot 6.25^2}{4} = 30.68\ cm^2$$

where A – surface area of the core, cm^2; d – the core diameter, cm.

The recorded pressure values for each flow rates before and after damage have been provided in **Table 5-29**. To convert from voltage to pressure, the values have been divided by 0.0029 based on the calibration data of the transducer for ΔP.

Calculation of Permeability Before and After Damage:

The obtained both slopes before and after damage, m = 0.0062 as shown in **Figs. 5-33a** and **5-33b**, respectively. The permeability of both became equal:

$$k_i = k_f = \frac{0.0062 \cdot 1.204 \cdot 5.1943}{30.68} \approx 0.0013\ D = 1.3\ mD$$

where, k_i and k_f – permeability before and after damage, mD, respectively.

$$Return\ Permeability = \frac{k_i}{k_f} \cdot 100\% = \frac{1.3}{1.3} \cdot 100\% = 100\%$$

This result means, in case of 100% filter cake removal, 100% return permeability is gained. Obtaining 100% return permeability presents that no solid invaded to the core sample. Therefore, it can be concluded that in real conditions, having zero-solid invasion will keep the well productivity of tight gas reservoirs same as an original productivity in case of 100% filter cake removal. Forming a very thin filter cake, like 0.7 mm, lets us also to claim that complete removal by washing with even 15 wt% HCl is possible and to get 100% return permeability. On the other hand, according to the solubility results, the minimum

return permeability will be more than 90-95%, as the expected filter cake removal efficiency will be more than 90-95% with added 4 wt% sodium silicate concentration to the base solution – 20 wt% K-DTPA + 6 wt% catalyst + 7 wt% enzyme for XC polymer + enzyme for starch. This is the worst scenario, which may happen due to a poor bridging and it can be resulted with the slightly increased filter cake thickness. All these results prove that formulated drilling fluid with added 0.075 wt% sodium silicate concentration is non-damaging and its return permeability is 100% with respect to having a good bridging, which may even eliminate the need for an expensive removal process by using only 15 wt% HCl. Furthermore, it should also be noted that doing a proper fracturing job may lead to improved permeability (higher than 100%), as the rock permeability will be kept almost as it is, because of using this drill-in fluid while drilling the formation part.

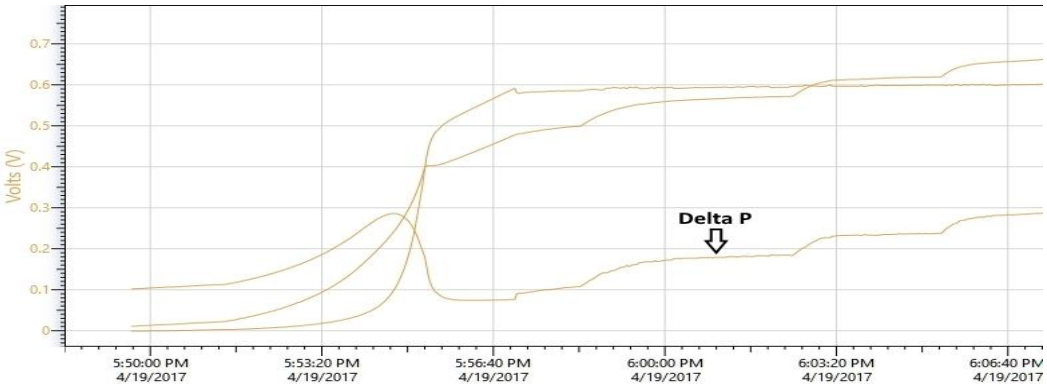

a)

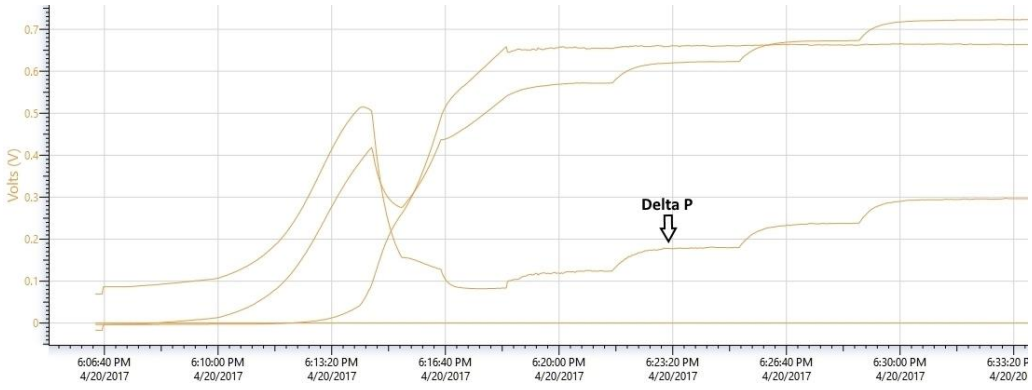

b)

Figure 5-32. Voltage Readings of *Omega* Software Before (a) and After (b) Damage

Table 5-29. Recorded Pressure Values for each Flow Rates Before and After Damage

Before Damage					After Damage				
q, ml/min	q, ml/sec	U, volt	ΔP, psi	ΔP, atm	q, ml/min	q, ml/sec	U, volt	ΔP, psi	ΔP, atm
0,5	0,008	0,116	40	2,7	0,5	0,008	0,1235	43	2,9
1	0,017	0,185	64	4,3	1	0,017	0,1805	62	4,2
1,5	0,025	0,2365	82	5,5	1,5	0,025	0,238	82	5,6
2	0,033	0,288	99	6,8	2	0,033	0,2965	102	7

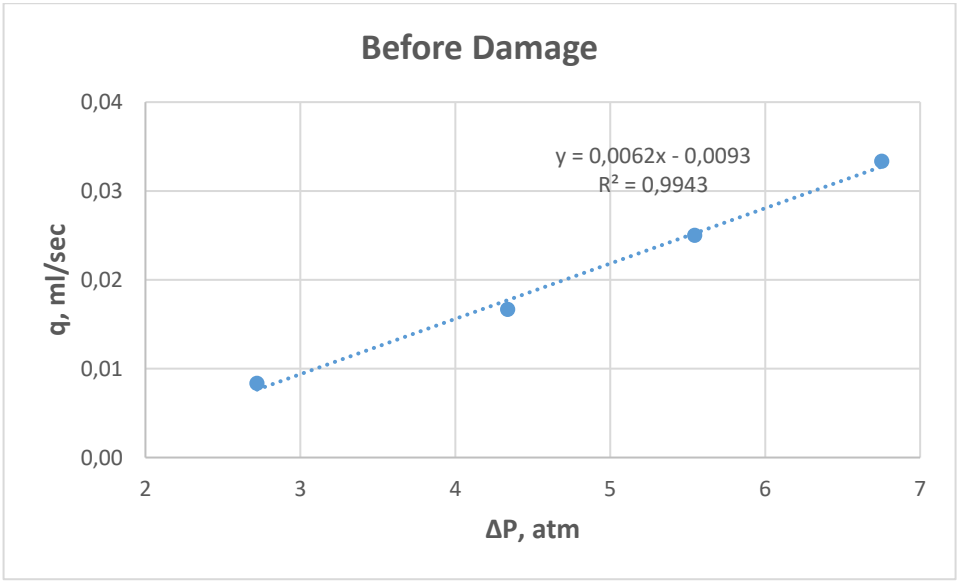

a)

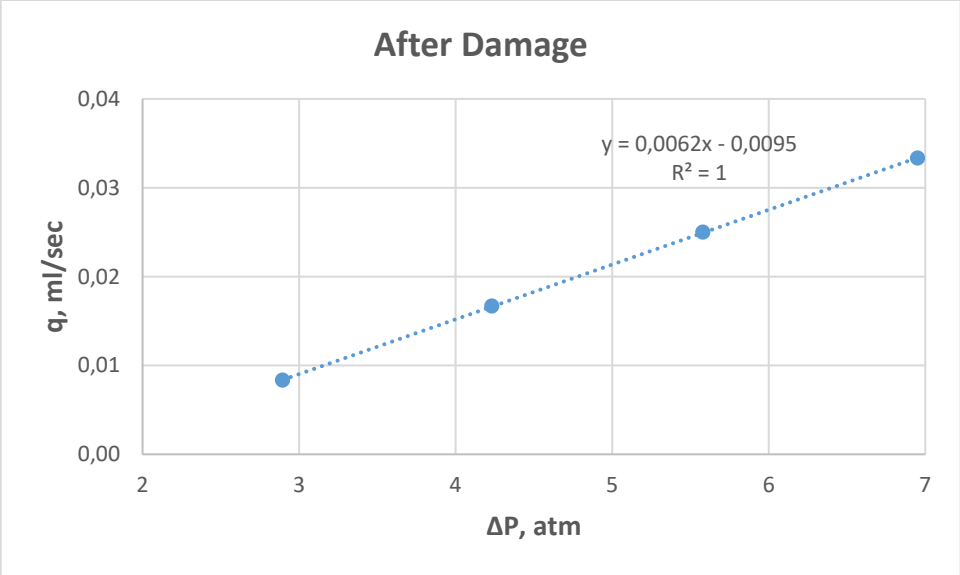

b)

Figure 5-33. Plotted q vs. ΔP Relationships Before (a) and After (b) Damage

5.5 Sag Test Results

Two static sag tests were performed to investigate the stability of base fluid and with added 0.075 wt% – the optimum sodium silicate concentration. The obtained sag factor for base fluid was 0.55 and for 0.075 wt% was 0.53. These results clearly showed that adding sodium silicate to the formula enhances its sag performance. According to the accepted standards in the industry, 0.53 is the sign of a good sag performance as discussed earlier. It can be concluded that the prepared drill-in fluid with 0.075 wt% sodium silicate concentration has a good sag performance at 300°F.

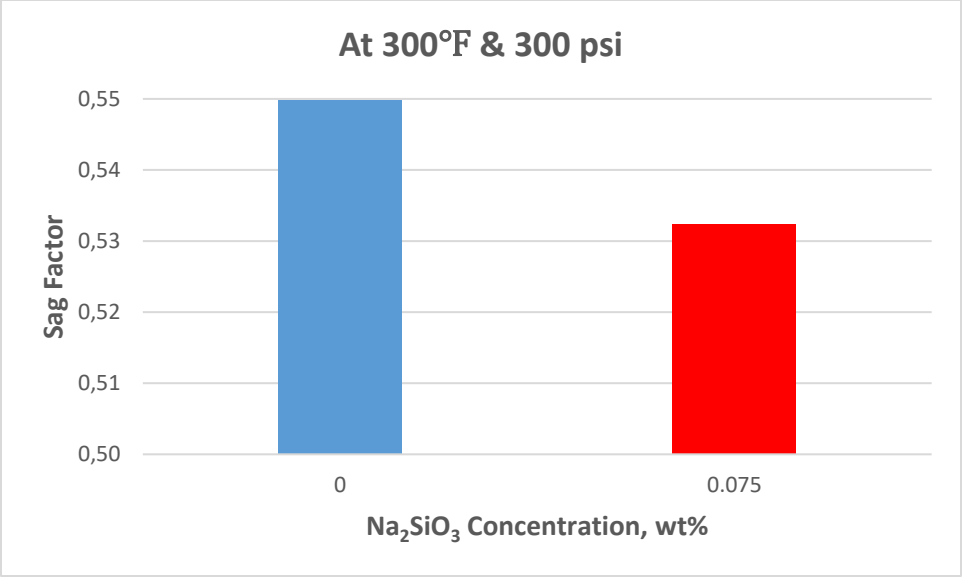

Figure 5-34. Sag Test Results with Base Fluid and 0.075 wt% Na_2SiO_3

Table 5-30. Summary of Sag Test Results with Base Fluid and 0.075 wt% Na_2SiO_3

Na_2SiO_3 Concentration, wt%	SG_{top}, g/ml	SG_{bottom}, g/ml	Sag Factor
0	2,08	2,54	0,55
0.075	2,02	2,3	0,53

5.6 Structural Analysis

The structural analysis has been done based on the slice-by-slice and cross-sectional views of the core samples as being before and after damage. The behavior of formed filter cakes with base fluid, 0.05, 0.075 and 0.1 wt% sodium silicate concentrations have been investigated. Regarding slice-by-slice analysis, 0.25” core samples have been sliced to six equal parts and the comparisons have been made for these parts. However, 2” core sample has been sliced to around fifty parts and the comparisons have been made for the selected

six slices – 1, 10, 20, 30, 40, 50, which are representing the other slices. This is simply because of difficulty in comparing all fifty slices.

5.6.1 Slice-by-slice Analysis and CT Numbers

As it is clearly observed from **Figs. 5-35a** and **5-35b**, the filtrate has invaded to all slices with base fluid. This has resulted in the highest increase in CT numbers, which ranges between 390 and 59 from first to the last slice as graphically illustrated in **Fig. 5-36**. **Figs. 5-37a** and **5-37b** are showing that fluid has invaded to the first four slices with 0.05 wt% sodium silicate concentration. This is following the CT numbers of base fluid with the slight decrease, which ranges between 313 and 51 that can be seen in **Fig. 5-38**. Investigating the behavior of 0.075 wt% on the slices before and after damage, in **Figs 5-39a** and **5-39b** obviously presents that 0.075 wt% has the least damage on the core sample. As it is shown, only first two slices have been invaded by filtrate. The bar chart of CT Numbers in **Fig. 5-40** shows that the damage rate with maximum difference is 150, while minimum is just 30. Analyzing **Figs. 5-41a** and **5-41b** demonstrate that fluid has invaded to first four slices with 0.1 wt% same as 0.05 wt%. However, the main difference is observed in the damage rate, where it is lower for 0.1 wt% than 0.05 wt% as presented in **Fig. 5-42**. The tabulated CT numbers of 0.25" core samples with each concentration have been provided in **Tables 5-31** and **5-32**. Moreover, **Fig. 5-43** graphically compares the average difference of CT numbers before and after damage for each concentration. 0.075 wt% sodium silicate concentration is the lowest with 60, while base fluid is the highest with around 150. **Table 5-33** provides the average difference of CT numbers before and after damage for each concentration.

When it comes to 2” core sample, result obtained is similar was obtained for 0.25” with 0.075 wt%. **Figs. 5-44a** and **5-44b** shows that only first slice has been affected with the fluid invasion. Since the length of the core is bigger compared to 0.25”, there is a significant decrease, about 5 times, in CT number differences starting from first to the last slice, where CT number of the last slice is 28 as given in **Fig. 5-45**. This is the prove of having very low fluid invasion through the core sample. Indeed, this result shows that achieving a good bridging could decrease a fluid invasion more and consequently, CT number could be even less than that value. The observations about 2” core sample proved the reason of getting 100% return permeability in case of 100% filter cake removal by not to invade to other slices except first. On the other hand, all the obtained CT numbers also proved the results of filtration tests and are consistent with them completely. **Table 5-34** summarizes the CT numbers of all slices of 2” core sample. It should also be stressed that 2” core sample is more representative than 0.25” with regard to near-wellbore conditions, which we observe that even with such not good bridging a fluid invasion becomes lower and lower with the increase of length. Therefore, the decrease in the near-wellbore damage can be investigated easily.

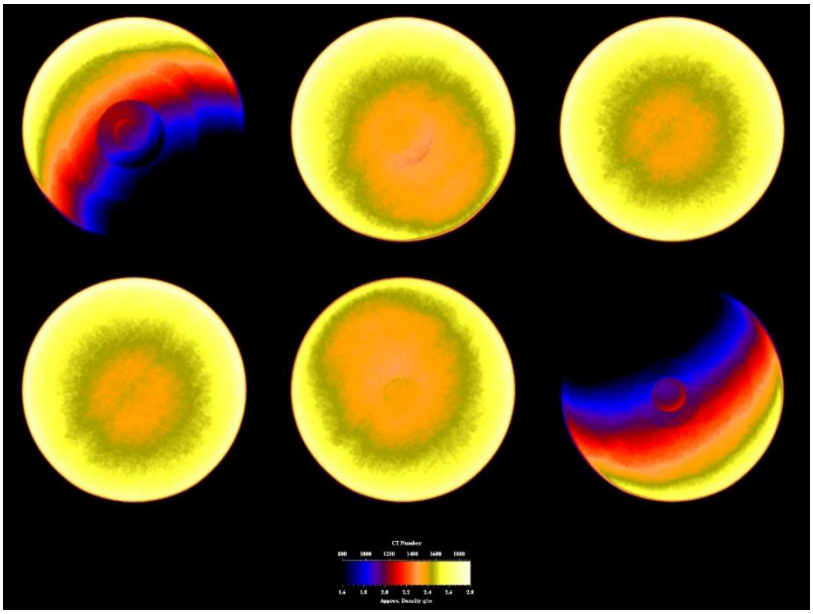

(a)

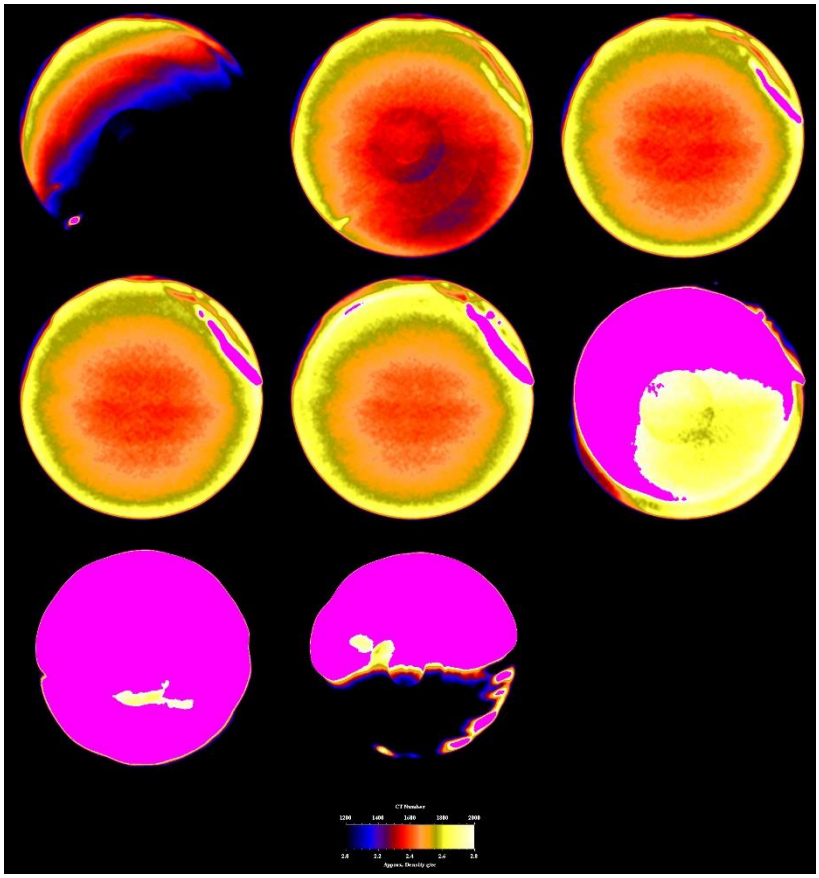

(b)

Figure 5-35. Slice-by-slice View of 0.25” Core Sample with Base Fluid Before (a) and After (b) Damage

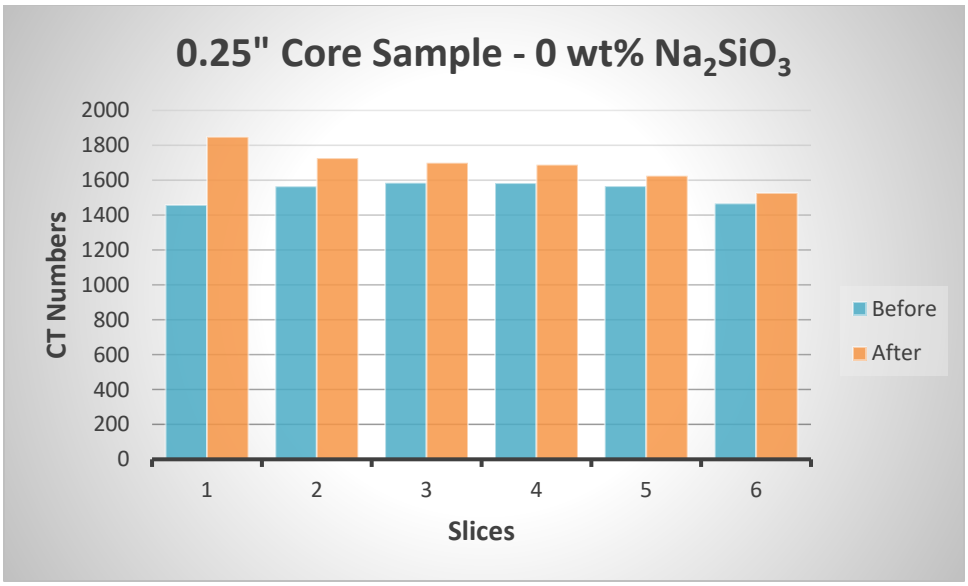

Figure 5-36. Comparison between CT Numbers of 0.25" Core Sample with Base Fluid Before and After Damage

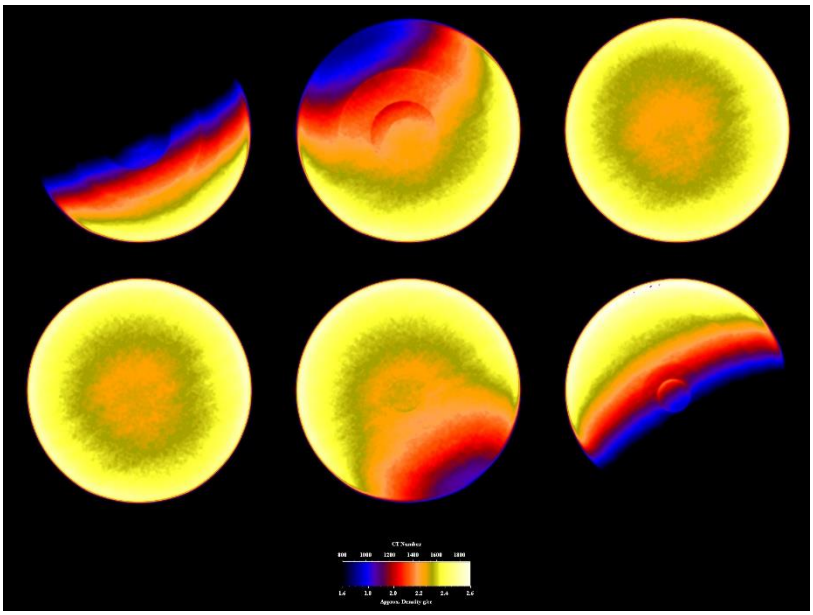

(a)

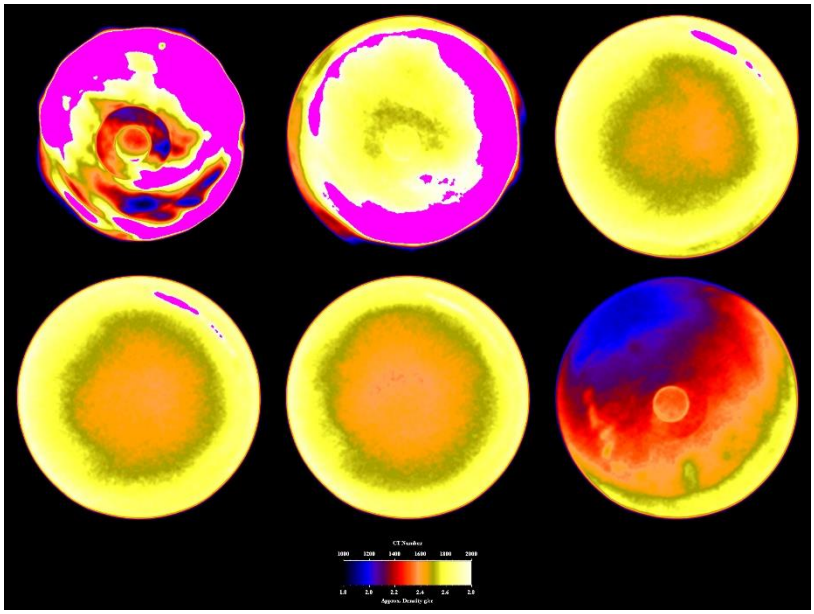

(b)

Figure 5-37. Slice-by-slice View of 0.25" Core Sample with 0.05 wt% Na_2SiO_3 Before (a) and After (b) Damage

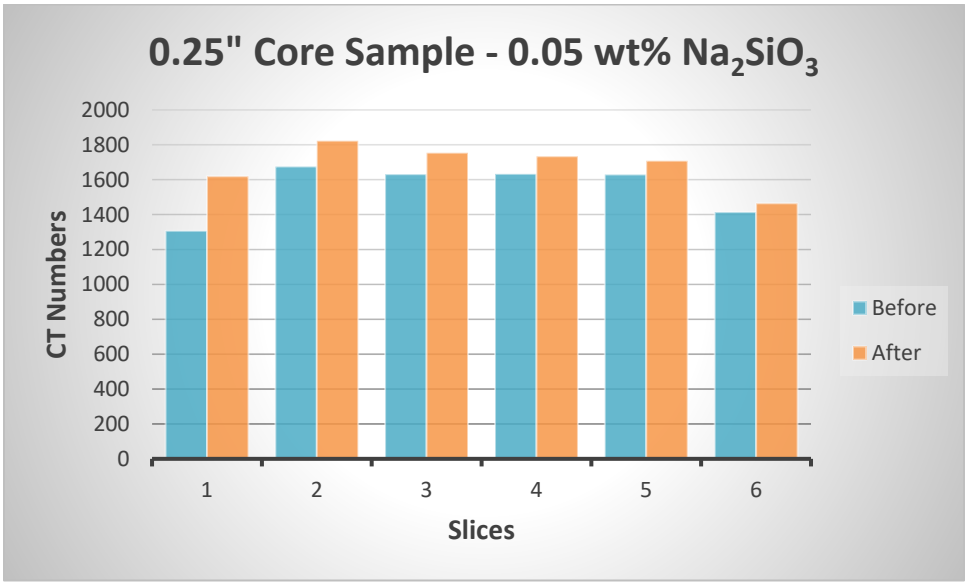

Figure 5-38. Comparison between CT Numbers of 0.25" Core Sample with 0.05 wt% Na_2SiO_3 Before and After Damage

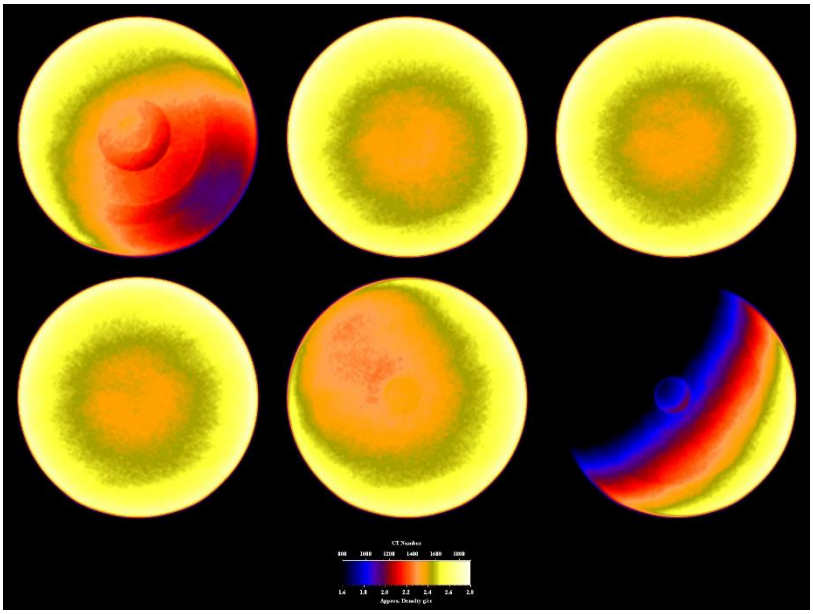

(a)

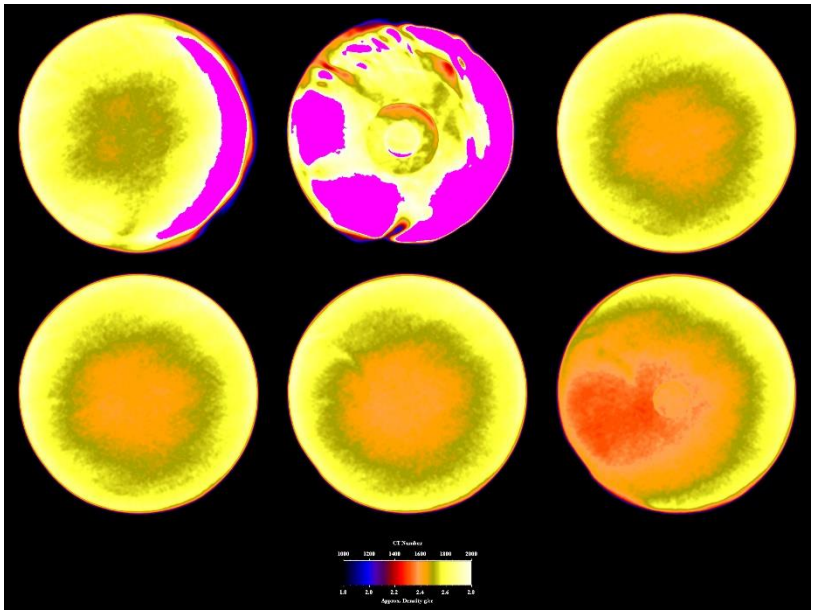

(b)

Figure 5-39. Slice-by-slice View of 0.25" Core Sample with 0.075 wt% Na_2SiO_3 Before (a) and After (b) Damage

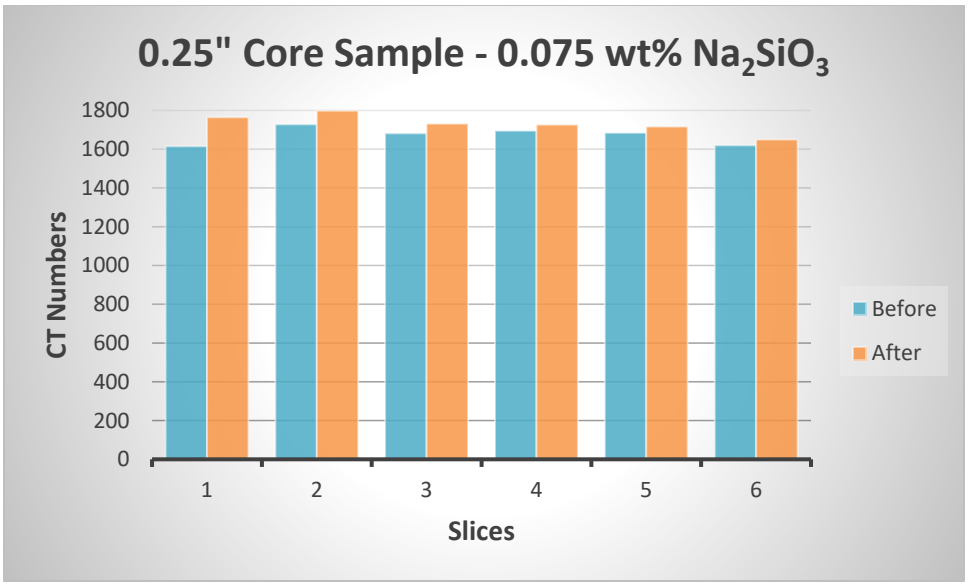

Figure 5-40. Comparison between CT Numbers of 0.25" Core Sample with 0.075 wt% Na_2SiO_3 Before and After Damage

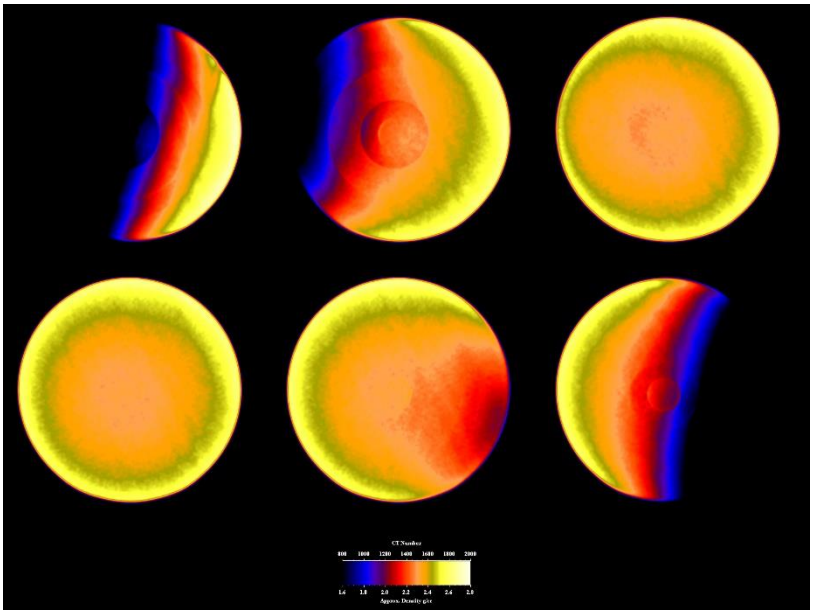

(a)

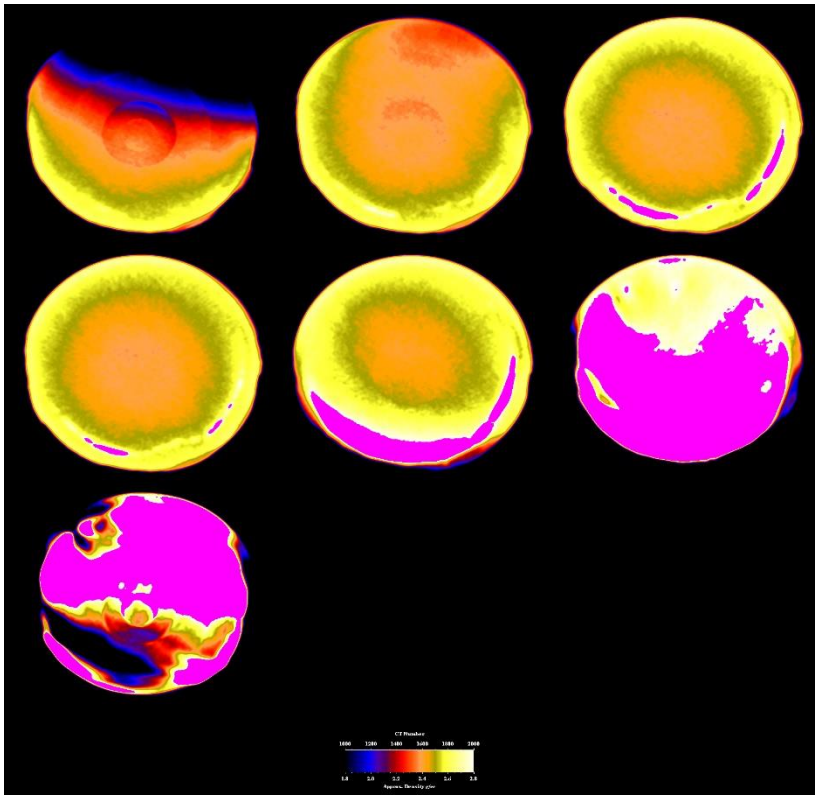

(b)

Figure 5-41. Slice-by-slice View of 0.25" Core Sample with 0.1 wt% Na_2SiO_3 Before (a) and After (b) Damage

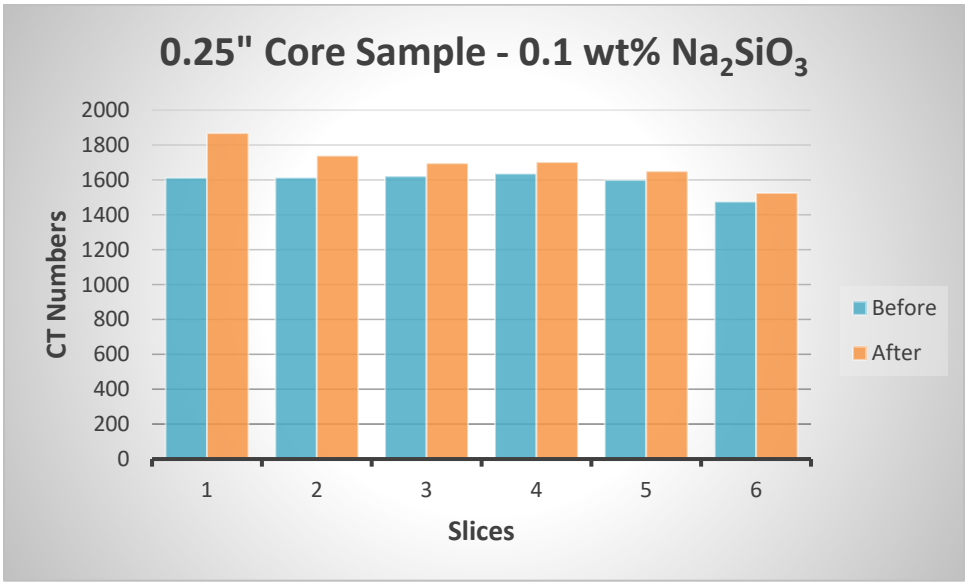

Figure 5-42. Comparison between CT Numbers of 0.25" Core Sample with 0.1 wt% Na_2SiO_3 Before and After Damage

Table 5-31. Summary of CT Numbers of 0.25" Core Sample with Base Fluid and 0.05 wt% Na_2SiO_3

Base Fluid				0.05 wt%			
Slice	Before Damage	After Damage	ΔCT Number	Slice	Before Damage	After Damage	ΔCT Number
1	1458	1848	390	1	1307	1620	313
2	1565	1726	161	2	1676	1824	148
3	1585	1700	114	3	1631	1754	123
4	1583	1689	105	4	1633	1734	100
5	1566	1625	59	5	1630	1708	78
6	1467	1526	59	6	1414	1465	51

Table 5-32. Summary of CT Numbers of 0.25" Core Sample with 0.075 and 0.1 wt% Na_2SiO_3

0.075 wt%				0.1 wt%			
Slice	Before Damage	After Damage	ΔCT Number	Slice	Before Damage	After Damage	ΔCT Number
1	1615	1765	150	1	1612	1867	256
2	1728	1798	70	2	1613	1738	125
3	1682	1731	49	3	1621	1695	74
4	1695	1727	32	4	1635	1701	66
5	1685	1717	32	5	1599	1649	50
6	1620	1650	30	6	1476	1525	49

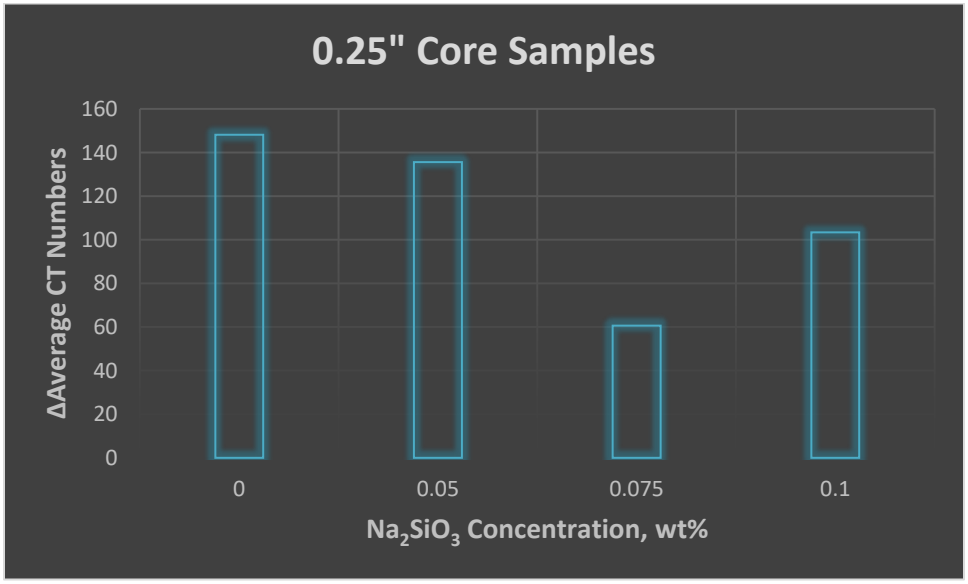

Figure 5-43. Average Difference of CT Numbers of 0.25" Core Samples Before and After Damage for each Na_2SiO_3 Concentration

Table 5-33. Summary of Average Difference of CT Numbers of 0.25" Core Samples Before and After Damage for each Na_2SiO_3 Concentration

Na_2SiO_3 Concentration, wt%	Average CT Number Before Damage	Average CT Number After Damage	ΔAverage CT Number
0	1538	1686	148
0.05	1549	1684	136
0.075	1671	1731	61
0.1	1593	1696	103

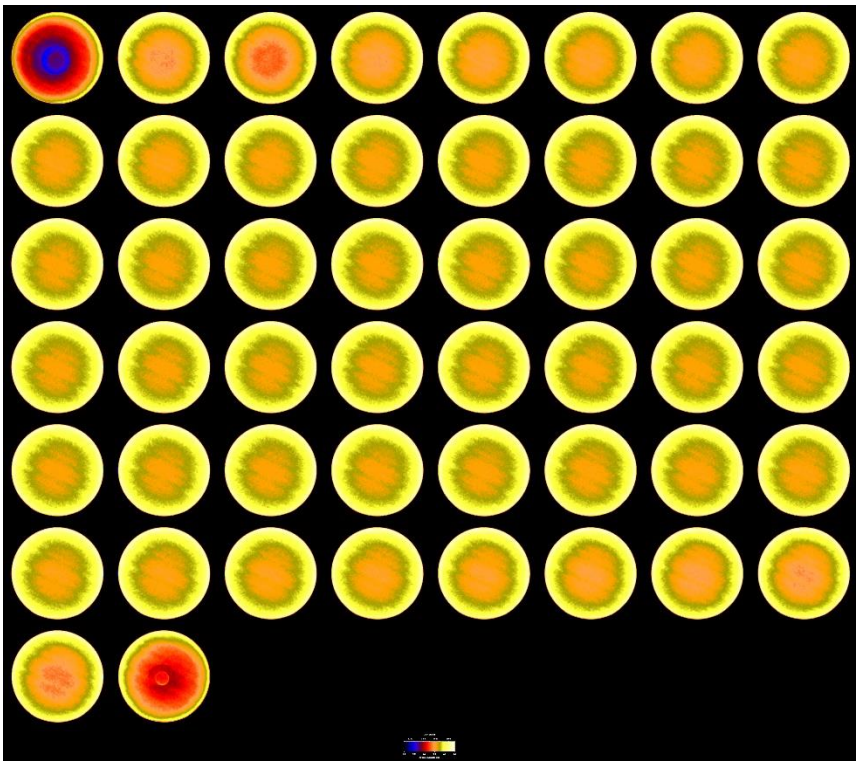

(a)

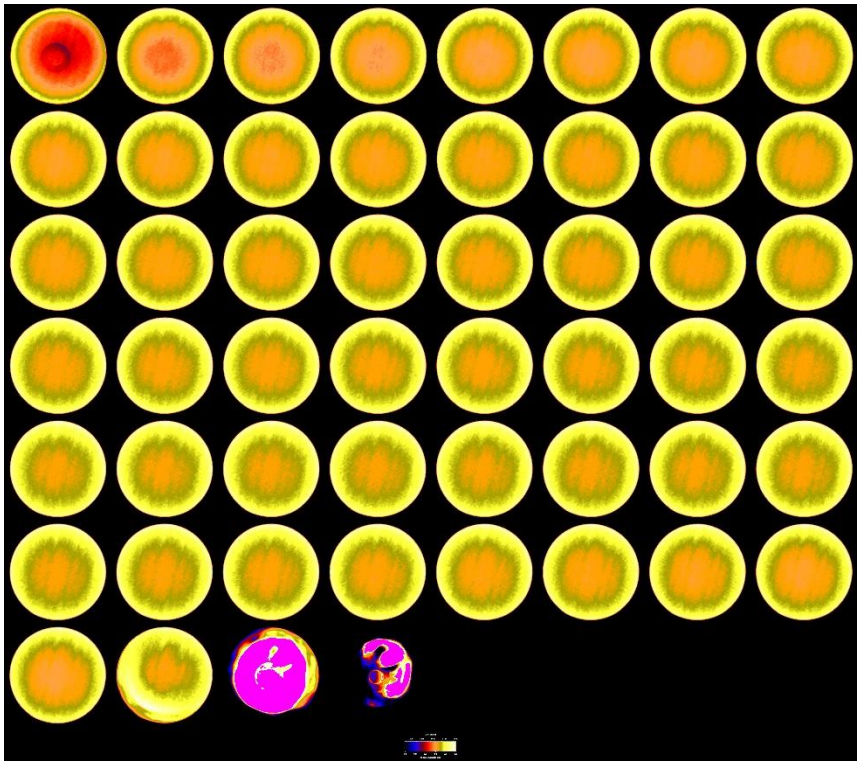

(b)

Figure 5-44. Slice-by-slice View of 2" Core Sample with 0.075 wt% Na_2SiO_3 Before (a) and After (b) Damage

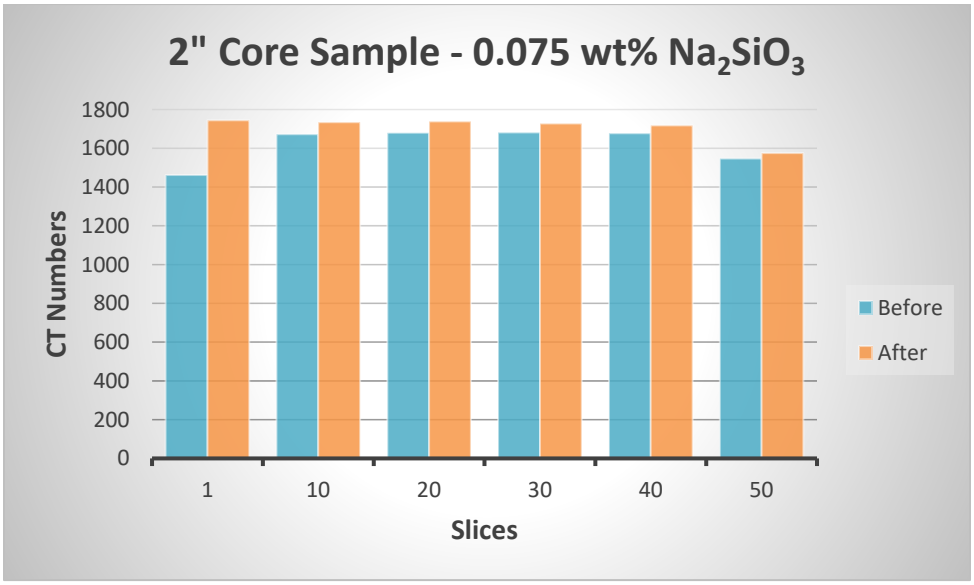

Figure 5-45. Comparison between CT Numbers of 2" Core Sample with 0.075 wt% Na_2SiO_3 Before and After Damage

Table 5-34. Summary of CT Numbers of 2" Core Sample with 0.075 wt% Na_2SiO_3

Slice	Before Damage	After Damage	ΔCT Number	Slice	Before Damage	After Damage	ΔCT Number	Slice	Before Damage	After Damage	ΔCT Number
1	1462	1744	282	11	1676	1736	60	21	1680	1738	57
2	1647	1766	119	12	1677	1737	59	22	1680	1736	56
3	1627	1709	82	13	1678	1737	59	23	1681	1735	54
4	1656	1716	60	14	1679	1738	59	24	1681	1733	53
5	1661	1721	60	15	1680	1739	59	25	1681	1731	50
6	1665	1726	61	16	1680	1739	59	26	1680	1732	52
7	1668	1728	60	17	1680	1739	59	27	1680	1730	50
8	1671	1731	60	18	1680	1739	59	28	1681	1729	48
9	1674	1733	59	19	1680	1739	58	29	1681	1728	48
10	1673	1734	62	20	1680	1739	58	30	1681	1727	46

Slice	Before Damage	After Damage	ΔCT Number	Slice	Before Damage	After Damage	ΔCT Number
31	1682	1726	45	41	1676	1717	40
32	1682	1726	44	42	1674	1715	41
33	1682	1725	43	43	1672	1713	41
34	1681	1723	42	44	1669	1709	40
35	1681	1723	42	45	1666	1706	39
36	1681	1722	41	46	1663	1701	38
37	1680	1721	41	47	1658	1695	37
38	1679	1721	41	48	1651	1686	35
39	1679	1719	41	49	1638	1669	30
40	1677	1718	40	50	1547	1575	28

5.6.2 Cross-sectional Analysis

Fig. 5-46 illustrates the cross-sectional view of typical 0.25" core sample before damage, whilst **Figs. 5-47**, **5-48**, **5-49** and **5-50** demonstrate the cross-sectional views of the damage of base fluid, 0.05, 0.075 and 0.1 wt% sodium silicate concentrations. By analyzing the figures, it is also observed that 0.075 wt% makes the lowest damage. Interestingly, the cross-sectional view of 0.1 wt% shows that filtrate invades from one side even more

compared than others. **Fig. 5-51** presents the cross-sectional view of 2” core sample before and after damage with 0.075 wt%. These graphs also prove how the fluid invasion is very low with 0.075 wt% on 2” core. All these results are compatible with the results of slice-by-slice views.

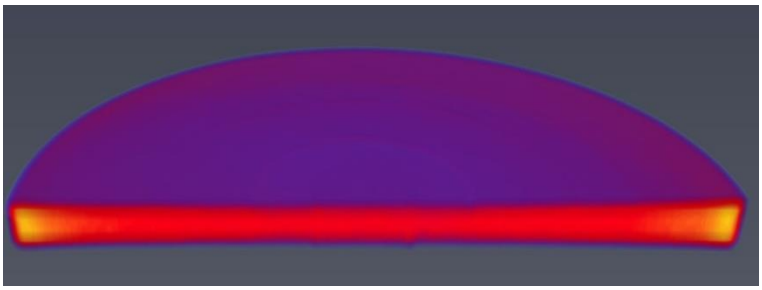

Figure 5-46. Cross-sectional View of Typical 0.25” Core Sample Before Damage

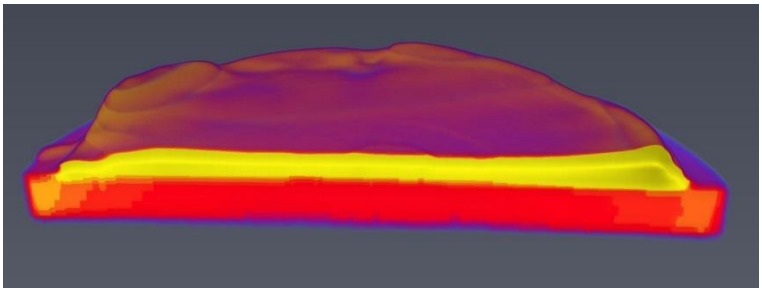

Figure 5-47. Cross-sectional View of 0.25” Core Sample with Base Fluid After Damage

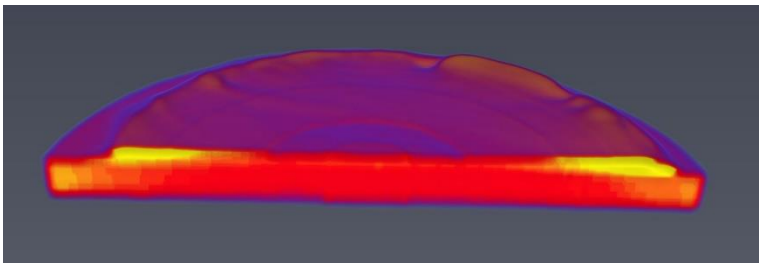

Figure 5-48. Cross-sectional View of 0.25” Core Sample with 0.05 wt% Na_2SiO_3 After Damage

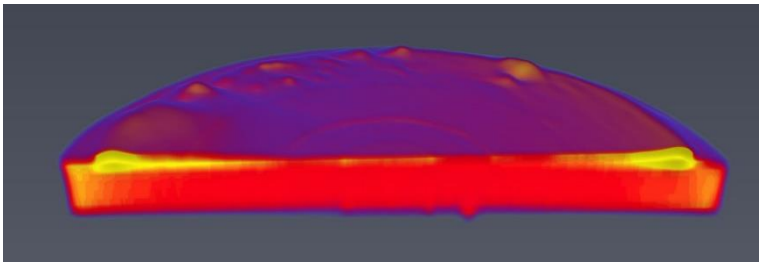

Figure 5-49. Cross-sectional View of 0.25" Core Sample with 0.075 wt% Na_2SiO_3 After Damage

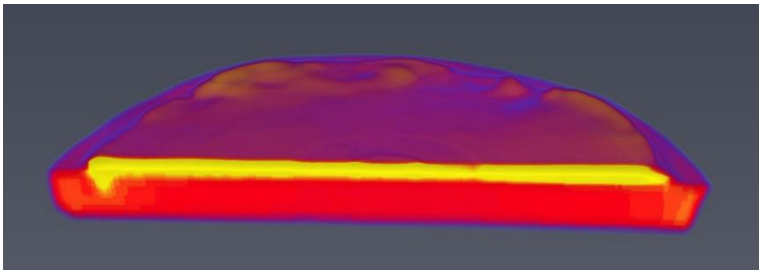

Figure 5-50. Cross-sectional View of 0.25" Core Sample with 0.1 wt% Na_2SiO_3 After Damage

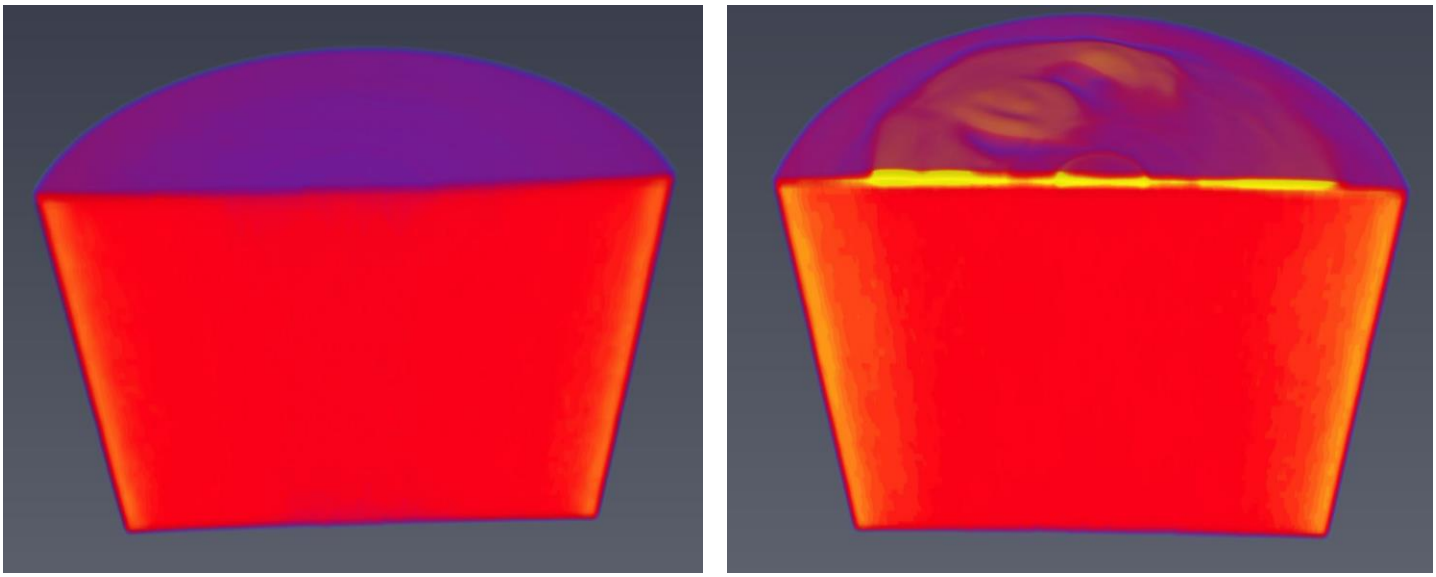

Figure 5-51. Cross-sectional View of 2" Core Sample with 0.075 wt% Na_2SiO_3 Before (left) and After (right) Damage

5.7 Mechanism of 0.075 wt% Na_2SiO_3

The mechanism of 0.075 wt% Na_2SiO_3 should be explained with two different approaches by combining and considering them together. They have been developed by chemists for processing of barite. However, these methods can be implemented to petroleum engineering as well. Since barite is the only non-soluble solid in the formulated drill-in fluid and the different concentrations of Na_2SiO_3 is the additive that shows an improvement through all the experiments, both approaches were considered together to explain our case as well. These approaches are barite flotation recovery with respect to Na_2SiO_3 concentrations and the solubility concentration of silicate with the PH value of the solution.

5.7.1 Barite Flotation Recovery

Flotation is a process that separates hydrophobic particles from hydrophilic ones. Na_2SiO_3 is one of the commonly used reagent for barite recovery in mining industry. Since it is acting as a dispersant, barite particles are suspended by Na_2SiO_3 and cannot settle down easily. Therefore, they start to float by being separated from other impurities. In 2015, Bulatovic offered the relationship between barite flotation recovery and Na_2SiO_3 concentrations per one ton barite as shown in **Fig. 5-52**. So, it means maximum $Na_2SiO_3/BaSO_4$ ratio is 0.002. In our case, the amount of 0.075 wt% Na_2SiO_3 and barite are 0.66 and 417 g in 360 ml drill-in fluid, respectively.

$$Na_2SiO_3/BaSO_4 = 0.675\ g/417\ g = 0.0016$$

The cross-section of the ratio of 0.075 wt% with the relationship curve shows that barite recovery is 91%, This percentage is desirable for us, because rest of the sank barite – 9%

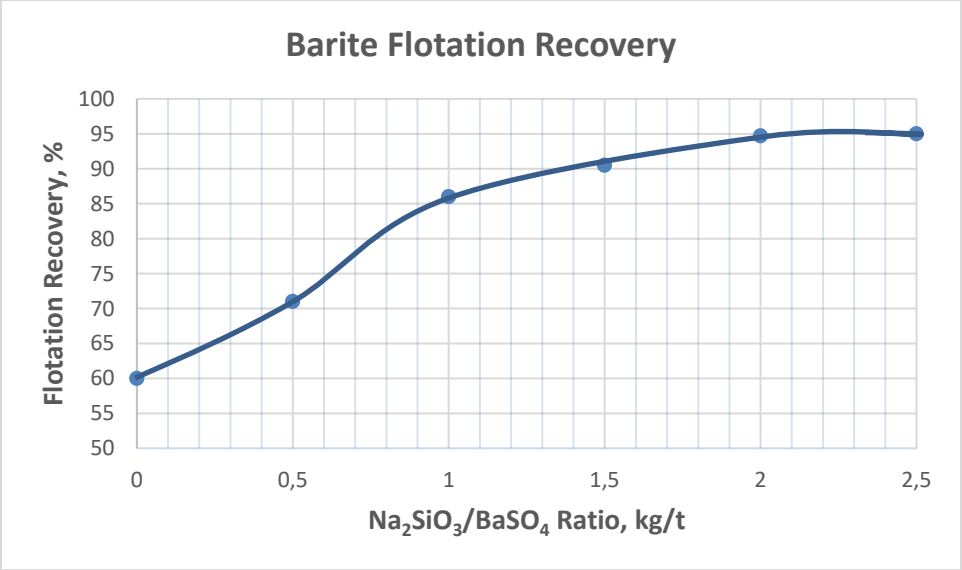

Figure 5-52. Barite Flotation Recovery with respect to $Na_2SiO_3/BaSO_4$ Ratio

is enough to form very thin filter cake. This relationship also explains the reason of having higher thickness of filter cake with 0.05 wt%. The ratio is 0.0011 with 0.05 wt%, which the recovery becomes around 86%. The decreased recovery means the increased sank barite and consequently, the increased filter cake thickness. However, this consideration is not enough to make a conclusion, because of higher concentrations, as in fact, still barite recovery can be increased up to 95%. The question can be raised "Why not to form more thinner filter cake with 5% sank barite by having 95% recovery?". To answer to this question, the second approach should be included.

5.7.2 Solubility Concentration of Silica with PH

The general formula of sodium silicate is $Na_2O{\cdot}SiO_2$. It has two parts: Na_2O and SiO_2. When Na_2SiO_3 is added to the aqueous solution, Na_2O enters to the reaction with water immediately:

$$Na_2O + H_2O \leftrightarrow 2NaOH \text{ (Caustic Soda)}$$

Caustic soda is obtained with this reaction and it dissolves in water easily. In brief, we are losing Na_2O and left with the most complex part – SiO_2 (silica).

To explain the solubility behavior of silica in water, Ives introduced an empirical correlation in 1984 as shown in **Fig. 5-53**.

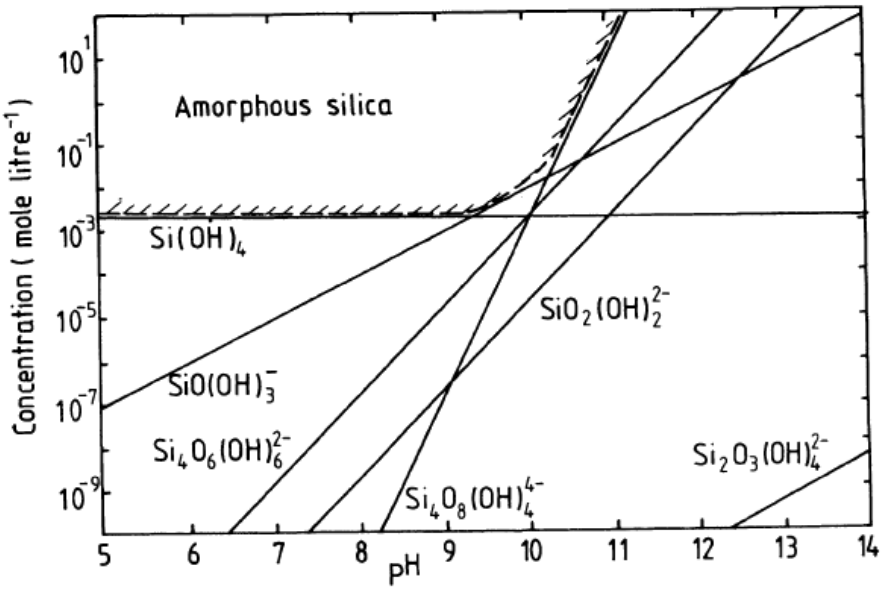

Figure 5-53. Solubility Concentration of SiO_2 with respect to PH

He mentioned that Na_2SiO_3 enters to the polymerization process if it can avoid from amorphous silica. Since amorphous silica dissolves in water slowly and needs 340℃ temperature, it takes long time. Therefore, it can't enter to the reaction with water easily and polymerization doesn't happen at the end. By his correlation, he presented that the rate of polymerization depends on the PH and temperature of the solution and silica

concentration in Na_2SiO_3. For our drill-in fluid PH = 10 regardless of Na_2SiO_3 concentration as it has been shown in rheology results section. The temperature is 300°F. The silica concentration in 0.075 wt% Na_2SiO_3 is determined with mol/litr unit as in below:

Molar Weight of Na_2SiO_3 = 122 g/mol

Molar Weight of SiO_2 = 60 g/mol

Weight of 0.075 wt% Na_2SiO_3 in 360 ml (0.36 litr) = 0.675 g

$$Weight\ of\ Silica = \frac{60 \cdot 0.675}{122} = 0.33\ g$$

$$Silica\ Concentration = \frac{0.33}{0.36 \cdot 60} = 0.015\ mol/litr$$

The cross-section of PH = 10 and Silicate Concentration = 0.015 mol/litr shows that we just could avoid amorphous silica region and the last polymer specie of silica is $Si_4O_8(OH)_4^{4-}$. Therefore, equilibrium reaction will be as in below:

$$SiO_2 + H_2O \leftrightarrow Si(OH)_4$$

$$Si(OH)_4 + OH^- \leftrightarrow SiO(OH)_3^- + H_2O$$

$$SiO(OH)_3^- + OH^- \leftrightarrow SiO_2(OH)_2^{2-} + H_2O$$

$$Si(OH)_4 + 2OH^- \leftrightarrow SiO_2(OH)_2^{2-} + H_2O$$

$$Si(OH)_4 + 2OH^- \leftrightarrow Si_4O_6(OH)_6^{2-} + 6H_2O$$

$$4Si(OH)_4 + 4OH^- \leftrightarrow Si_4O_8(OH)_4^{4-} + 8H_2O$$

The possible siloxane bonds of $Si_4O_8(OH)_4^{4-}$ becomes:

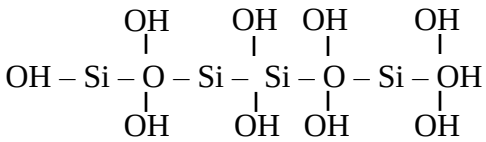

The interaction between barite and polymerized $Si_4O_8(OH)_4^{4-}$ resulted in the suspension of barite particles, which keeps barite in colloid. The last part of the polymerization process is gelation. At this stage, when the gelly polymer is exposed to the ΔP, it is flushed out of the solution and plugs the formation face by making a film-like barrier. As a result, fluid invasion minimizes and solid invasion completely stops because of polymerization effect of 0.075 wt% Na_2SiO_3.

However, at higher concentrations than 0.075 wt%, amorphous silica effect is observed. $Na_2SiO_3/BaSO_4$ ratio of 0.1 wt% is around 0.0022, with which maximum barite flotation recovery – 95% can be obtained. Although, maximum recovery is obtained, but the filter cake thickness also increases with 0.1 wt% Na_2SiO_3. The silica concentration is 0.02 mol/litr and it can be clearly observed from the silica solubility correlation that amorphous silica effect shows itself starting with this concentration at PH = 10. Since amorphous silica dissolves in water slowly, its ions bind together and make a very permeable layer between barite and the bridging material – $CaCO_3$. Moreover, as the density of silica is 2.65 g/cc, which it is close to the density of $CaCO_3$ (2.71 g/cc), it settles down and doesn't let $CaCO_3$ to make a good bridging by taking its place. As a result, fluid finds an easy path through amorphous silica to enter to the formation and the amount of invasion increases. At the end, this causes to the settling of barite particles and increase of filter cake thickness because of loosing more fluid. To avoid amorphous effect at 0.1 wt%, PH of the drill-in

fluid has to be increased. On the other hand, having high PH is not preferable, because of corrosion issue. This limitation should also be taken into account.

Additionally, it should also be noted, no segregation occurs for both polymerization and amorphous silica effect in aqueous solution, due to being lost of Na_2O. However, observing the original structure of Na_2SiO_3 without any reaction under microscope shows that Na^+ ions make clusters by being surrounded with O^{2-} ions. Having no segregation in aqueous solution is another prove why barite particles can't settle down easily and suspend as colloid.

In conclusion, polymerization effect at $\leq$0.075 wt% Na_2SiO_3 and amorphous silica effect at >0.075 wt% are observed at PH = 10. Polymerization effect is the evidence of minimizing fluid invasion to the possible lowest level and obtaining 100% return permeability by having zero-solid invasion with 0.075 wt% Na_2SiO_3.

CHAPTER 6

CONCLUSIONS AND RECOMMENDATIONS

6.1 Conclusions

The aim of this work was to prepare non-damaging drilling fluid for tight gas reservoirs that should reduce fluid invasion and eliminate water blockage problem and enhance well productivity by obtaining high return permeability. The findings showed that we reached to our goal even with zero-solid invasion and 100% return permeability. Based on the experimental results, below conclusions were made:

- ✓ Up to 2 wt% concentration, sodium silicate doesn't have any significant effect on density and PH
- ✓ Eliminating high temperature fluid loss additive resulted in fully deflocculation at 300°F under 300 psi, in which both PV and YP were reduced for lower sodium silicate concentrations. Similarly, 10-second and 10-minute gel strength also decreased. 0.075 wt% showed higher PV, YP and gel strength compared with other low concentrations
- ✓ The filtrate volume and filter cake thickness was reduced by 53% and 65% with 0.075 wt% sodium silicate through 0.25" core sample, respectively.
- ✓ The minimized fluid invasion is the evidence for the elimination of water blockage problem of the wells drilled into tight gas reservoirs

- ✓ The formed 0.7 mm filter cake is very thin and can be completely removed by washing it with 15 wt% HCl
- ✓ High concentrations have a reverse effect on filtration, with which both volume and filter cake thickness increased
- ✓ Bridging has an important effect on filtration test. Poor bridging reduces the effect of Na_2SiO_3. The experiment with 0.075 wt% sodium silicate on 2" core sample presented slightly higher fluid loss volume and filter cake thickness due to a poor bridging
- ✓ Based on the filtration test results, 0.075 wt% sodium silicate concentration was determined as an optimum
- ✓ Measured permeability values of 2" core sample before and after damage remained constant at 1.3 mD, which means return permeability is 100% in case of 100% filter cake removal
- ✓ The highest solubility result obtained with 4 wt% sodium silicate. It improved the barite solubility method of Ba geri et al (2015) up to 82% by acting as a catalyst. This means filter cake removal efficiency will also increase up to 90-95%. In the worst scenario, if the thin filter cake couldn't be formed, this method can be used and around 95% return permeability can be obtained
- ✓ 0.075 wt% concentration improved sag performance with 0.53, compared to the value of base fluid – 0.55.
- ✓ Slice-by-slice and cross-sectional structural analysis and the obtained CT numbers confirmed the filtration test results.

- ✓ Barite flotation recovery and solubility concentration of silica with PH empirical correlations should be considered together to optimize sodium silicate concentration
- ✓ Polymerization effect of 0.075 wt% sodium silicate was the mechanism for minimized fluid and zero-solid invasion with this concentration. It proved obtaining of 100% return permeability
- ✓ Sodium silicate concentrations higher than 0.075 wt% give poor results due to amorphous silica effect.

6.2 Future Work Recommendations

The followings are recommended for future work:

- ❖ To observe the effect of sodium silicate on calcium carbonate and manganese tetra oxide-weighted water-based drilling fluids
- ❖ To optimize the enzyme concentration for starch so that to perform filter cake removal experiment with 20 wt% K-DTPA + 6 wt% catalyst + 7 wt% enzyme for XC polymer + 4 wt% sodium silicate
- ❖ To check the effect of more finer bridging materials on the filtration tests with tight core samples depending on their permeabilities.

References

[1] Al-Abdullatif Z.A., Al-Yami A.S., Wagle W., Bubshait A.S. 2015. Development of New Kill Fluids with Minimum Sagging Problems for High-Pressure Jilh Formation in Saudi Arabia. *Saudi Aramco Journal of Technology*.

[2] Al-Yami A.S., Nasr-El-Din H.A., Al-Shafei M., Bataweel M.A. 2010. Impact of Water-Based Drilling-in Fluids on Solids Invasion and Damage Characteristics. *SPE Production & Operation* **25**(1):40-49.

[3] Amanullah Md., Allen T. 2013. Extended Aramco Method – Its Technico-Economic Significance in Non-Damaging Drill-in Fluid Design. SPE/IADC Paper 166694 presented at the SPE/IADC Middle East Drilling Technology Conference and Exhibition, 7-9 October, Dubai, UAE.

[4] Ba geri B.S., Mahmoud M. 2017. Zero-Invasion Acidic Drilling Fluid. Pub No.: US9657214 B2.

[5] Ba geri B.S., Mahmoud M., Abdulraheem A., Al-Mutairi S.H., Elkatatny S.M., Shawabkeh R.A. 2016. Single Stage Filter Cake Removal of Barite Weighted Water Based Drilling Fluid. *J. Pet. Sci. Eng.* Vol. **149**, p. 476-484.

[6] Barry M.M., Jung Y., Lee J., Phuoc T. X., Chyu M.K. 2015. Fluid Filtration and Rheological Properties of Nanoparticle Additive and Intercalated Clay Hybrid Bentonite Drilling Fluids. *J. Pet. Sci. Eng.* Vol. **127**, p. 338-346.

[7] Bulatovic S.M. 2015. Handbook of Flotation Reagents: Chemistry, Theory and Practice – Flotation of Industrial Minerals. Vol. **3**. Elsevier, Amsterdam, Netherland.

[8] Caenn R., Darley H.C.H., Gray G.R. Composition and Properties of Drilling and Completion Fluids. 6th Edition. 2011. Gulf Professional Publishing, Massachusetts, USA.

[9] Cobianco S., Bartosek M., Lezzi A., Guarneri A. 2001. How to Manage Drill-in Fluid Composition to Minimize Fluid Losses During Drilling Operations. *SPE Drilling & Completion* **16**(3):154-158.

[10] Conners J.H., Bruton J.R. 1979. Use of Clear Brine Completion Fluids as Drill-in Fluids. SPE Paper 8223 presented at the 54th SPE Annual Fall Technical Conference and Exhibition, 23-26 September, Las Vegas, Nevada, USA.

[11] Dobson J.W., Harrison J.C., Hale A.H., Lau H.C., Bernardi Jr.L.A., Kielty J.M., Albrecht M.S., Bruner S.D. 2000. Laboratory Development and Field Application of a Novel Water-Based Drill-in Fluid for Geopressured Horizontal Wells. *SPE Drilling & Completion* **15**(2):105-111.

[12] El Bialy M., Mohsen M., Ezell R.G., Abdulaziz M.E., Kompantsev A., Khakimov A., Ganizade F., Ashoor A. 2011. Untilization of Non-Damaging Drilling Fluid Composed of Potassium Formate Brine and Manganese Tetra Oxide to Drill Sandstone Formation in Tight Gas Reservoir. SPE/IADC Paper 147983 presented at the SPE/IADC Middle East Drilling Technology Conference and Exhibition, 24-26 October, Muscat, Oman.

[13] El Essawy W.M., Hamzah R., Malik M.M., Knox D., Monem M.R., Oswald R.J. 2004. Novel Application of Sodium Silicate Fluids Achieves Significant Improvement of the Drilling Efficiency and Reduce the Overall Well Costs by Resolving Borehole Stability Problems in East Africa Shale. SPE Paper 88008 presented at the IADC/SPE Asia Pacific Drilling Technology Conference and Exhibition, 13-15 September, Kuala Lumpur, Malaysia.

[14] Fraser L.J., Reid P.I., Williamson L.D., Enriquez Jr.F.P. 1999. Formation-Damaging Characteristics of Mixed Metal Hydroxide Drill-in Fluids and a Comparison with Polymer-Base Fluids. *SPE Drilling & Completion* **14**(3):178-184.

[15] Gaiser C.J. 1969. Amorphous Sodium Silicate Having Inherent Binding Properties and Method of Producing Same. Pub. No.: US3450494 A.

[16] Han L., Clinch D., van der Zwaag C., Galletti E., Fornasier F., Estevez F., McMillan N., Green J., Patey I. 2012. Customizing Drill-in Fluid for Peregrino Project in Brazil: Laboratory Development and Field Experience. SPE Paper 151824 presented at the SPE International Symposium and Exhibition on Formation Damage Control, 15-17 February, Lafayette, Louisiana, USA.

[17] Hossain M.E., Al-Majed A.A. 2015. Fundamentals of Sustainable Drilling Engineering. Scrivener Publishing, Massachusetts, USA.

[18] Huang T., Crews J.B., Clark D.E. 2011. Protecting the Reservoir with Surfactant Micellar Drill-in Fluids in Carbonate-Containing Formations. *SPE Drilling & Completion* **26**(4):492-498.

[19] Ismail A.R., Aftab A., Ibupoto Z.H., Zolkifile N. 2016. The Novel Approach of the Enhancement of Rheological Properties of Water-Based Drilling Fluids by Using Multi-Walled Carbon Nanotube, Nanosilica and Glass Beds. *J. Pet. Sci. Eng.* Vol. **139**, p. 264-275.

[20] Ives K.J. The Scientific Basis of Flotation. 1984. Martinus Nijhoff Publishers, The Hague, Netherland.

[21] Lakatos I., Bodi T., Lakatos-Szabo J., Szentes G. 2010. Mitigation of Formation Damage Caused by Water-Based Drilling Fluids in Unconventional Gas Reservoirs. SPE Paper 127999 presented at the SPE International Symposium and Exhibition on Formation Damage Control, 10-12 February, Lafayette, Louisiana, USA.

[22] Lake L.W., Fanchi J.R., Mitchell R.F., Arnold K.E., Clegg J.D., Holstein E.D., Warner Jr.H.R. 2007. Petroleum Engineering Handbook. Vol. **6**. Society of Petroleum Engineers, Texas.

[23] Mahmoud O., Nasr-El-Din H.A., Vryzas Z., Kelessidis V.C. 2016. Nanoparticle-Based Drilling Fluids for Minimizing Formation Damage in HP/HT Applications. SPE Paper 178949 presented at the SPE International Conference and Exhibition on Formation Damage Control, 24-26 February, Lafayette, Louisiana, USA.

[24] Mandal N.G., Jain U.K., Anil Kumar B.S., Gupta A.K. 2006. Nondamaging Drilling Fluid Enhances Borehole Quality and Productivity in Conventional Wells of Mehsana Asset, North Cambay Basin. SPE/IADC Paper 102128 presented at the SPE/IADC Indian Drilling Technology Conference and Exhibition, 16-18 October, Mumbai, India.

[25] Marinakis K.I., Shergold H.L. 1985. Influence of Sodium Silicate Addition on the Adsorption Oleic Acid by Fluorite, Calcite and Barite. *Int. J. Miner. Process.* Vol. **14**, p. 177-193.

[26] Meunier M. 2012. Industrial Applications of Molecular Simulations. CRC Press, Boca Raton, Florida, USA.

[27] McDonald M. 2012. A Novel Potassium Silicate for Use in Drilling Fluids Targeting Unconventional Hydrocarbons. SPE Paper 162180 presented at the SPE Canadian Unconventional Resources Conference, 30 October-1 November, Calgary, Alberta, Canada.

[28] Nasr-El-Din H.A., Lynn J.D., Al-Dossary K.A. 2002. Formation Damage Caused by a Water Blockage Chemical: Prevention Through Operator Supported Test Programs. SPE Paper 73790 presented at the SPE International Symposium and Exhibition on Formation Damage Control, 20-21 February, Lafayette, Louisiana, USA.

[29] Rao M.A. Rheology of Fluid and Semisolid Foods. 2nd Edition. 2007. Springer Science + Business Media LLC, New York, USA.

[30] Recommended Practice for Field Testing Water-Based Drilling Fluids. API Recommended Practice 13B-1. 3rd Edition. December 2003.

[31] Sanchez A., Audibert-Hayet A., Rousseau L. 2004. Influence of Drill-in Fluids Composition on Formation Damage. *SPE Journal* **9**(4):403-410.

[32] Siddiqui M.A., Nasr-El-Din H.A. 2005. Evaluation of Special Enzymes as a Means to Remove Formation Damage Induced by Drill-in Fluids in Horizontal Gas Wells in Tight Reservoirs. *SPE Production & Facilities* **20**(3):177-184.

[33] Tropea C., Yarin A.L., Foss J.F. Springer Handbook of Experimental Fluid Mechanics. Springer-Verlag Berlin Heidelberg, Berlin, Germany 2007.

[34] Van Zanten R., Horton D., Tanche-Larsen P. 2011. Engineering Drill-in Fluids to Improve Reservoir Producibility. SPE Paper 143845 presented at the SPE European Formation Damage Conference, 7-10 June, Noordwijk, The Netherlands.

[35] William J.K.M., Ponmani S., Samuel R., Nagarajan R., Sangwai J.S. 2014. Effect of CuO and ZnO Nanofluids in Xanthan Gum on Thermal, Electrical and High Pressure Rheology of Water-Based Drilling Fluids. *J. Pet. Sci. Eng.* Vol. **117**, p. 15-27.

[36] Yadav P., Kosandar B.A., Yadhav P.B., Ishaq L.G., Addagalla A.K.V, Al-Rabah M. 2015. Customized High-Performance, Water-Based Mud for Unconventional Reservoir Drilling. SPE Paper 172603 presented at the SPE Middle East Oil & Gas Show and Conference, 8-11 March, Manama, Bahrain.

[37] Young S., Friedheim J. 2013. Environmentally Friendly Drilling Fluids for Unconventional Shale. Paper OMC-2013-102 presented at the 11th Offshore Mediterranean Conference and Exhibition, 20-22 March, Ravenna, Italy.

[38] Zabala E., Luongo A., Parra E., Mendez J., Arocha J., Carrasquero J. 1999. Field Experiences with Stable Mul, a Non Damaging Micro Emulsion Used as Drilling Fluid for Heavy Oil Formations in Venezuela. SPE Paper 54113 presented at the SPE International Thermal Operations and Heavy Oil Symposium, 17-19 March, Bakersfield, California, USA.

Vitae

Name	: Tural Jafarov
Nationality	: Azerbaijani
Date of Birth	: 5/6/1990
Email	: tural.ceferov@gmail.com
Address	: Baku, Azerbaijan
Academic Background	: KFUPM - MSc Petroleum Engineering, May 2017, Dhahran, Saudi Arabia Khazar University – MSc Petroleum Engineering, June 2014, Baku, Azerbaijan Azerbaijan State University of Oil & Industry – BSc Petroleum Engineering, June 2011
Work Experience	: KFUPM – Teaching Assistant, September 2016 – June 2017 Baker Hughes (Azerbaijan) – Field Engineer I – Open Hole Completion, May 2013 – May 2014 AMEC Foster Wheeler (Azerbaijan) – Graduate Mechanical Engineer, November 2012 – May 2013

Schlumberger (Azerbaijan) – Field Engineer – Open Hole Completion (intern), September – October 2011

McDermott Caspian Contractors Inc. (Azerbaijan) – Field Engineer (intern), August – September 2011

Trainings : PETREL, KFUPM, November 2016

International Well Control Forum Level 1 Programme, June 2016

CMG-IMEX Modelling. KFUPM, February 2016

Engineering Development Program I, Baker Hughes. September – October 2013

Leadership for Industrial Professionals, Caspian Engineers Society, April 2012

Skills : Programming Languages – MATLAB

Software Packages – PETREL, Eclipse, CMG, PIPESIM

Languages – Azerbaijani, English, Turkish, Russian

Publication : Critical Review of the Existing Liquid Loading Prediction Models for Vertical Gas Wells (OTC-26526-MS) presented at the OTC ASIA, March 2016, Kuala Lumpur, Malaysia

Honors & Awards : Full Scholarship for Master Degree by KFUPM, August 2014

Caspian Engineers Society Student of the Year, November 2012

Full Scholarship of the Republic of Azerbaijan for Master Degree, June 2011

BP Bursary, December 2007

Full Scholarship of the Republic of Azerbaijan for Bachelor Degree, August 2007

Membership : Society of Petrophysicists & Well Log Analysts (SPWLA),

Society of Petroleum Engineers (SPE)

Caspian Engineers Society (CES)